Università degli Studi di Ferrara

International Erasmus Mundus Master in
QUATERNARY AND PREHISTORY

Erasmus Mundus

Mandibular angle variation in Middle Pleistocene *Homo*, *Homo neanderthalensis* and *Homo sapiens*

Larissa Docal Spina

Supervisor: Prof. Julie Marie Arnaud

Academic year 2024/2025

Acknowledgments

Although writing may seem a lonely task, no reasoning process is entirely developed by one single person alone. In the research processes, there are countless exchanges, contributions we are sometimes unaware of. Besides the works cited throughout the text, I take a few words to recognize the impact of some very special people and institutions.

First of all, to the Erasmus International Master Quaternary and Prehistory for giving me the tools to prosper and develop into a well-rounded archaeologist. For the *Universitá di Ferrara* for welcoming me so well, especially in the figures of professors Marta Arzarello and Julie Arnaud. I thank you for the courses and the internship opportunities, both at excavation and at the lab. I appreciate the Paris *Musée Nationale d'Histoire Naturelle* for receiving me in exchange, in particular for Professor Amélie Vialet for taking the time to show me around the *Institut de Paléontologie Humaine* and accepting to evaluate this work.

In the scope of this research, I highlight that the development of this study would not have been possible without the contribution of Professor Julie Arnaud. Her work as my supervisor was fundamental in guiding and teaching me the methodological framework, in discussing the results and offering new perspectives about the written arguments. She is truly an inspiration as a paleoanthropologist and a professor, available and understanding at the same time. I hope one day to have the same attention to students and other researchers as she did with me.

I express my deepest gratitude to my husband, Tiago, who stood at my side through it all. Beyond the emotional support, as a statistician, he helped me to understand the mathematical nuances of the methods I worked with and improve the results' analysis. In many ways we complemented each other, both of our fields of expertise meet in this work, which made for some interesting conversations, even if sometimes the specific terminology escaped our comprehension. I hope to always help you the way you did with me.

My heartfelt acknowledgements go out to my friends and colleagues that made these two years memorable, for all the laughs and shared experiences. Devi and Ambre, I thank them for all their perspicacity and bravery, in sharing together the "italian life-style" - and also a bit of gossip. For Trish, I am grateful for the companionship on the *Bibliothèque Nationale de France* days and candid conversations. Last, but not the least, I thank Macchiato, for being such an outstanding and courageous cat, exploring the world with me.

List of figures

List of tables

Summary

Introduction

The current human fossil record holds a considerable amount of mandibles, especially for the Middle Pleistocene period (Rosas et al, 2019). Some specimens have particular importance in the European contemporary paleoanthropological framework - the Mauer mandible, for instance, is the holotype for the *Homo heidelbergensis* species, at the center of debate for the evolution of the *Homo neanderthalensis* lineage (Mounier et al, 2009; Hublin et al, 2009; Tattersall, 2011; Vialet et al, 2018; Quam et al, 2024) and their last common ancestor with *Homo sapiens* (Stringer, 2012; Rightmire, 2015; Roksandic et al, 2018; Di Vincenzo and Manzi, 2023). Thus, the mandible has features that are phylogenetically significant, which dictates further studies for their better comprehension (Rosas and Bastir, 2004; Nicholson and Harvati, 2006; Harvati et al, 2011).

The mandible is a complex bone, one of the most plastic in the human body, since it is constantly subject to biomechanical constraints, such as chewing patterns and bite forces. Therefore, its remodelling also responds to the biomechanical action from muscles attached and the articulation at the tempo-mandibular joint (Aiello and Dean, 1990; Lieberman, 1997; Van Eijden, 2000; Ruff, 2018; Sella-Tunis et al, 2018). At the same time, the association between mandibular and cranial-facial morphological changes dictated the activity in resorption and deposition sites (Enlow et al, 1996; Rosas and Bastir, 2004; Rosas et al, 2006). Therefore, it is essential to consider aspects of the growth trajectory, including different morphological integration patterns, as well as the biomechanical morphological implications.

These issues are at the core of current discussion about Neanderthal emergence and the allocation or not of Middle Pleistocene specimens into the lineage (Mournier, 2009b; Stringer, 2012; Rosas et al, 2019; Quam et al 2024). The *H. neanderthalensis* key mandibular features are fixated first in their differentiation process (Rosas et al, 2006), in comparison to other cranial aspects, such as the typical Neanderthal occipital bun. However, their early appearance is not linear, different specimens show an inconsistent combination of different plesiomorphic features and Neanderthal apomorphies - the very definition for the proposed ancestor *H. heidelbergensis* (Mounier, 2009b). Therefore, it is yet unclear what these morphological configurations represent, if they refer to intra-specific populational variation or represent the coexistence of different lineages.

Among Neanderthal derived features, the gonion region is significant for the particular truncated shape observed in many specimens. The mandibular outline studied in this research captures the variation in the gonion region, at the junction of the mandibular posterior and basal borders. While the truncated and inverted gonion morphology is typical

for *H. neanderthalensis* (Rosas, 2001; Mounier, 2009b), different configurations are observed for Middle Pleistocene *Homo* (Vialet et al, 2018; Quam et al, 2024) and some Neanderthals. Identifying the main axis of variation for this feature may provide insights into the processes driving these morphological changes and, in turn, contribute to a better understanding of Middle Pleistocene *Homo* variability.

On the other hand, *Homo sapiens* show some variations to their typical regularly curved gonion. Upper Pleistocene *H. sapiens* show a general mandibular pattern that is more related to the Neanderthal morphology than to later *H. sapiens* (Bergmann et al, 2021). Additionally, the Iberomaurusian, a North-African Upper Paleolithic population, tends to have a more expressive gonion eversion, the outward orientation of the angle (Irish, 2000; De Groote and Humphrey, 2016; Humphrey et al, 2021). A trend towards gracilization may also be identified in the Holocene, recent *H. sapiens* sample (Sella-Tunis et al, 2018; Bergmann et al, 2021), impacting both the gonion and ascending ramus morphology.

Therefore, this study focuses on the analysis of gonion morphology variation, also connecting it to the posterior ascending ramus morphology. Besides a morphological investigation, Geometric Morphometrics is applied through landmark and Elliptical Fourier-based Principal Component Analysis (Kuhl and Giardina, 1982; Lestrel, 1989; Easton, 2000; Claude, 2008; Arnaud, 2021).

The main goals are to identify intra and inter-specific variations, correlating gonion and posterior border morphologies. The distinctions between *H. neanderthalensis* and *H. sapiens* are described, and the Middle Pleistocene *Homo* compared. Moreover, Upper Pleistocene and the Upper Paleolithic Iberomaurusians are compared to the more recent Holocene *H. sapiens* sample, attesting to the differences produced in a gracilization process and between the male and female specimens.

This work is divided into five chapters. Chapter I introduces the mandible morphological and biomechanical aspects, as well as the state of art in paleoanthropological research. Chapter II describes the studied sample and methods employed. The results are given first at chapter III, for the morphological investigation, and at chapter IV for the Geometric Morphometrics. The results are discussed in chapter V, divided by the analysed species and followed by the conclusions.

Chapter I: State of the art

This chapter provides a concise review of the main anatomical and paleoanthropological aspects of the mandible for *Homo sapiens*, *Homo neanderthalensis* and Middle Pleistocene *Homo*. It is structured in two parts: first, an anatomical and biomechanical discussion; second, an examination of the evolutionary significance of mandibular morphology. As this study focuses on the gonion angle, particular attention is given to its morphological variation, highlighting the implications for human evolution and musculoskeletal reorganization.

1.1 Mandibular angle anatomy and biomechanical implications

The mandible, a horseshoe-shaped bone, corresponds to the lower jaw and integrates the cranial-facial complex. Chewing is its main function, through a biomechanical system of muscle attachment and the involvement of the temporomandibular joint. In general terms, the mandible is divided into two parts: 1) the *ascending ramus*, vertical and posterior, from the inferior border to the condylar articulation surface; 2) the *body*, or horizontal ramus, an U-shaped structure in which, at the superior margin, the alveolar sockets hold the lower teeth (White et al, 2011).

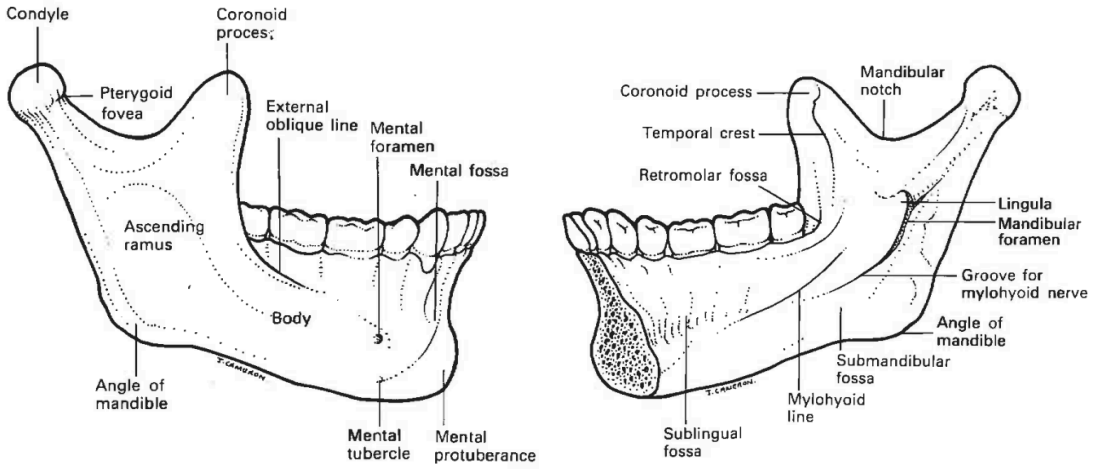

Fig. 1.1. Lateral and medial views of a human hemi-mandible. From Aiello and Dean (1990).

On lateral view (Fig. 1.1), a few key features are noticeable. The *condyle* is the most posterior rounded-process, articulating with the temporal bone by a cartilaginous disk. In front of it, the *coronoid process*, thin and triangular, is the anterior portion of the ascending ramus. Both structures are separated by an U-shaped *mandibular notch*, or incisura. At the root of the anterior portion of the ramus is the *oblique line,* a feeble eminence that extends

below the last molars. The posterior part of the ramus meets the inferior border of the body at the *mandibular angle*, or *gonion*. This is where the masseter masticatory muscle attaches, extending over the ascending ramus until the origin point at the zygomatic arch. On the medial aspect (Fig. 1.1), the ramus also has muscular and ligament insertions. At the *lingula*, a tiny and sharp projection, the sphenomandibular ligament attaches. Right below, the *mandibular foramen* allows the passage and nerves, as well as the *mylohyoid groove* marks their lodging. Lastly, the insertion of the medial pterygoid muscle at the postero-inferior part of the gonion.

At the mandibular body, there are other important bone structures for the well-functioning of the cranio-facial system. On the lateral and external side, the *mental foramen,* usually under the second premolar, serves for the passage of vessels and nerves. At the symphysis, a triangular bone chin forms the *mental protuberance*. On the internal side, important muscular attachments are present. The *mylohyoid line*, running anteroinferiorly, from the last molar alveolar margin, is where the mylohyoid muscle inserts, important for the oral cavity floor. At the symphysis, the *mental spines* are the insertion site for tongue muscles (White et al, 2011; Aiello and Dean, 1990).

This osteological description is very brief, but it substantially highlights the features to be most considered in this work. The focus on the outline of the posterior and inferior borders sheds a spotlight on their adjacent structures, in particular the gonion outline as a point of muscular insertion. Thus, understanding the bone configuration is important to interpret the variation observed in the outlines. These varied morphologies reflect the responses of the human mandible to multiple factors. The forces applied when chewing and the integration of the cranial-mandibular complex during growth are all to be regarded as possible influences on muscular configuration, bone modelling and remodelling. As such, it is important to comprehend both the mandibular development from birth and its response to biomechanical forces during life.

As a matter of fact, mandible formation begins even before birth, as one of the first bones to begin the ossification process still intra-uterine, around seven weeks of gestation, second only to the clavicle. Its development is characterized by an intramembranous ossification, the direct mineralization of a connective tissue membrane. Different from the endochondral ossification, in which a cartilaginous model of the bone is first formed and later on ossified, the intramembranous process directly ossifies the mesenchymal tissue, following a highly vascularized area, for the proliferation of the center of ossification along this capillary line. This type of ossification is mostly common in plate-like bones, such as the

skull or face. It results in dense, compact bone, whereas trabecular, cancellous bone is formed by the endochondral process (Scheuer & Black, 2000; Scheur & Black, 2004).

At the perinatal stage (Fig.1.2), the hemi-mandible morphology is very different from the later adult one. It is in fact not one bone, but two halves with independent ossification processes that are joined at the symphysis by a fibrocartilaginous joint. Teeth gems are already present, although not erupted, and the mandibular body and ramus are connected. Nevertheless, their positioning, in relation one to the other, is quite different (Aiello and Dean, 1990; Scheuer & Black, 2000).

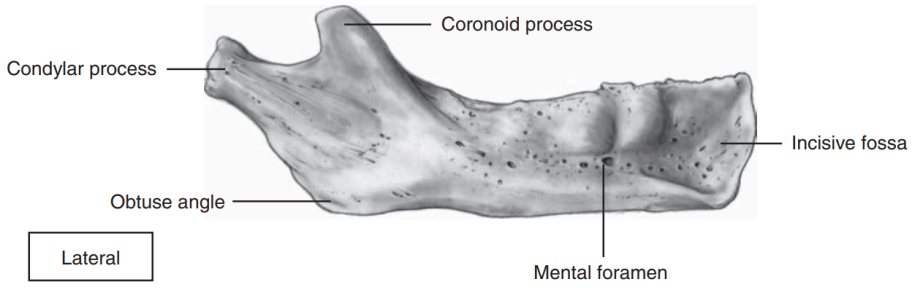

Fig. 1.2. Lateral view from right perinatal hemi-mandible. From Black, Schaefer and Scheuer (2009).

In modern humans, the gonial angle is very obtuse, varying from 135º to 150º, causing the condyle to be almost aligned to the occlusal plane, much lower than it will be in later stages of life. Indeed, the mandible is the facial bone that undergoes most postnatal variation in size and shape, according to dentition turnover and maxillary size for occlusion. Initially, the mandibular body undergoes a more rapid growth and, to maintain the relation as size increases, bone is deposited at the ascending ramus posterior border and reabsorbed from the anterior. This process creates space for dentition, elongating the body, as well as placing the condyle in a higher position, more vertical when the ramus increases in height. The gonial angle reduction is visible throughout this course: by the time of complete eruption of deciduous teeth, it varies between 130º - 140º; after the eruption of the second molar (permanent), it is at 120º - 130º (Scheuer & Black, 2000).

As such, this period is essential to the comprehension of the configuration that is to be settled onwards, into adulthood. Morphological integration plays its part for the coherence of the whole cranial-mandibular system, which denotes that alterations on the mandible may be correlated with other changes in the cranium (Rosas and Bastir, 2004; Rosas et al, 2019). Likewise, muscles are also part of this system, on one hand responding to morphological

reconfiguration and on the other hand influencing it, since bone is also subject to the forces applied by muscles.

The principle behind this idea is that bone is responsive to mechanical strain, and as such its morphology may reveal biomechanical information (Ruff, 2018). Bone is stiff to resist, but it has some deformation capability to withstand loading, and it may adapt to reach optimal form accordingly. Based on Wolff's law, bone is a functional adaptation, a feedback mechanism in which bone deposition or loss responds to an increase or decrease in strain (Aiello and Dean, 1990; Lieberman, 1997; Van Eijden, 2000; Sella-Tunis et al, 2018). In other words, from an optimal strain level, if mechanical loading increases, more bone is deposited; if it decreases, more bone is resorbed. Thus, bone may be altered in a life-long modelling or remodelling process, depending on the type of response adopted.

Forces of the same magnitude may cause bone to become thicker, change its shape or alter its internal structure. Modelling will involve the addition of new tissue, while remodelling usually entails the removal of bone tissue and changements in shape or structure. The variation in morphology is accounted for by the diversity in cellular activity, its onset, rate and duration. In line with the prevailing activity, it can be classified as depository, when osteoblast cells deposit new bone tissue, resorptive, if osteoclasts remove it, or resting if cells are quiescent. In general, thicker or more mineralized bone is formed for a greater resistance to strain (Liberman, 1997).

The mandible, due to its functional aspects, is one of the most plastic bones, since it is constantly under the masticatory forces, which in turn may vary in accordance with diet and activities. The condyle plays a major role in movement, since it articulates at the glenoid fossa for the temporo-mandibular joint (TMJ). There are four main pairs of muscles which act for this articulation movement: the temporalis, the masseter, the medial and the lateral pterygoid (Fig. 1.3).

The temporalis muscle extends upwards from its insertion at the coronoid process, anterior ramus border, to the lateral of the skull, overlaying parts of the temporal, parietal and sphenoid bones. The lateral pterygoid muscle is split in two, one originating from the lateral pterygoid plate, the other from the sphenoid great wing, until both meet to insert at the condyle articulation, at the fovea level (Aiello and Dean, 1990).

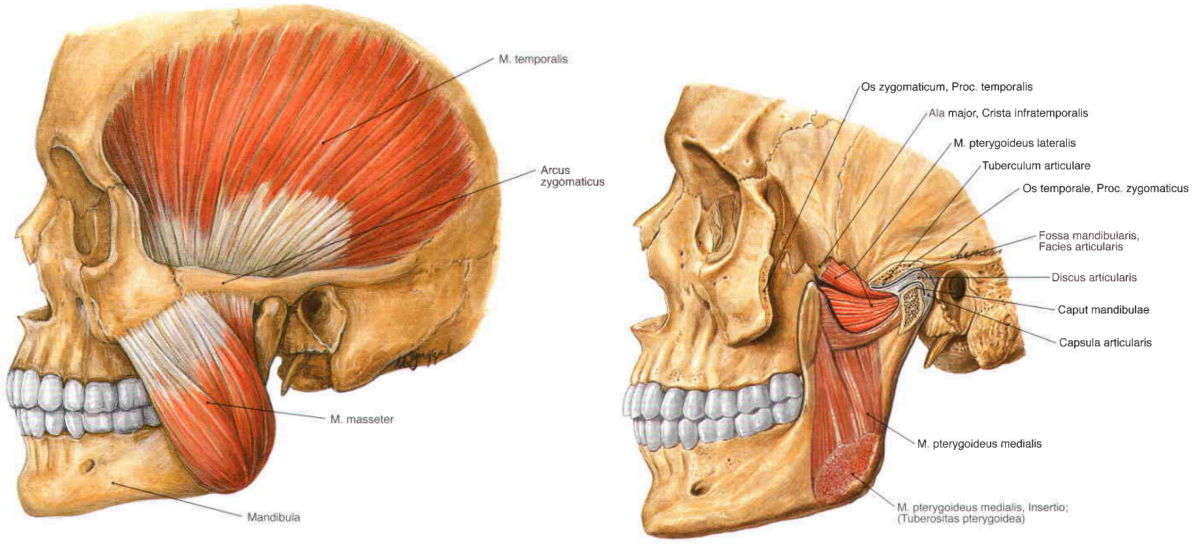

Fig. 1.3. Masticatory muscles. From Putz and Pabst (2006) .

When considering the gonion outline, the masseter and the medial pterygoid have a major role, since they insert, respectively, at the lateral and medial side of the gonion, acting primarily as elevators to close the mouth (Aiello and Dean, 1990). The masseter runs over the ascending ramus in a right angle, from its origin at the zygomatic arch inner border to its insertion at the mandibular angle. On the medial aspect of the ramus runs the medial pterygoid muscle, called as such because its main origin point is the medial aspect of the lateral pterygoid plate on the sphenoid bone. Differently from the masseter, its insertion at the gonial angle is medial and occupies only a small triangular area (Aiello and Dean, 1990).

In the mandibular movement, all these muscles act primarily as elevators: they contract to pull the mandible upwards closing the bite and tense during mouth opening. A chewing cycle can be divided into three continuous phases: the opening stroke, the closing stroke, the power stroke (when the teeth actually meet) (Aiello and Dean, 1990). However, the masticatory movement is not as simple as an up and down motion, but it is rather multidirectional, which implies differences in function for both the TMJ and the muscles, depending if they are on the working-side (where the bite happens) or on the balancing one.

For an unilateral molar bite, the mastication cycle follows an overall ellipsis: the mandible first moves downward, then laterally towards the working-side, and returning to the midline by the pull of the balancing-side. The temporalis is equally active on both sides, but masseter and medial pterygoid are more involved in the working-side. Primary roles also change according to the function: in the working-side, muscles act more as elevators and the

condyle rotates mostly in place at the TMJ; on the balancing-side muscles pull the mandible laterally and the condyle translates instead (Aiello and Dean, 1990; Van Eijden, 2000).

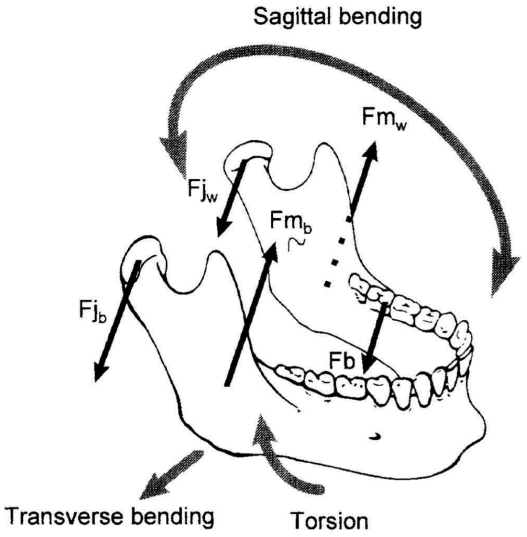

Fig. 1.4. Forces applied at the mandible in unilateral biting. Fj is joint force, Fm is muscular force and Fb is bite force. "w" stands for working-side (left) and "b" balancing-side (right). From Van Eijde (2000).

Hence, different forces are applied at the mandible, throughout all these movements (Fig. 1.4). Joint, muscle and bite forces create an overall vertical component, producing a primary sagittal bending moment, which is resisted by the great thickness of the mandible along this plane (Van Eijde, 2000). Moreover, due to the lateral movements of the mandible, transverse bending also occurs later in the powerstroke, requiring greater activation of the balancing-side muscles. Likewise, there is significant torsion on the working-side, caused by the twisting of the mandibular body along its axis. This rotation, or torque, can be defined by the force applied times the distance between the joint (TMJ) and where the force is applied (the bite). A stronger rotation may cause the lower border to evert, and the alveolar margin to invert. On both sides, the largest moment is at the ramus and adjoining mandibular areas (Lieberman, 1997; Van Eijde, 2000).

Regarding from a biomechanical perspective, Lieberman (1997) approaches the masticatory system through a lever arm/ load arm analysis, in which the first is the distance from the force produced (by the muscle) to the joint, and the second is the distance between the joint and where the bite force is applied. Torque is then, as previously mentioned, given by both force and lever arm. Therefore, both the ascending ramus height, as the lever, and the mandibular body length, as the load arm, will influence force magnitude. In these terms, a taller ascending ramus increases the lever arm for the masticatory muscles, allowing greater

torque generation. On the other hand, a longer mandibular body augments the load, but decreases the power applied.

Chewing strains can in fact influence mandibular height, as argued by controlled experiments on primates and rodents in which a hard food diet caused an elongation of the ramus, probably in response to sagittal strain (Lieberman, 1997). Such would suggest that the decrease in ramus height when comparing farmer populations to hunter-gathers could be a response to a softer diet, representing changes in the functional demands. Notwithstanding, there are other factors to be considered, in particular when comparing different species, since considerable aspects may vary differently. A greater muscle mass, for instance, may compensate for a smaller ramus, increasing the force applied.

Another morphological variation was observed by Sella-Tunis et al. (2018) when comparing cross-sectional muscle areas (CSAs) for the masseter and temporalis as a proxy for bite force. There was indeed a correspondence between the ascending ramus morphology and the muscle, especially significant for ramus breadth. The taller and narrow ramus, with an obtuse gonion angle, was connected to smaller muscle CSAs, indicating weaker bite force. Instead, a trapezoid-like ramus, wider, with a greater coronoid process was associated with greater CSA. Thus, the distance between the ramus posterior and anterior borders seems to indicate considerable involvement of both temporalis and masseter muscles shaping the morphology, considering also this thickening as an indicator of resistance to parasagittal and transverse bending.

This brief description accounts for some of the main aspects influencing the mandible morphology, highlighting those to be particularly considered in this study. Growth and modelling during life are important factors to its shape. Due to its functional character, the mandible is a very plastic bone, and as such, its study must include said aspects.

1.2 State of the art of paleoanthropological research on mandible remains

One of the core practices in paleoanthropological research is the establishment of phylogenetic relations based on the evaluation of bone morphology. Albeit the advances in ancient DNA studies in the last couple of decades, morphological study remains relevant and particularly significant to establish ancestor-descendent relations, in particular in older periods with no DNA data available (Bastir, 2018). However, the aforementioned multifactorial basis for osseous morphology may cloud the comprehension of evolution, since non-genetic stimuli can also explain certain features. Bone thickness, for instance, may be a poor indicator, since the deposition of bone matrix also responds to its activity. Addressing

these points should involve an approach that integrates functional and developmental studies (Lieberman, 1997).

The mandible presents some challenges in this case, since its morphological variability is influenced by its functional aspects. Nevertheless, there are some important arguments in favor of its study (Rosas et al, 2019). First of all, mandibles have some key features, fairly stable, which allow for species identification and a better comprehension of their variability. Second, the abundance of jaws on the fossil record is worth noting and an incentive to address the issue. Third, some specimens are central to the discussions, such as the Mauer holotype for *H. heidelbergensis* and other very complete mandibles in a sparse record. Therefore, the mandible continues to be an essential element to understand human evolution, since several integrate the Middle and Upper Pleistocene records and are key to the comprehension of the emergence of sister-species *H. neanderthalensis*, in Eurasia, and *H. sapiens*, in Africa[1].

a. Paleoanthropological studies on the *Homo sapiens* mandible

The fossil record holds evidence of *H. sapiens* speciation in Africa, around 300 thousand years ago (Hublin et al, 2017). The mandible has some of the key features for this process, since the mental eminence is a diagnostic apomorphy, although some primitive specimens may present a chin-like mental bump, such as Tigheniff (Mounier et al, 2009). Moreover, a gracilization process can be observed by the progressive change of the mandibular features through time.

In fact, early *H. sapiens* mandibles were intermediate between Middle Pleistocene morphology and nowadays modern humans. In many cases, including Upper Pleistocene mandibles, they resemble Neanderthal mandibles, with a wide ramus, large gonion area and retromolar space. These features, however, are related to an allometric signal, proving static allometric to be also an influential factor in bone morphology, besides phylogeny and masticatory adaptation. In other words, for *H. sapiens,* this Neanderthal-like mandibular shape may be varying according to size, correlating to bicondylar and bigonial breadth (Bergmann et al, 2021).

Later, the main differences between *H. sapiens* and Neanderthals are in corpus height, the mental eminence, retromolar space, gonion shape and ramus configuration (Bergmann et

[1] The Denisovans might be included as a sister-group that differed in the Middle Pleistocene. However, they are defined on a DNA basis, extracted from a pahalange (Sawyer et al, 2015). There are very few remains assigned to the species, which make it impossible to include them in a morphological comparison study.

al, 2021). Furthermore, a trend of gracilization is recorded by an obtuse gonial angle, the increase in prominence of the chin, reduction in dental arcade length and ramus breadth (Bergmann et al, 2021). Holocene *H. sapiens*, then, is more distant from the Neanderthal morphology, aligned with bone and muscular changes driven by changes in diet and behaviour, from a hunter-gatherer, forager community, to agriculture, pastoralism and the post-industrial society. This is also supported by a study correlating mandibular morphology and the masseter muscle cross sectional area, in which narrow ramus and obtuse angles are associated with weaker masticatory muscles (Sella-Tunis et al, 2018).

b. Neanderthals: mandibular features and evolutionary implications

The Neanderthal mandibular morphology has some very particular features and differs a lot from the *H. sapiens* described in section one. Apomorphies for Neanderthals are described as: posterior position of mental foramen, under the first molar; retromolar space between the ramus anterior border and the third molar; medial position for the intersection of the condyle and the mandibular notch; diagonally oblique mylohyoid line; deeply excavated pterygoid fossa; and a truncated gonion profile (Rosas, 2001). The gonion could be further described as inverted, the ramus wide and the symphysis straight, in opposition to the chin characteristic of *H. sapiens* (Bergmann et al, 2021).

Some of these traits could be related to growth, since different development units are integrated into the mandible (Rosas and Bastir, 2004), forming a complex growth pattern, simplified as bone deposition at the posterior ramus border and resorption at the anterior (Rosas, 2001; Enlow et al, 1996). The backward growth of the ramus for the forward displacement of the mandible also causes the posterior move of structures such as the mental foramen and the creation of a retromolar space. Allometry, the relation between shape and size, explains these features, considering they may also be present in some large Upper Pleistocene *H. sapiens* fossils (Rosas and Bastir, 2004; Bergmann et al, 2021).

Another set of features could indicate changes in the muscular organization for Neanderthals, which would accompany other changes. The forward displacement of the mandible is related to the midfacial prognathism, in coordinated growth between the different craniofacial anatomical units, to maintain the occlusal position of maxillary and mandible. Reconfiguration to stabilize the tissue matrix is also necessary, and some apomorphic features indicate muscular reorganization, such as the gonion, truncated, or the mylohyoid line, oblique (Rosas, 2001).

Considering all these characteristics, the *H. neanderthalensis* mandible has a clear set of apomorphies that allows its recognition as a species. The problem is they do not appear as a package, but rather irregularly in Middle Pleistocene forms, which complicates the identification of a speciation event for Neanderthals (Hublin, 2009). Two main models for the emergence of the species were proposed, trying to account for the evolution of the derived features for *H. neanderthalensis* and its impact on the mandible.

The two-phase model is based on two different moments for morphological change that would at the Late Pleistocene culminate in what we know as *H. neanderthalensis* (Rosas et al, 2006; Rosas et al 2019). The 1st phase, around 600 thousand years ago, is related to mid-face prognathism, with the anterior displacement of facial units, in mid-sagittal growth. Cranio-mandibular integration would require the jaw bone to also adapt, which is reflected in the dental arcade and external features. This phase is yet poorly understood, with significant variation (Rosas et al, 2006). The 2nd phase of morphological change takes place after 300 thousand years ago, characterized by cranial reorganization, with the increase in size of temporal and occipital areas, reflected on internal features. In this model, the second phase would be an speciation event for Neanderthals, which would differentiate from their ancestor, recognizing them as two different species (Rosas et al, 2006; Hublin, 2009).

On the other hand, the Neanderthal evolution model can be described as a progressive appearance of its derived features, which throughout the Middle Pleistocene increase in frequency and become fixated by the Upper Pleistocene. Dean et al (1998) identifies four main stages in Neanderthal evolution, by the amount of characters already present. The accretion model considers the *H. neanderthalensis* evolution as a continuum, from the appearance of the first characteristic traits, starting mainly by the dentition, face and mandible and later on the skull, in particular the occipital bone (Hublin, 2009). This model would favor a chronospecies concept, a clear connection between Neanderthals and their Middle Pleistocene ancestors, placing them in the same clade.

Although most scientists tend to favor the perspective from an accretion model, these questions still remain under debate. Who were the first Neanderthals? How did they evolve and how do they relate to us, in terms of a Last Common Ancestor (LCA)? Understanding the emergence of *H. neanderthalensis* is fundamental for the comprehension of Middle Pleistocene human history, regarding *H. sapiens* speciation in Africa, Denisovans in Asia and the candidates for a LCA (Roksandic et al, 2021; Di Vincenzo and Manzi, 2023).

c. Middle Pleistocene human evolution in Europe

The Middle Pleistocene (MP) fossil record is discontinuous, in the sense that fossils cannot be aligned to show progressive Neanderthalization through time (Vialet et al, 2018). In other words, older specimens may show more Neanderthal features than their more recent counterparts. This puzzling nature of the record is ground for multiple interpretations and species attributions for the hominins of the period. Multiple proposals have been done regarding the name and reach of these specimens, limiting them to Europe, or proposing Afro-European extensions. According to the line of research, MP *Homo* may be referred to as *Homo heidelbergensis*, *Homo rhodesiensis, Homo bodoensis*, or even as *H. neanderthalensis* if this species is defined by the first appearance of its derived features. In the next few paragraphs we briefly address this confusion that has come to be defined as "the muddle in the middle" (Roksandic et al, 2021).

H. heidelbergensis was suggested as a classification for MP *Homo*, since its holotype, the Mauer mandible, is one of the oldest human remains in MP Europe. Despite the specimen containing only the mandible, it shows a clear combination of plesiomorphies and Neanderthal-like apomorphies (Mounier et al, 2009; Mounier, 2009b), for instance the posteriorly positioned foramina mentale, retromolar space and truncated gonion. This unique combination of primitive and derived Neanderthal-like features was the definition proposed for *H. heidelbergensis,* noting that Mauer differentiates from *H. neanderthalensis* for a receding symphysis and a parallel mylohyoidal line (Mournier, 2009b).

The fact that the holotype for the species is a mandible complicates the identification of other fossils belonging to the group, since many are skulls or other bones. Some researchers have, however, approximated the face of *H. heidelbergensis* by comparison. The Arago mandibles are morphologically similar to Mauer and they have associated craniums, which in turn are comparable to Petralona, and from Petralona to African MP specimens Broken Hill, Kabwe and Bodo (Rightmire, 2008; Stringer, 2012).

Due to the similarity between European and African counterparts, it is argued that *H. heidelbergensis* is a stem species for both *H. neanderthalensis* and *H. sapiens* (Rightmire, 2008; Mounier et al, 2009; Di Vincenzo and Manzi, 2023). Mounier (2009b) comparative morphological analysis supports the phenetic basis of *H. heidelbergensis* as an Afro-European group, ancestral to both species. The African specimens would not present Neanderthal apomorphies, but derived features which would later on be related to *H. sapiens*, such as Tigheniff modern human-like chin (Mounier et al, 2009). There is significant morphological variability in the assemblage, nonetheless it is not excessive to that observed

in other species (Rightmire, 2008; Di Vincenzo and Manzi, 2023), but regional variances would ultimately lead to the different species (Mounier et al, 2009).

This would imply that *H. heidelbergensis* is the Last Common Ancestor between *H. sapiens* and *H. neanderthalensis*, which is in line with current nuclear DNA estimates for the divergence of the two clades, around 500 thousand years ago (Prufer et al, 2014; Di Vincenzo and Manzi, 2023). Not everyone agrees with the interpretation, though. Other authors (Rosas and De Castro, 1998; Hublin, 2009) define *H. heidelbergensis* as an only european chronospecies of the Neanderthal evolutionary lineage. Contemporarily, the African specimens would be considered as *H. rhodesiensis*, ancestor to *H. sapiens*, with the Kabwe fossil as the holotype. Then, this interpretation does not consider *H. heidelbergensis* as the LCA for Neanderthals and *H. sapiens*.

We can summarize a few issues stemming from these considerations about *H. heidelbergensis*. Which specimens are included in the group? What are their phylogenetic relations? Likewise, the heterogeneous distributions of Neanderthal apomorphies in MP fossils unsettles the debate about ancestor-descendent relation between *H. heidelbergensis* and *H. neanderthalensis*. The question in this case is rather if Mauer predates or postdates the beginning of Neanderthal features (Hublin, 2009). Even if Mounier et al (2009) identify the Neanderthal apomorphies in the holotype mandible, it is not a consensus.

For other researchers (Tattersall, 2011; Roksandic et al, 2018; Quam et al, 2024), Middle Pleistocene specimens with a clearer Neanderthal affinity, such as Sima de los Huesos (SH), in Atapuerca, should rather be defined as *H. neanderthalensis*, pushing the emergence of the species to around 430 thousand years ago. This is done because SH and Neanderthals features are not just synapomorphic, but indicate the same morphological configurations (Stringer, 2012). For Quam et al (2024), while the phylogenetic structure of the Sima de los Huesos mandibles is fairly stable, placing it into the Neanderthal variability, Mauer lacks most of the Neanderthal apomorphies. Therefore, two groups are divided, one with Neanderthal-like configuration is *H. neanderthalensis* (Sima de Los Huesos, l'Aubesier and Ehringsdorf), and the other *H. heidelbergensis* (Mauer, Montmaurin and Visogliano).

This implies the coexistence of two evolutive lineages in Europe, as a way to explain the morphological variability observed in Middle Pleistocene Europe. Another similar proposal was done by Roksandic et al (2021) with the creation of *H. bodoenses*, with Bodo 1 as holotype, to replace *H. rhodesiensis* in Africa and assign many specimens in Eastern Europe. Other specimens in Western Europe would be considered as *H. neanderthalensis* (including both Mauer and Atapuerca) to indicate the early differentiation of the clade. Both

approaches also push back the date of the Last Common Ancestor, in Africa, according to Roksandic et al (2021), probably around 1 million to 700 thousand years ago.

This Middle Pleistocene morphological variability, however, is tackled by other approaches that consider *H. heidelbergensis* as an Afro-European species ancestor to both *H. neanderthalensis* and *H. sapiens*. How much morphological difference is necessary to the separation of species? On one hand, Rosas et al (2019) adopts a structuralist approach and concludes that Mauer and the SH mandibles belong to one single deme, reflecting early stages of Neanderthal lineage. The variability in mandibular features is, instead, explained by structural differences reflecting growth patterns for the vertical configuration of the face. On the other hand, for other authors, migration and population processes can explain morphological variability. Multiple demes of the same species may have been created, by isolation processes due to the worsening climate conditions and the arrival of several population waves (Vialet et al, 2018; Di Vincenzo and Manzi, 2023; Hautavoine et al, 2024).

The MP is the period of the onset of glaciation cycles lasting 100 thousand years, marking a high degree of climatic heterogeneity (Di Vincenzo and Manzi, 2023). During the glacial periods, most of Europe would be almost unpopulated, in what could be considered a "sink" place, where, for the lack of individuals, reproductive rates are not enough to maintain population without new incomers (Dennel et al, 2011). These new migrations would come from warmer "source" areas, where populations survived, but perhaps after periods of isolation. These repeated population contractions and migration flows would cause extinction events, genetic drift and hybridization between surviving populations (Hautavoine et al, 2024).

These complex and not yet well understood processes could account for the variability and discontinuity of the MP fossil record. The isolation events and genetic changes do not imply a separation of lineages, but are, instead, morphological variation still in the same species. This is possible because evolutive lines start to diverge before there is an actual split, before the species is divided into two clearly separated monophyletic groups.

For Di Vincenzo and Manzi (2023), in respect to the Middle Pleistocene evolutive scenario, there would be a first process, between 600 and 300 thousand years ago, of intraspecific differentiation into paleodemes or subspecies, in which all individuals still belong to *H. heidelbergensis* (the LCA). In a second moment, after 300 thousand years ago, genetic and morphological differences would become fixed and account for defined descendent species. This proposal considers the Accretion model for Neanderthal emergence, in a "phylogeographic" evolutive pattern, in which features become first fixed in Neanderthal

populations isolated to the West and Atlantic and then expand to the East, replacing ancestral populations.

1.3 Hypothesis and goals of this study

The study of mandibular morphology is of great significance to the comprehension of evolutionary processes, growth and biomechanical implications. The multifactorial character of the bone morphology is a challenge, but also a window into other aspects. The gonion morphological configuration is very complex, since there are bone deposition and resorption centers that respond to different stimuli - growth, biomechanical and cranial-mandibular integration. Therefore, mapping the variation patterns enhances the comprehension of factors involved in gonion morphology and addresses its effectiveness as a distinguishing feature between species, since it is often listed as a phylogenetically significant trait for *H. neanderthalensis.* With these considerations, the main purpose of this work is to investigate the axis of variation in gonion morphology. The results are discussed regarding the following hypothesis:

1. *H. neanderthalensis* differentiates from *H. sapiens* by a truncated gonion;
2. Middle Pleistocene *Homo* gonion morphology approximates *H. neanderthalensis*;
3. There is significant variability between *H. sapiens* populations, considering specimens from Upper Pleistocene, Iberomaurusian populations and Holocene.
    a. Upper Pleistocene *H. sapiens* may present a gonion outline intermediate to *H. neanderthalensis* and later *H. sapiens*;
    b. Iberomaurusian specimens differ from other *H. sapiens* by an expanded and everted gonion.
4. Consider if molar antemortem tooth loss explains any of the of the observed axis of gonion morphological variation.

Chapter II: Materials and Methods

To understand the implications of variation in gonion morphology, a thorough process of data retrieval and analysis was followed. First of all, to comprise the variability, the specimens and the reference collections were selected: a total number of 165 individuals were included, divided into *Homo neanderthalensis*, Middle Pleistocene Hominins, *Homo sapiens* Upper Pleistocene *H. sapiens* and iberomaurusian *H. sapiens*, for their particular morphology. The state of conservation varies, requiring mirroring technique and adaptations, but all present a clear hemi-mandible outline.

The obtention of data was a second step, through the management of 3D models, some from the original mandible, others from a research-appropriated replica. On the software 3D Slicer (Fedorov et al, 2012), 70 landmarks were positioned to draw the mandibles' curves. Next, the analysis streamed from three main methods: a morphological investigation of gonion characteristics; the Geometric Morphometrics, through landmarks configurations for all the specimens and Elliptic Fourier analysis on outlines (Arnaud, 2021; Claude, 2008; Easton, 2000; Lestrel, 1989) . In this chapter, each of these processes is further described.

2.1 Materials

a. Middle Pleistocene *Homo*

The specimens with the oldest chronology are referred to in this study as "Middle Pleistocene *Homo*", designating their allocation to a period of diversity in human evolution, when different lineages coexisted, and it is not yet agreed on the phylogenetic relations. For some researchers, the specimens in this group are *Homo heidelbergensis* (Mounier, 2009), to others they may refer to more than one phylogenetic lineage (Quam et al, 2024). The name choice acknowledges this debate.

The chronologically older individual in this group is dated to around 700 thousand years ago, by biostratigraphy and paleomagnetism. *Tighenif 3,* the best preserved exemplar of the sandpit site, in Algeria, is massive and robust and shows a primitive structure pattern (Bermúdez de Castro et al, 2007). Since its first definition as *Atlanthropus mauritanicus*, by Arambourg (1954), it has since been attributed to *H. heidelbergensis* (Mounier et al, 2009*), H. erectus* sensu lato (Bermúdez de Castro et al, 2007), encompassing North African variants of *H. ergaster*.

The holotype for the *H. heidelbergensis* is the *Mauer* mandible, an indeterminate individual, represented by this single bone. In 1908, recognizing human characteristics in a at

the time unparallel ancestor, Schoetensack attributed the species name after the valley of Heidelberg in which it was found. The robust mandible was found in excellent condition, the only damage to some tooth crows occurred during cleaning preparations at a time methods were not as rigorous as today (Mounier et al, 2009).

The *AT-888* mandible is one of the specimens at the Sima de los Hueso site, in Atapuerca, known for its unparalleled Middle Pleistocene fossil abundance. The mandible was found in several fragments, but was later reconstructed to a good standard, although the right condyle is chipped, the left ascending ramus is missing, as well as the frontal dentition. However, from molars and premolars wear, a mature age was indicated. From the association with skull 5, possibly belonging to individual XX1, the male sex was estimated (Rosas, 1997).

The *Montmaurin* specimen was originally found in two pieces which were later on assembled to form a remarkably complete mandible, with all molars still in the alveolar sockets. Considering the lack of wear on the fully erupted third molars, this is a young adult with very small dimensions. When compared to Mauer, the Montmaurin was estimated as female; however sexual dimorphism is not yet well established for the *H. heidelbergensis* species (Billy and Vallois, 1977).

In the 50 years of excavation in Caune de l'Arago site, in Tautavel (1964 - 2014), five human mandibles have been retrieved, dating around 400 to 350 thousand years ago. Of those, two are included in the sample. *Arago 13* is a right hemi-mandible, with all molars and premolars in the dental alveolars. It stands out from the other four mandibles in the series for its size, which led to its attribution as male, while the others, more gracile, are considered females. Among these is *Arago 2*, a complete specimen, with two molars present on either side and one premolar on the left. The right ascending ramus has undergone some reconstruction, so the better-preserved left side was preferred for this analysis, applying the mirroring technique. The different morphological analyses diverge in species attribution. For Mounier (2009), the Arago specimens are phylogenetically connected to Mauer, thus assigned to *H. heidelbergensis*, whereas for de Lumley (2015) they are different from Mauer and closer to Tighenif, and as such, *H. erectus* sensu lato.

Middle Pleistocene Hominins		
Specimen	**Chronology**	**Bibliographical Reference**
Tighenif 3	~700 ka	(Bermúdez de Castro et al, 2007)
		(Arambourg, 1954)
		(Zanolli and Mazurier, 2013)
Mauer	609 ± 40 ka	(Mounier et al, 2009)
AT-888	530 ka	(Rosas, 1997)
Montmaurin	400 ka	(Billy and Vallois, 1977)
Arago 2	400 - 350 ka	(Lumley, 2015)
Arago 13	400 - 350 ka	

Table 2.1. List of Middle Pleistocene Hominins included in this study.

b. Homo neanderthalensis

Twelve *Homo neanderthalensis* were included in the sample, comprising a variety of chronology, geographical location and age at the time of death. Sex is also a variable, although a large part are males (8 in total), with only one female and three indeterminate. Three are dated to the end of Middle Pleistocene and transition into the Upper Pleistocene (around 126,000 years ago), and the others extend through this last geological period, until the beginning of the culturally-defined Upper Paleolithic (from 40,000 years ago). As for the location, seven were found in Western Europe, five in the Middle East and one in Eastern Europe. Here is a brief description of each specimen.

L'Aubesier 11 is an indeterminate sex individual dated from the Middle Pleistocene and excavated in the beginning of the 2000's. A description of the mandible indicates only a partial mandible is present, but containing the full outline of the right side. There is some surface bone loss to the gonion area, but most of the posteroinferior gonion margin is retained (Lebel and Trinkaus, 2002). Severe pathological alterations to the alveolar bone make this an even more intriguing specimen, since antemortem tooth loss and impairment of the remaining teeth imply feeding adaptations prior to death, although wear in C1 and P3 roots indicate L'Aubesier 11 was still chewing (Lebel et al, 2001).

Tabun II is an isolated mandible found in Israel, associated with other Neanderthals, dated to the Upper Pleistocene transition. Its pristine condition, with only the left condyle and central incisor missing, allows one to estimate sex and age, even if only the mandible is present. In fact, to McCown and Keith (1939), its massive proportions could only attribute it

to a male, especially when compared to the contemporaneous Tabun I, much more gracile and considered a female (not included in this study sample).

The only Eastern Europe Neanderthal in the sample is *Krapina J*, a male mandible, the most complete mandible of the site series, and dated to the Riss-Wurm Interglacial. It was excavated in the beginning of the XXth century at the eponymous Croatia town. Regarding the conservation, only the posterior part of the right ascending ramus is missing and only the left P3 was lost in life and the M3 post-mortem (Smith, 1976).

Malarnaud was discovered inside a cave in 1888, becoming the first Neanderthal to be found on French soil. With a fairly good bone preservation, the specimen has almost no teeth, only the right M1 is still in the alveolar socket and M3 is visible through the bone, in the eruption process. Indeed, this individual of indeterminate sex is classified as an young adult, some studies attributing ages as young as 11 to 13 years old (Heim, 1995). The chronology is still uncertain, a long period was attributed because the fauna in the biostratigraphy could refer either to an interglacial period or a glacial one (Heim, 1995).

Shanidar caves in Iraq provide some of the most famous Middle East Neanderthals. In this study are the mandibles from *Shanidar I,* excavated in the 1950's, and *Shanidar IV*, the famous "flower burial" Neanderthal (Solecki, 1975), in the 1960's. Both mandibles belong to adult males, attributed with significant evaluation of teeth, cranial and pelvis remains (Trinkaus, 1983). Shanidar 1, chronologically younger, is the best preserved of the two, with no significant damage or distortion. It is large, compared to other Neanderthals and is only missing the frontal incisors. Shanidar IV, on the other hand, has marked tooth loss, with signs of alveolar reabsorption on the right side. The five original pieces went through great reconstruction, making it possible to analyse the main structures.

Both the Israeli mandibles *Kebara* and *Amud 1* are in pristine condition, only tips of the condyle are missing, in the left side for the first, and in the right for second. Furthermore, all teeth are present, allowing both to be classified as young adults (Tillier, 1989) (Hovers et al, 1995). Considering other anatomical elements, Amud 1 is classified as male (Maureille and Vandermeersch, 2007) and Kebara indeterminate.

Some of the most famous *Homo neanderthalensis* from France are included in the sample. They mark the discussion about Neanderthal morphology and burials. *La Ferrassie 1*, a male in supine position discovered in 1909, is the first finding in a site that holds 17% of Neanderthal burials. *St. Césaire 1*, also a male excavated in 1979, was not as complete as the Ferrassie counterpart, and the cranium went through great reconstruction (Maureille and Vandermeersch, 2007).

La Chapelle-aux-saints 1, excavated in 1908, is a very particular case in regards to its mandible, since it shows extreme pathological alterations, which earned him the nickname of "the old man" (Trinkaus, 1983). He is indeed a male with severe bone reabsorption for post-canine teeth, although Tappen (1985) indicated that recovered teeth and alveolar analysis suggest that on the left side both incisors, canine and premolars were functional, in occlusal position. On the other hand, for the right side, the situation is dubious at least for frontal teeth, due to damage. According to the author, it is possible some of these teeth were present or lost little before death, but they would be in any case tilted medially.

The most recent of the *H. neanderthalensis* specimens is the *Zafarraya 2* mandible, found at the entrance of Boquete de Zafarraya karstic cave in southern Spain. The bone was broken in two pieces, at the symphyseal region, but was later reassembled, resulting in an overall well-preserved state. Based on morphological estimations, the remains belong to an adult male adult, who died at approximately 25 to 30 years of age. Gamma-ray spectrometry dating places the specimen at the beginning of the Upper Paleolithic (Barroso, 2001).

Homo neanderthalensis		
Specimen	**Chronology**	**Bibliographical Reference**
L'Aubesier	> 169 ka - 191 ka.	(Lebel and Trinkaus, 2002)
		(Lebel et al, 2001)
Tabun II	165 ka - 143 ka	(McCown and Keith, 1939)
Krapina J-59	130 ka	(Smith, 1976)
Malarnaud	100 ka - 50 ka	(Heim, 1995)
Shanidar IV	80 ka	(Trinkaus, 1983)
Shanidar I	60 ka	
Kebara	64 ka - 59 ka	(Tillier, 1989)
Amud 1	60 ka - 50 ka	(Hovers et al, 1995)
La Ferrassie 1	55 ka - 61 ka	(Maureille and Vandermeersch, 2007)
Saint Césaire	55 ka - 61 ka	
La Chapelle-aux-Saints	56 ka - 47 ka	(Trinkaus, 2011)
		(Tappen, 1985)
Zafarraya 2	50 ka - 42 ka	(Barroso, 2001)

Table 2.2. List of *Homo neanderthalensis* specimens included in this study.

c. Iberomaurusian *Homo sapiens*

The Iberomaurusian, a population from the Maghreb during the Upper Paleolithic period, are in this study separated from other *Homo sapiens* due to their morphological

significance. They are overall a skeletal-robust population and their mandibular angle displays a particular shape, usually with a strong extroversion (Irish, 2000). It is also worth noting that they practice, as a ritual behaviour, the removal or ablation of teeth, typically the upper central incisors (De Groote and Humphrey, 2016). Taking into account the possible impact from such teeth alteration and the particular morphology, thirty-six iberomaurusian mandibles from two different sites were included as a group for the analysis.

From the Afalou necropoli, dated between 14910 to 11450 thousand years ago, there are eighteen specimens included, nine male, three female and six indeterminate (De Groote and Humphrey, 2016). From Taforalt, ages between 15000 to 13000 years ago, there are also eighteen mandibles, nine male and nine female (Mariotti et al, 2009). The conservation is excellent for most of them, with minor chippings and occasionally a missing part that does not impede this study.

d. Upper Pleistocene *Homo sapiens*

Upper Pleistocene individuals provide an understanding of the mandibular angle morphological evolution, since they differ from later Holocene *H. sapiens*. Five mandibles integrate this sample. AP/58-2-37807, from the *Abri Pataud* site in France, is well preserved, with only incisors, canines and the second premolar missing. Initially excavated in the Movius campaign (1958 - 1963), it was, in later works, connected to other bones that compose one single person (P1), a female from the coxae bone (Henry-Gambier et al, 2013). Both *Skhul IV* and *Skhul V* were excavated in the 1930's and were subject to several treatments, not in all regards up-to today standards (Schwartz and Tattersall, 2005). Consequently, even if both are almost complete, there are fragmentations and reconstruction work. In both male mandibles all the teeth are still attached to the alveolus.

Upper Pleistocene *Homo sapiens*		
Specimen	**Chronology**	**Bibliographical Reference**
Grimaldi		
Abri Pataud - AP/58-2-37807	22 ka	(Henry-Gambier et al, 2013)
Skhul IV	100-130 ka	(McCown and Keith, 1939), (Schwartz and Tattersall, 2005)
Skhul V	100-130 ka	

Table 2.3. List of Upper Pleistocene *Homo sapiens* included in this study.

e. Recent *Homo sapiens*

This is the largest group in the analyzed sample, with individuals from two main categories. North African *H. sapiens* allow for interpretation of populational continuity in the region, since an evaluation on the Iberomaurusian particular morphology is necessary. Comprising most of the specimens, the reference collections, recent *Homo sapiens,* dated from the Holocene, representing a control sample in this study. They are stored in several Parisian institutions, the Musée de l'Homme, the Musée Nationale d'Histoire Naturelle and the Institut de Paléontologie Humaine.

i. North African *Homo sapiens*

Ten other specimens from North Africa were included, in order to assess population continuity in the region, since the iberomaurusian population presents such a unique morphology. The individuals here included span from possibly contemporaneous, in the Upper Paleolithic, mandible H3 from El Harhoura 2 site and L14-190 from M'Tsogatin, both showing cultural and morphological similarities to the traditional site of the iberomaurusian culture, Taforalt (Oujaa and Lacombe, 2012) (Sens et al, 2016).

Regarding the following periods, the individuals from Ain Meterchem, Ain Dokhara, El Harhoura 2 (H5 and H6), from Neolithic and Capsian traditions, may reflect some continuity in population and cultural practices (De Groote and Humphrey, 2016)(El Hahraoui et al, 2012). A mandible from the upper disturbed layers Kehf Hammar completes the North African sample with its most recent specimen (Barton et al, 2005).

North African *Homo sapiens*		
Specimen	**Chronology**	**Bibliographical Reference**
Ain Meterchem	Capsian	(De Groote and Humphrey, 2016)
Ain Dokhara	Capsian	
A5_1918-2	Capsian	
El Harhoura 2 (H3)	Upper Paleolithic	(Oujaa and Lacombe, 2012)
		(Humphrey et al., 2021)
El Harhoura 2 (H5)	Neolithic	(El Hahraoui et al, 2012)
El Harhoura 2 (H6)	Neolithic	
Gambetta 1	Mesolithic?	(Humphrey and Bocaege, 2008)
		(Balout and Briggs, 1949)
Kehf Hammar	500 AC	(Barton et al, 2005)
Mechta-Chateaudun	Capsian	(Mercier, 1915)
M'Tsogatin 1 - L14-190	Upper Paleolithic	(Sens et al, 2016)

Table 2.4. List of North African *Homo sapien*s included in this study.

ii. Reference collections

Musée de l'Homme: the Georges Olivier and Cantacuzène Collections

The oldest of the two Trocadero's collections was donated in the 1870's by its namesake, Don Prince de Cantacuzène, containing 46 skulls from XIXth century Turks, Bulgarians, Serbs and Romanians (Broca, 1873). It is an effort to improve the available anthropological material, taking into account other donations and Broca's engagement to built a laboratory museum, in which collections with French and foreign individuals would be easily available to students (Broca, 1872). From this collection, 17 mandibles were included in this study, of Bulgarian and Romanian origin, 5 of those being female and the others indeterminate (Ely, 1967).

With respect to the Georges Olivier collection, it was formed significantly later, in the second half of the XXth century. Olivier was in fact the creator of the Biological Anthropology lab in the University of Paris 7 (old Faculté des Sciences de Paris) (Demoulin, 1996). The conceived collection became a reference for anthropological and medico-legal studies in France (Knusel, Maureille, 2018). 33 individuals are included from this collection, as well as 1 middle aged mandible from the Saint Anna site.

The collections at the MNHN and the IPH

Both the *Musée National d'Histoire Naturelle* and the *Institut de Paléontologie Humaine* have human remains from different periods and origins. For this research, there are 29 individuals from the MNHN, 11 female and 18 male, spanning from Neolithic France to more recent Japan. From IPH, there are 13 individuals of indeterminate sex, from Poland, Italie, and Finland.

2.2 Methods

a. Morphological investigation and classification of the gonion

The classification proposed here for morphological variation in the mandibular angle is based on the specific traits of the aforementioned sample. The approach adopted draws on Mounier (2009b), who included the gonion as one of the features he analysed, labelling it as "everted", "regular" and "truncated". Modifications were introduced to better suit the sample in question and further assess the variability in each category. For this purpose, a system was developed considering separately "gonion shape" and "gonion orientation" (Quam et al, 2024).

In this process, the observations were recorded in two different steps. Initially, when also retrieving data for the curves, the mandibular angle was sorted into the Mounier (2009b) categories. When the full extent of the specimens was evaluated, a more refined classification was applied. Thus, in the second step the gonion classification was divided. While "shape" here is considered the outline, the boundary structure of the angle, "orientation" regards the direction of this structure.

A shape can be: expanded (E), if the gonion area extends beyond the expected curve and in relation to the mandibular body; regular (R), if the gonion follows a clear curve; truncated (T) if the angle is "formed as a third arista between the posterior border of the ramus and the basal border" (Rosas, 2001, p.78). On the other hand, orientation refers to an angle which is: everted (E), when it projects outward; straight (S), if it is aligned to the mandibular plane; inverted (I), if the direction is inward.

Variable	Possible Values
Gonion shape	**E** = expanded
	R = regular
	T = truncated
Shape expression	**1** = subtle
	2 = moderate
	3 = pronounced
Orientation	**E** = everted
	S = straight
	I = inverted
Orientation expression	**1** = subtle
	2 = moderate
	3 = pronounced

Table 2.5: Classification system for the mandibular gonial angle.

To account for the inter-individual difference for the same feature, a classification of the degree of expression was implemented, in which score 1 indicates subtle expression, score 2 moderate, and score 3 pronounced (table 2.5). For instance, a specimen with a T1 shape has a subtly truncated gonion. If we included the orientation, it could be T1 / I2, as an example, meaning the gonion is subtly truncated and moderately inverted. This is particularly relevant for investigating the range of variations in the everted orientation, but also affects inversion, as well as expansion and truncation regarding shape. The regular and straight categories were considered non-expressive (score 0), since they don't have such a visible difference. Therefore, the investigation into two aspects, combined with the degree of each

category's expression, enables a more nuanced understanding of the gonion morphological variability.

Besides this classification system, other parameters were taken into consideration to investigate mandibular angle aspects, such as the visibility of the gonion in frontal and occlusal view. A binary system was implemented, in which zero indicates the absence of the feature and one the presence. There are, of course, other structural factors that influence the visibility of the gonion, but it could demonstrate a stronger degree of extroversion or inversion.

Likewise, binary values were attributed to the presence of ante-mortem tooth loss (1) and absence of it (0). Signs of alveolar resorption and bone remodelling were considered for the exclusion of post-mortem loss. On a side column, there are specifications about the precise tooth lost in life and its laterality. Considering the posterity of the tooth is also important for possible plasticity and remodelling effects. It is worth noting that only the 3D models were observed on two different occasions.

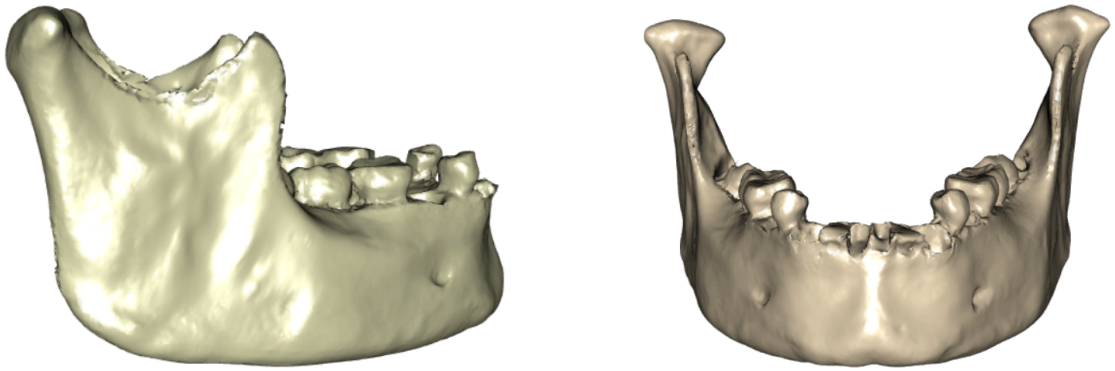

Fig 2.1. Pataud AP/58-2-37807, *Homo sapiens*, female. Regular and straight gonion (R0 / S0). On the right, lateral view, frontal view on the left. Gonion is not visible on the frontal view (0).

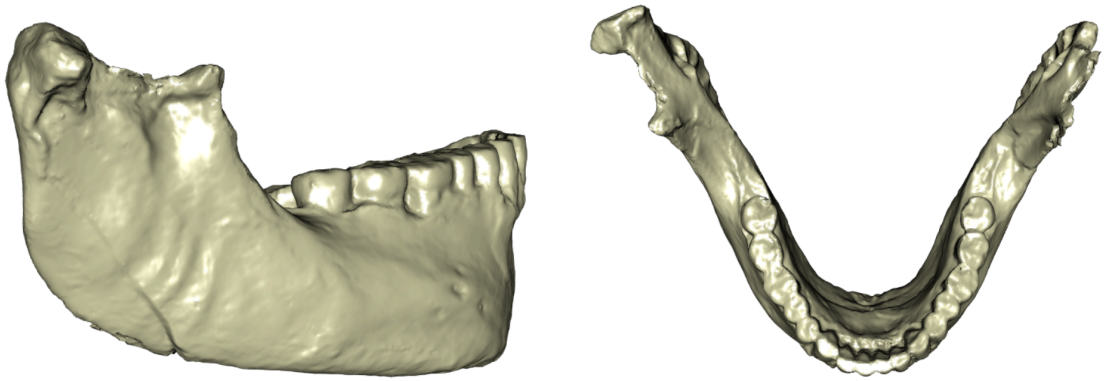

Fig. 2.2. Kebara, *Homo neanderthalensis*, indeterminate sex. Regular gonion with pronounced inversion (R0 / I3). Lateral view on the left and occlusal view on the right. Gonion inversion is visible on the occlusal view (1).

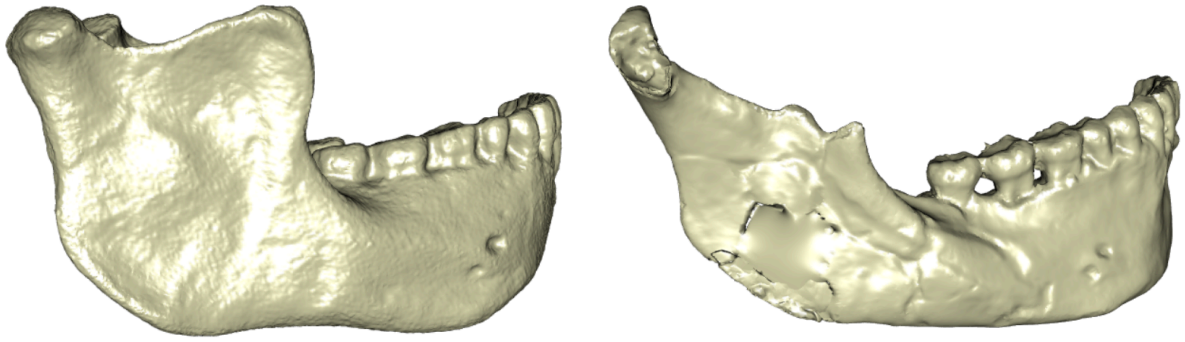

Fig 2.3. On the left, Mauer mandible, *Homo heidelbergensis*, indeterminate sex. Gonion truncation is pronounced and orientation straight (T3 / S0). On the right, Saint Césaire *Homo neanderthalensis*, male, pronounced truncation and straight gonion.

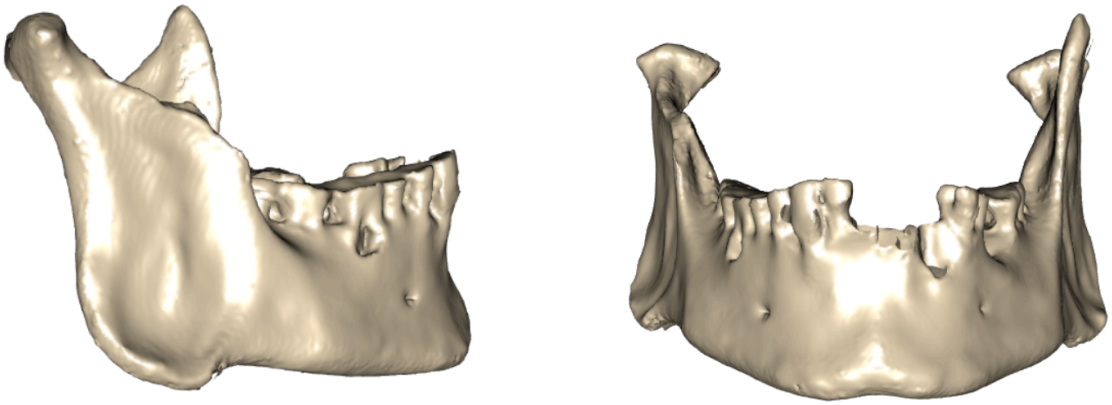

Fig 2.4. Mechta-Châteaudun, *Homo sapiens*, male. Gonion with pronounced expansion and eversion (E3 / E3). Lateral view on the right and frontal view on the left. Gonion extroversion is visible on the frontal view (1).

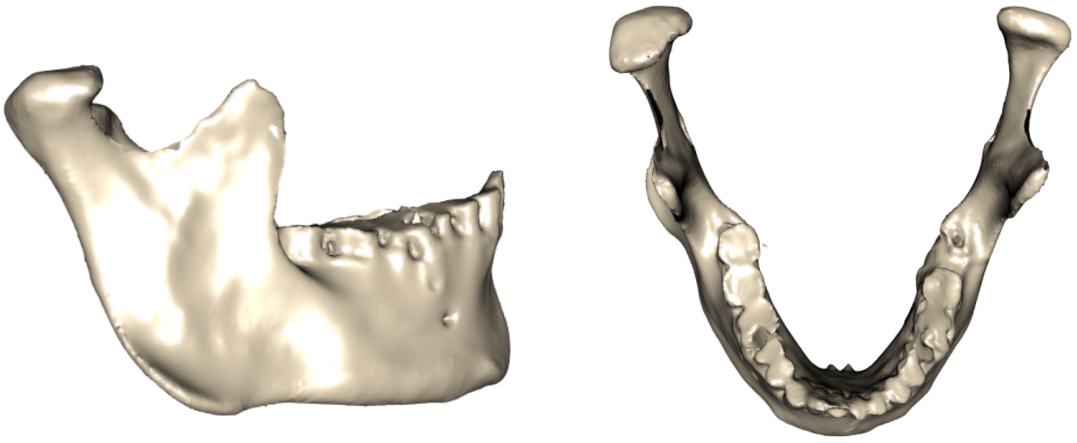

Fig 2.5. Taforalt XVIII, *Homo sapiens*, female individual from Iberomaurusian population. Gonion is regular and pronouncedly everted (R0 / E3). Lateral view on the right and occlusal view on the left. Gonion extroversion is visible on the occlusal view (1).

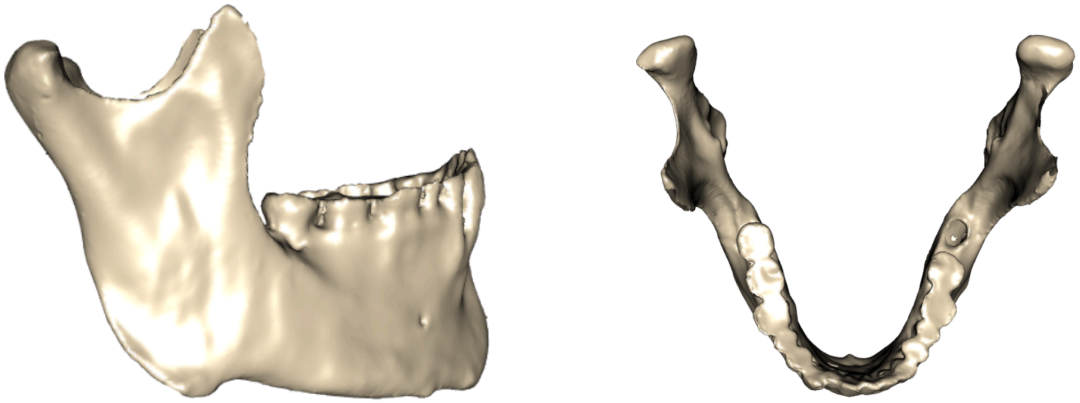

Fig 2.6. Afalou 47, specimen is *Homo sapiens* of indeterminate sex and Iberomaurusian population. Gonion is moderately expanded and straight (E2 / S0). Lateral view on the left, occlusal view on the right. Gonion is visible on the occlusal view (1), but follows a more straight profile.

b. Curve creation with 3D slicer

Data collection was done with the intention to comprehend the gonion morphology and expression from the mandible outline, to be analysed though landmarks based geometric morphometrics and Elliptic Fourier analysis. It was thus necessary to gather the points forming the shape of a hemi-mandible, in this case the right side was chosen.

The curves were created on 3D slicer (Fedorov et al, 2012), a software for image computing that works on 3D surface models, in this study uploaded in .ply format. In this platform, the function "curve" allows for the insertion of a string of landmarks, according to the model's shape (Fig. 2.7). The outline of the mandible was followed in lateral view for landmark placement, considering as anchors points the condylion superior, the gonion and the gnathion, as defined in table 2.6, besides semi-landmarks.

Landmark	Definition
Condylion Superior	The most superior point on the mandibular condyle
Gonion	Angle on the posteroinferior corner of the mandible, between the ascending ramus and the body
Gnathion	The most inferior midline point on the mandible

Table 2.6. Definition of reference landmarks after White et al. (2011).

After drawing the curve and adjusting its shape to the bone's conformity, a "resample" was made, in order to standardize the number of landmarks equidistantly placed on each specimen. Therefore, each mandible was analyzed from these 70 points, with x, y and z

coordinates. This data was then exported in .fcsv format, ideal for the planned analysis in R language.

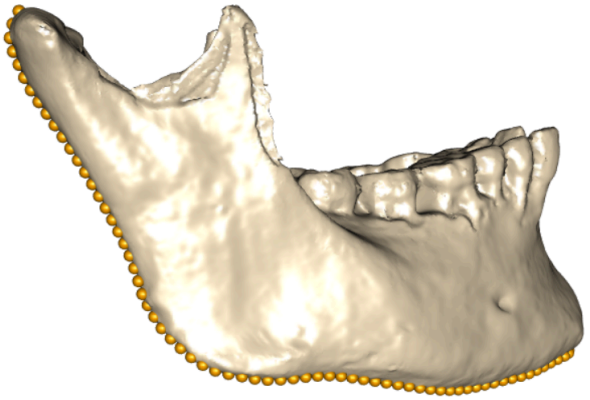

Fig. 2.7. Mandible MNHN 20752 and its outline curve. 70 semi-landmarks are equally spaced. *Homo sapiens* individual, female, MNHN collections.

For a correct comparison between the different specimens the curves must be homologous, which means the landmarks must be placed on the same side, referring to the same structures. The right side was chosen in this study, when it was fragmented or missing, mirroring techniques were applied to the left side. In 3D slicer, on surface tools, there is the possibility of mirroring a model in the x axis, which enables the landmarks to be placed as if it were on the right side. As a result, the mandible is incorporated in the comparison.

c. General Procrustes and Principal Component analysis with R

In morphometric data analysis it is important to approach scale, size and orientation differences among specimens, before applying statistical and mathematical procedures, to ensure the variation observed truly refers to morphological differences rather than artifacts of position or size. The Procrustes superimposition (Fig. 2.8) offers an effective method for fitting and scaling multiple landmark configurations onto a common reference (Claude, 2008), while still maintaining their geometric properties. The procedure begins with translation, aligning all configurations by their centroids. In the second step, the shapes are scaled to standardize size across specimens. Finally, rotation is applied to minimize the distance between corresponding landmarks, thereby bringing homologous structures into closer alignment (Claude, 2008; Arnaud, 2021). After it is done, multivariate analysis can be performed.

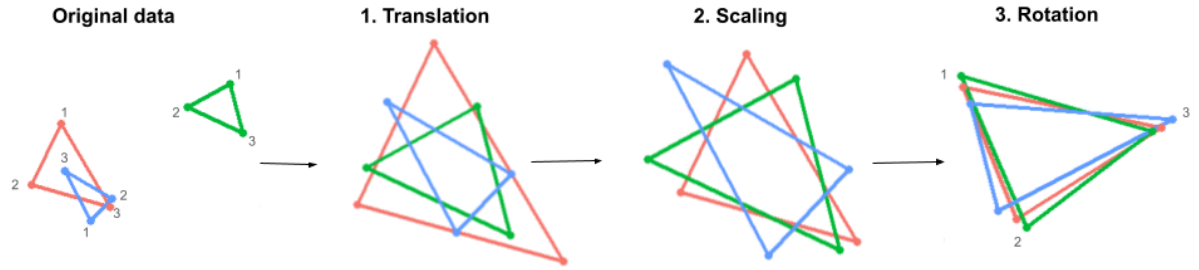

Fig 2.8. Schematic representation of Procrustes superimposition method. Three phases are presented: the translation into the centroid; the scaling into a standard, comparable size; the rotation to approximate homologous landmarks, minimizing their distance. After Arnaud (2021) and Claude (2008).

Principal Component Analysis is one of the possible statistical methods, in which the maximum of variation and covariation is reflected through the main axis. Essential to this process is the transformation of the coordinate system, through the manipulation of data matrices. More precisely, the data that was before organized in different observations is then correlated into the main axis of variance (principal components), in which the individual observations can be plotted. This method is effective because it reduces the variable dimensions and offers an understanding of which ones are more influential in each component.

Looking at it more thoroughly, each principal component is actually formed by a linear combination of the original variables, which are multiplied by their weight. These weights are calculated through a series of operations that target a maximum variance. Thus, the variables with great input in the axis are also multiplied by higher coefficients (Claude, 2008). According to the function, the value of the first principal component for the individual n is defined as:

$$PC1_{(n)} = u_{n1}x_1 + u_{n2}x_2 + \ldots + u_{nj}x_j$$

In which x_j is the observed value for the variable j, and u_{nj} is the coefficient (or loading) for variable j in individual n. In a morphometric study, each variable j corresponds to a landmark coordinate in three-dimensional space. In this case, the dataset includes 70 landmarks, each with x, y and z coordinates, resulting in a total of 210 observed values (x_j) per individual. The coefficients u_{nj} reflect the weight, or loading, of each variable and serve as one of the correlated factors used to analyze shape variability.

The direction of principal components variability is expressed by eigenvectors, which are always in an orthogonal position in relation to each other, meaning the PCs are always

uncorrelated. Eigenvectors and eigenvalues result from the same eigen decomposition: while eigenvectors represent the directions of maximum variability in the data space, eigenvalues quantify the amount of variance captured along those directions. Loadings, derived by scaling eigenvectors by the square root of their corresponding eigenvalues, indicate how strongly each original variable contributes to a principal component (Claude, 2008).

When working with morphometrics, Principal Component Analysis is an essential tool to identify and explain group definitions, since the method tends to maximize intergroup variance and minimize intra-group (Arnaud, 2021). In practical terms, the procrustes superimposition was first executed with the *procSym* function, from Morpho package (Schlager, 2017) in the R software (R Core Team, 2024). One of the returns from this function is the PC scores for the specimens set, which can therefore be plotted.

d. Elliptic Fourier analysis with R

Elliptic Fourier Analysis (EFA) is a mathematical method that was originally created by Kuhl and Giardina (1982) for aircraft identification, but was later applied to the study of complex biological forms. This adaptation of the convention Fourier function allows it to work independently of a coordinate system and to study shapes that curve over themselves. Therefore, it is a suitable method to identify variation in anatomical structures, such as the contour of the mandible in this case.

Substantially, EFA can represent and reconstruct outlines by the superimposition of harmonical ellipses which increase accuracy of the figure as they are added. Every harmonic is defined by four coefficients (a_n, b_n, c_n and d_n), which in turn define the x and y positions, capturing the harmonic contribution in both directions. As a parametric function, x and y in EFA are both in function of a third variable (t), which is a curvilinear abscissa (Easton, 2000; Lestrel, 1989). The x and y positions of the n-esimal harmonic/ellipse is defined as:

$$x(t) = A_0 + \sum_{n=1}^{k} a_n \cos(nt) + \sum_{n=1}^{k} b_n \sin(nt)$$

$$y(t) = C_0 + \sum_{n=1}^{k} c_n \cos(nt) + \sum_{n=1}^{k} d_n \sin(nt)$$

Where k is the maximum number attained. According to the Nyquist theorem, the maximum number of harmonics can only be equal to half the points in the outline, since the

higher harmonics represent details and there would be overfitting over that number. Therefore, $k = n/2$ or $k = (n-1)/2$, for an odd number of points (Easton, 200).

Looking at the equations, it is yet important to consider the coefficients, since this is the data analyzed to understand the variability. For each harmonic the four coefficients are compared, so if we were working with ten harmonics, there would be forty coefficients involved, plus A_0 and C_0. They are discrete estimators (Kuhl and Giardina, 1982) defined as:

$$a_n = \frac{1}{n^2\pi} \sum_{p=1}^{q} \frac{\Delta x_p}{\Delta t_p} [\cos(nt_p) - \cos(nt_{p-1})]$$

$$b_n = \frac{1}{n^2\pi} \sum_{p=1}^{q} \frac{\Delta x_p}{\Delta t_p} [\sin(nt_p) - \sin(nt_{p-1})]$$

in which q is the total of points, tp the distance between point p and $p+1$, and xp is the projection of the segment on the x axis. Coefficient a_n involves the cosine, whereas b_n the sine. The same applies respectively to coefficients c_n and d_n, except that it uses yp for the y axis projection, instead of the xp.

$$c_n = \frac{1}{n^2\pi} \sum_{p=1}^{q} \frac{\Delta y_p}{\Delta t_p} [\cos(nt_p) - \cos(nt_{p-1})]$$

$$d_n = \frac{1}{n^2\pi} \sum_{p=1}^{q} \frac{\Delta y_p}{\Delta t_p} [\sin(nt_p) - \sin(nt_{p-1})]$$

A_0 and C_0 are constant and refer to the centroid of the shape. A normalization process is required so that the different outlines analyzed are actually comparable and the coefficients reflect such correlation. They are dependent on the following factors: outline orientation, position of the starting point and outline size (Claude, 2008). Normalizing according to the centroid allows for a neutral point to be used, since it is invariant with rotation. Size is another factor to be considered because substantial differences may overwhelm shape variation (Easton, 2000). When working with landmarks, a possibility is to normalize using the Procrustes superimposition method.

An important part of the EFA is to understand the input of the different harmonics. Some characteristics of the ellipses can be used for such purposes: amplitude indicates the ellipse range in x and y directions, and power, measured by the square of the amplitude, provides a numerical comparison of which harmonics carry the most information. For better visualization, a reconstruction of the process can be done, showing the effect of adding each harmonic in the draw shape, compared to the original outline (Fig. 2.9).

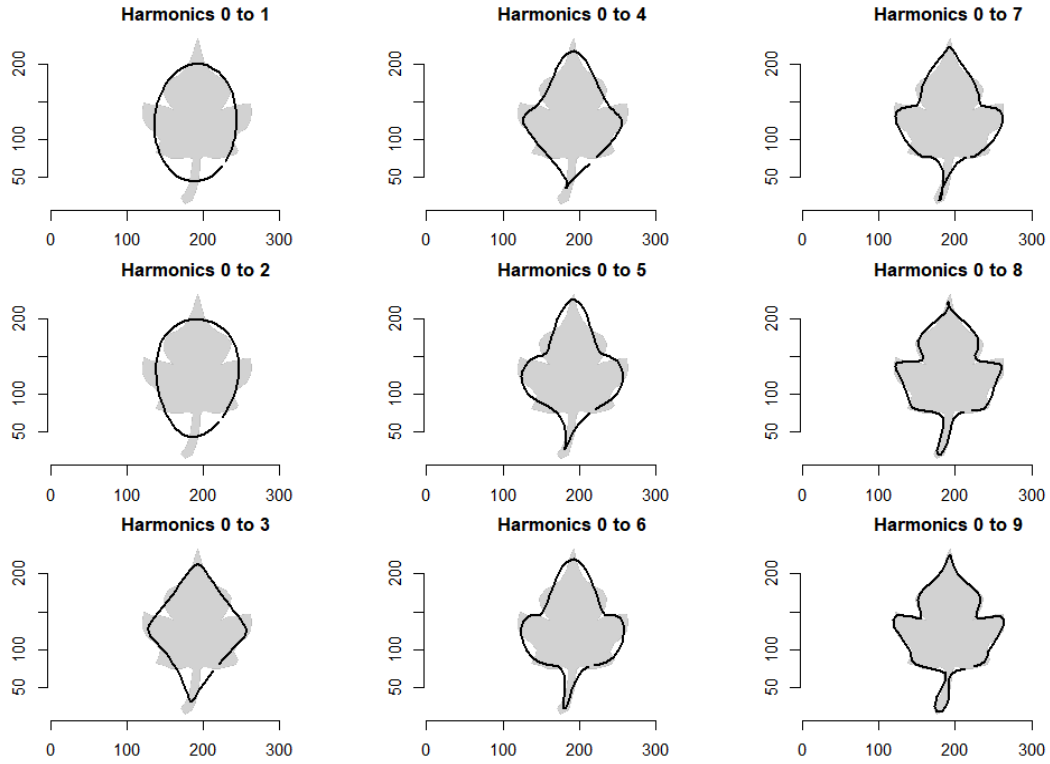

Fig 2.9. Outline when adding harmonics 1 to 9. Leaf shape from Momocs R package shapes dataset.

In general, the first harmonics tend to be the biggest contributors to the general structure, while the others are mostly responsible for finer details in the shape. For an analysis of the mandibular symphysis, Arnaud (2021) uses the first 9 harmonics, since their sum comprises 99% of cumulative power (Claude, 2008; Lestrel, 1989). On the other hand, in Easton (2000) methodological study, 20 harmonics were taken into account for the outline of complete mandibles. This choice was based on the residual values, since they decrease as more harmonics are added, indicating the fitness of the outline. The author considered a residual value between 0.3 - 0.2mm, which was obtained by the 20th harmonic.

In this study, the Procrustes method is used for the normalization of the mandible outlines, described by seventy landmarks, as previously pointed-out. As such, the maximum number of harmonics (k) is thirty-five, equating half the landmarks. Data treatment and

analysis were run on the R software (R Core Team, 2024), using the Momocs library package (Bonhomme et al, 2014), especially the functions *dfourier*, *mshapes* and *stack*. The nine first harmonics were considered, applying *PCA* and *plot_PCA* functions.

Chapter III: Morphological Investigation

This chapter briefly presents the results of the gonion classification regarding its shape and orientation. The relation between both categories is considered, as well as their distribution between the species and population groups. The results improve the comprehension of morphological variability, aligned with previous studies (Rosas, 2001; Mounier, 2009; Bergmann et al, 2021) and confirming the gonion as a distinguishing feature to be considered. *H. neanderthalensis* (HN) and Middle Pleistocene *Homo* (MP) are recognizable for the higher frequency of gonion truncation and/or inversion. On the other hand, *H. sapiens* populations may present varying amounts of everted and expanded gonions.

3.1 General distribution of gonion shape and orientation

For a more detailed understanding of gonion angle variability, a correlation between shape and orientation is proposed in table 3.1, where the categories for orientation (everted, inverted and straight) are disposed according to the shape (expanded, regular or truncated). It is worth noting that there is a great difference in sample size for each species, therefore, the morphological prevalences should be taken into account considering the distribution per species/group. It is, however, interesting to note the displayed associations between gonion orientation and shape.

Gonion orientation	*Gonion shape*			**Total**
	Expanded	Regular	Truncated	
Everted	16	39	3	**58**
Inverted	0	5	6	**11**
Straight	7	79	10	**96**
Total	**23**	**123**	**19**	**165**

Table 3.1. Morphological distribution of gonion shape per gonion orientation.

In terms of gonion orientation, the sample is distributed as *straight* (58.18%), a large portion is *everted* (35.15%) and only a little part is *inverted* (6.67%). Most of these mandibles have a gonion shape classified as a *regular* - 123 out of 165, representing 74.55% of the total. Of those, 79 also display a straight orientation (47.88% of the total), but a significant part is regular and everted - 39 specimens, representing 23.64% of total sample.

For the *expanded* shape (13.94%), the majority is also everted (16 out of 23), but a considerable portion is also straight (7 out of 23). There are no observed cases of an expanded gonion shape with an inverted gonion orientation. For the *truncated* gonions

(11.52%), the majority also has a straight profile (10 out of 19), but there is considerable *inversion* (6 out of 19) and few cases of eversion even (3 out 19).

To a more in-depth understanding of gonion morphological variability, the degree of expression of features can be correlated with their counterpart category. For instance, the frequency of each eversion level (gonion orientation) by the gonion shape categories. Likewise, the levels of a shape feature can be analyzed by their distribution in gonion orientation categories.

a. The level of gonion eversion according to gonion shape

Out of the 165 mandibles, 58 have an everted gonion, representing 35.15% of the sample. Nonetheless, there are differences in the degree of the outward flip of the mandible. In some cases the flip is very pronounced and can be observed from a frontal or occlusal view; in others, it is very subtle and may only be visible from a posterior view. Therefore, this level of eversion may be differentiated and taken into account when analysing the distribution for shape. The table 3.2 presents frequency for each eversion level according to expanded, regular or truncated shape.

Eversion level	*Gonion shape*			**Total**
	Expanded	Regular	Truncated	
1	6	30	0	**36**
2	6	5	3	**14**
3	4	4	0	**8**
Total	**16**	**39**	**3**	**58**

Table 3.2. Eversion level according to the gonion shape. (1) is subtle; (2) moderate; (3) pronounced eversion.

Even though a great part of regularly shaped gonions are also everted, more often than not this eversion is present to a mild degree. Of the 39 regular and everted gonions, 30 are everted on a subtle level (1), which is equal to 76.92% of the regular and everted gonions.

On the other hand, for the less numbered expanded and everted gonions (16), the distribution among the levels is more balanced. The eversion in only 37.5% is subtle (1), in 37.5% it is moderate (2) and, in the last 25% it is pronounced (3). Therefore, regular gonions, when everted, tend to exhibit it in a lesser degree of expression. In contrast, expanded gonions are better distributed into the three levels of eversion, and are proportionally more likely to have a pronounced eversion.

Only three cases of truncated and everted gonion were observed and they all exhibit moderate eversion, which does not allow particular conclusions. We may also observe the distribution of eversion levels per species or group.

Eversion level	*Species*		**Total**
	HS	IB	
1	25	11	**36**
2	7	7	**14**
3	2	6	**8**
Total	**34**	**24**	**58**

Table 3.3. Eversion level distributed per (HS) is *H. sapiens* and (IB) Iberomaurusian *H. sapiens* population. (1) is subtle; (2) moderate; (3) pronounced eversion.

The gonial eversion is only observed in modern humans, as evidenced in table 3.3. This morphology is only observed in the recent *H. sapiens* group and the Iberomaursian population, an Upper Paleolithic North-African *H. sapiens* group. However, Iberomaurusians differ proportionally from other *H. sapiens* for the higher level of gonial eversion presented. In total, the sample has 107 *H. sapiens* and 36 Iberomaursians.

Of the first group, 31.78% has an everted gonion (34 out of 107), but of these eversions 73.5% are subtle (25 out of 34). On the other hand, for the last group, most have an everted gonion (24 out of 36), representing ⅔ of the group, or 66.67%. The majority of these Iberomaurusian eversions are still subtle (45.83%), but their frequency increases for moderate (29.17%) and pronounced eversion (25%), in relation to the other *H. sapiens* samples. Thus, the results indicate that the Iberomaurusian gonial morphology may be present in other *H. sapiens* populations, but they differ by both the frequency and level of gonial eversion.

b. The level of gonion truncation according to species or group

The table 3.4 shows the levels of truncation for the 19 specimens with this gonion shape and their associated orientations. From the total truncated sample, 11 specimens exhibit a subtle truncated gonion (57.89%), 5 moderate (26.32%) and 3 pronounced (15.79%).

Truncation level	*Gonion orientation*			**Total**
	Everted	Inverted	Straight	
1	3	3	5	**11**
2		3	2	**5**
3			3	**3**
Total	**3**	**6**	**10**	**19**

Table 3.4 Truncation level according to gonion orientation (1) is subtle; (2) moderate; (3) pronounced eversion.

The truncated and straight gonions represent 52.63% of the sample (10 out of 19), of which 5 have a subtle truncation, 2 moderate and 3 pronounced. It is important to note that these are the only 3 pronounced truncated gonions in the whole sample and they all have a straight orientation. The inverted gonions are equally distributed between a subtle and moderate truncation, without any pronounced expression. For the only 3 everted and truncated gonions, the truncation is subtle.

Moreover, the feature levels can be considered according to their distribution by the species and groups analysed, according to table 3.5.

Truncation level	HN	MP	HS	IB	UP
1	3	2	4	2	
2	3			1	1
3	1	2			
Total	**7**	**4**	**4**	**3**	**1**

Table 3.5. Truncation level according to species and group. The truncated shape is (1) subtle; (2) moderate; (3) pronounced. (HN) is *H. neanderthalensis*; (MP) Middle Pleistocene *Homo*; (HS) *H. sapiens*; (IB) Iberomaurusian *H. sapiens* population; (UP) Upper Paleolithic *H. sapiens.*

Most of the truncated gonions are *H. neanderthalensis* (7 out of 19) and are distributed by all levels of truncation. Out of the 12 Neanderthals in the sample, the truncation is present in 7 of them, or 58.33% of the Neanderthal sample. These are equally distributed between subtle and moderate levels and only one individual has a pronounced truncation. Middle Pleistocene *Homo* is the only other group that shows a pronounced level of truncation, with 2 out 6 MP individuals having a pronounced truncated gonion morphology. The other 2 have subtle gonion truncation.

All the *H. sapiens* groups, although registering a few truncated gonions, are mostly at the subtle expression level. Only one Iberomaurusian and one Upper Paleolithic *H. sapiens* have a moderate truncated gonion. This indicates that, although *H. sapiens* may have a truncated gonion, it is unlikely to be as pronounced as the truncation exhibited by *H. neanderthalensis* and Middle Pleistocene *Homo*.

3.2 Gonion shape and orientation per species/group

For a general overview, table 3.6 presents the total sample distributed by gonion shape, gonion orientation and species, or *H. sapiens* population.

Gonion shape	*Gonion orientation*	HN	HS	IB	MP	UP	**Total**
Expanded	Everted		9	7			16
	Straight		3	4			7
Total Expanded			12	11			23
Regular	Everted		24	15			39
	Inverted	3			2		5
	Straight	2	67	7		3	79
Total Regular		5	91	22	2	3	123
Truncated	Everted		1	2			3
	Inverted	4			1	1	6
	Straight	3	3	1	3		10
Total Truncated		7	4	3	4	1	19
Total		**12**	**107**	**36**	**6**	**4**	**165**

Table 3.6. Morphological distribution of gonion shape and gonion orientation per species/ group. (HN) is *H. neanderthalensis*; (MP) Middle Pleistocene *Homo*; (HS) *H. sapiens*; (IB) Iberomaurusian *H. sapiens* population; (UP) Upper Paleolithic *H. sapiens.*

a. *Homo neanderthalensis* and Middle Pleistocene *Homo* compared:

For the two groups, there is no expanded gonion shape, nor everted gonion orientation, as observed in table 3.6. In terms of shape, they all vary between *truncated* and *regular*, associated with *inverted* or *straight* orientation.

For the 6 Middle Pleistocene *Homo* in the sample, 4 have a truncated gonion shape, with an inverted orientation for Arago 13 and straight for Mauer, Tighenif 3 and AT-888. Arago 2 and Montmaurin have a gonial shape that is not truncated, but regular, and the orientation is inverted for both. It is worth noting that the most frequent morphology in the sample, a regular and straight gonion, is absent for Middle Pleistocene Hominins. All specimens from this group have gonion truncation or inversion.

The 12 *H. neanderthalensis* are well distributed in the combination of these shape and orientation categories. For the truncated shape, 4 Neanderthals have a truncated and inverted gonion, 3 truncated and straight. For a regular curved gonion, 3 are regular and inverted, and the last 2 regular and straight. Eventhough the majority of Neanderthals have truncated and inverted gonions (⅓ of the sample), the difference in absolute numbers is small. There is no prevalent morphology for the *H. neanderthalensis* gonion, but there is a tendency for the truncation or inversion features, since at least one of them is observed in 10 out of the 12 specimens. This association is similar to the one highlighted for the MP *Homo* group.

When studying the gonion variation according to sex, a key point is the distribution for Middle Pleistocene *Homo*, shown in table 3.7. Although only 6 specimens from this group were included in the sample, they show a coherent distribution. The 2 male and the 2

indeterminate sex individuals all have a truncated gonion, while the 2 females have the only regular gonions in the group, also inverted. For Neanderthals, it is not possible to analyse sex differences due to the absence of females in the group sample. Still, we point out that 6 of 9 males have truncated gonions and only 3 regular. They are fairly distributed between inverted and straight orientations.

Gonion shape	*Gonion orientation*	HN		MP		
		Indeterminate	Male	Female	Indeterminate	Male
Regular	Inverted	2	1	2		
	Straight		2			
Truncated	Inverted	1	3			1
	Straight		3		2	1
Total		**3**	**9**	**2**	**2**	**2**

Table 3.7. Gonion distribution for (HN) *H. neanderthalensis* and (MP) Middle Pleistocene *Homo* by sex.

b. *Homo neanderthalensis* and *Homo sapiens* compared

The two groups exhibit a different pattern for gonion morphology, although there may be some overlap between them. For *H. sapiens*, 91 out of 107 individuals have a regularly curved gonion, representing 85% of the group. Out of those, 67 have a regular and straight gonion, in terms of orientation. This classification corresponds to 62.62% of the *H. sapiens* group, indicating that it is the prevalent morphological configuration.

The other possible morphologies displayed are infimal. In regards to the other shape categories, there are only 12 expanded gonions (11.21%) and 4 truncated (3.74%). In terms of gonion orientation, for all the 107 *H. sapiens*, 73 have a straight gonion (68.22%), 34 an everted one (31.78%) and there are no inversions. Thus, for this species, gonions are usually regular, and often straight, but for a considerable portion they may be everted.

For *H. neanderthalensis* the morphological variation observed is quite different. In the 12 individuals, no gonion expansion or eversion is observed and only 2 exhibit a regular and straight curve, the typical *H. sapiens* morphology. The Neanderthal morphology is fairly distributed between truncated and regular shapes, inverted and straight orientation. From the observed sample, there is no clear correlation between shape and orientation. In total, 7 Neanderthals have a truncated gonion, 5 regular; regarding the orientation, 7 are inverted, 5 straight. 10 out of the 12 exhibit at least truncation or inversion, features that clearly distinguish Neanderthals and *H. sapiens*, since the first trait is hardly ever present and the second is absent.

c. *Homo sapiens* intra-specific variability: populations compared.

i. Recent *H. sapiens* sample

The *H. sapiens* group is the largest in the whole sample, composed of 107 specimens out of the 165. According to table 3.6, 91 of these individuals have a regularly curved mandibular gonion (85.05% of the group), 67 of which are also straight in terms of orientation. Thus, a regular and straight gonion is prevalent for the species recent group, representing 62.62% of the observed cases.

Nevertheless, everted gonions compose still a crucial portion of the group, since they are present in 31.78% of individuals (34 out of 107), associated with all possible shapes - expanded, regular or truncated. It is noteworthy that most of these eversions continue to be associated with the regular shape, the regular everted gonion representing 22.43% of the group sample (24 out of 107).

Only 12 individuals have an expanded shape (11.20% of the sample), 9 are everted and 3 straight. The truncated gonions are even less present, with only 4 individuals (3.83% of group), 3 truncated and straight, 1 truncated and everted.

Gonion shape	*Gonion orientation*	HS		
		F	I	M
Expanded	Everted		7	2
	Straight		2	1
Total Expanded			9	3
Regular	Everted	2	15	7
	Straight	14	40	13
Total Regular		16	55	20
Truncated	Everted		1	
	Straight		3	
Total Truncated			4	
Total		**16**	**68**	**23**

Table 3.8. Gonion morphology distribution for (HS) *H. sapiens* by sex.

When considering the *H. sapiens* distribution per sex (table 3.8), 63.55% of the group's specimens are indeterminate sex (68 individuals), spread among all possible morphological configurations. However, 80.88% have a regular shaped gonion (55 out of the 68), and 58.82% it is regular shaped and straight oriented (40 out of 68), reinforcing the prevalent *H. sapiens* morphology. Males follow a similar distribution pattern, with 86.95% of their gonions regularly shaped (20 out of 23) and 56.52% regular and straight (13 out of 23).

For females, 100% have regular shaped gonions, 87.50% have regular and straight gonions (14 out of 16).

ii. The Upper Pleistocene *H. sapiens* compared to recent *H. sapiens*

The 4 individuals of this group do not exhibit expansion or eversion of the gonion. Out of them, 3 have the prevalent *H. sapiens* morphology - a gonion with a regular curve and straight. Only 1 of them varies in the classification, however, in a combination of gonion characters more typical to *H. neanderthalensis* or Middle Pleistocene *Homo*. The Skhul 5 mandible has a truncated gonion. Although large in area, there is the formation of a third arista between the ramus posterior margin and the basal border. On the posterior view, it is possible to notice a slight inversion.

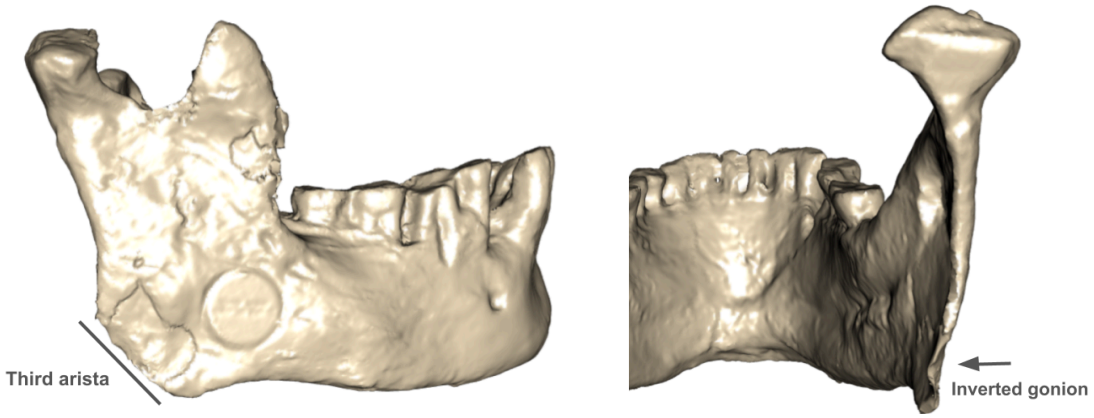

Fig. 3.1. Skhul V, Upper Pleistocene male *Homo sapiens*, moderate truncation and subtle inverted gonion.

It is worth noting that the morphological configuration displayed by Skhul V (Fig. 3.1) is very different from that observed in the Holocene *H. sapiens* sample. In the 107 individuals, no cases of inversion were observed and there were only 4 truncated gonions, representing 3.74% of the group. Accordingly, it is stunning that out of the 4 Upper Paleolithic *H. sapiens*, one exhibits this very particular morphology for the species.

iii. Iberomaurusian population

For both the *H. sapiens* and the Iberomaurusian population, the gonion shape is in most cases regular. However, the expanded gonion is also significant for both groups, and there are just a few cases of a truncated gonion. In terms of orientation, there are two morphologies that can be associated with the shapes described above for the two groups: a straight or eversion, without any observed inversions.

We may compare them by percentages because sample sizes are very different, *H. sapiens* has 107 individuals and Iberomuaurusian 36 (table 3.9). The main difference between the two groups is the proportion of each morphological combination, since for Iberomaurusians the eversion is present to a much more significant degree. Therefore, even if the configuration is the same, the frequency and distribution are not.

Gonion shape	*Gonion orientation*	HS	IB
Expanded	Everted	8.41%	19.44%
	Straight	2.80%	11.11%
Total Expanded		11.21%	30.56%
Regular	Everted	22.43%	41.67%
	Straight	62.62%	19.44%
Total Regular		85.05%	61.11%
Truncated	Everted	0.93%	5.56%
	Straight	2.80%	2.78%
Total Truncated		3.74%	8.33%
Total		**100%**	**100%**

Table 3.9. Percentages of gonion morphology for (HS) *H. sapiens* and (IB) Iberomaurusians.

For the recent *H. sapiens* group, a regular gonion represents 85.05% of its individuals (91 out of 107), whereas for the Iberomaurusian population it is only present at 61.11% of the cases (22 out of 36). Considering the combination of a regular gonion and orientation, 62.62% of *H. sapiens* display a gonion that is both regular and straight (67 out of 107). For the Iberomaurusians, this percentage is significantly lower, down to 19.44% (7 out of 36). Instead, 41.67% of the group (15 out of 36) has eversion combined with the regular shape. For *H. sapiens*, only 22.43% have a regular and everted gonion (24 out of 107).

The expanded shape represents only 11.21% of cases (12 out of 107) for *H. sapiens*, but it is more frequently associated with an eversion (8.41%) than with a straight orientation (2.80%). For Iberomaurusians, the expanded gonion is 30.56% of the group (11 out of 36), 19.44% combined with everted orientation (7 out of 36) and 11.11% straight (4 out of 36).

The truncation is only present in a few cases, for both *H. sapiens* and Iberomaurusians, but it can have straight or everted orientation. One of the examples is the mandible Taforalt XIV (Fig. 3.2), who has a slightly truncated gonion, by the formation of a subtle third arista. This shape is associated with the moderate everted gonion, visible in posterior view.

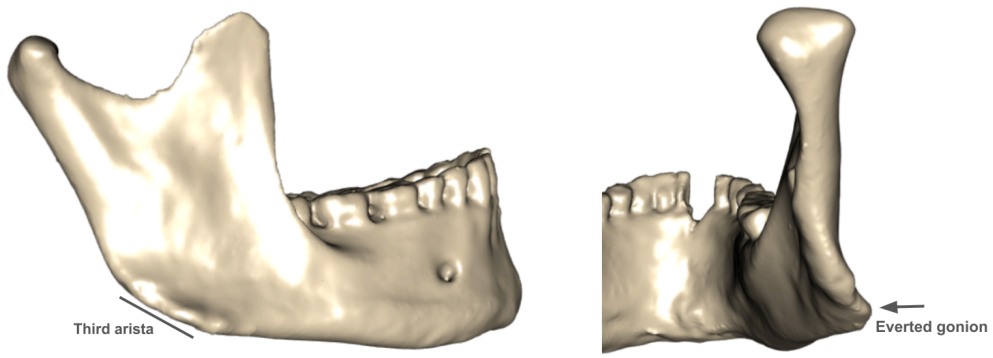

Fig. 3.2. Taforalt XIV, Iberomaurusian male mandible with subtle truncation and everted gonion.

Gonion orientation	HS	IB
Eversion	31.78%	66.67%
Straight	68.22%	33.33%
Total	**100%**	**100%**

Table 3.10. Distribution of gonion orientation for (HS) *H. sapiens* and (IB) Iberomaurusian.

Thus, Iberomaurusians have a particular distribution, when compared to other *Homo sapiens*, mainly in respect to its orientation. When looking at gonion orientation, in table 3.10, there is an proportionally inverse distribution. For Iberomaurusians, an everted gonion represents 66.67% of the cases, and 33.33% are straight oriented. For *H. sapiens*, it is approximately the opposite: 68.22% of the gonions are straight and only 31.78% everted.

Gonion shape	*Gonion orientation*	HS			IB		
		F	I	M	F	I	M
Expanded	Everted		7	2		1	6
	Straight		2	1		1	3
Regular	Everted	2	15	7	8	1	6
	Straight	14	40	13	3	2	2
Truncated	Everted		1			1	1
	Straight		3		1		
Total		**16**	**68**	**23**	**12**	**6**	**18**

Table 3.11. Gonion morphology distribution for (HS) *H. sapiens* and its (IB) Iberomaurusian population by sex.

In terms of variation per sex, it is worth noting that almost all females have a regular shaped gonion, as shown in table 3.11. In fact, the only female with no regular shape is Iberomaurusian Taforalt XVI C1 (Fig. 3.3), who has a moderately truncated gonion. On the contrary, males and indeterminate sex are split between expanded and regular shapes. 86.95% of male *H. sapiens* have regular gonions (20 out of 23), while for Iberomaurusians they are more equally divided between regular and expanded shapes, with 44.44% for the first (8

individuals) and 50% for the second (9 out of 18). Hence, the expanded shape is significantly more frequent for Iberomaurusian males than other *H. sapiens*.

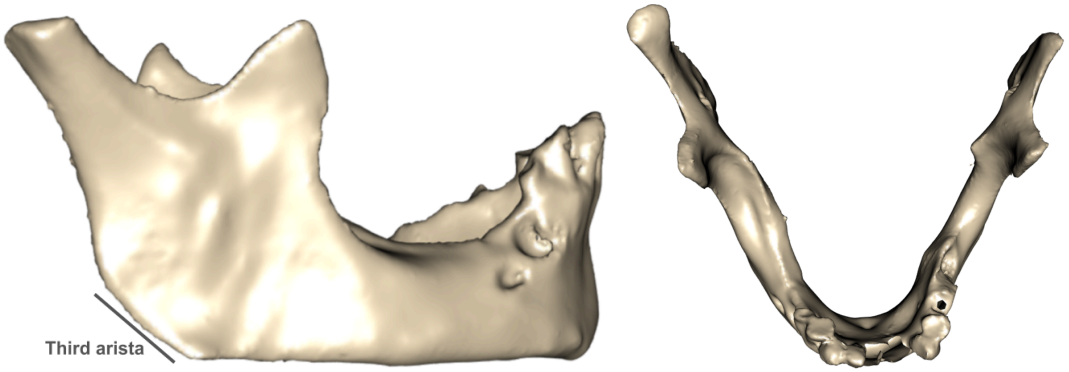

Fig. 3.3 Taforalt XVI C1, Iberomaurusian female, mandible with moderate truncation and straight gonion.

Considering the orientation, according to table 3.12, there are important distinctions in all sex categories. Females present the biggest difference in distribution because, while for *H. sapiens* 87.50% of females have straight gonions (14 out of 16), 66.66% of Iberomaurusians females have some level of eversion (8 out of 12), representing two thirds of the sample.

Gonion orientation	HS			IB		
	F	I	M	F	I	M
Everted	2	23	9	8	3	13
Straight	14	45	14	4	3	5
Total	**16**	**68**	**23**	**12**	**6**	**18**

Table 3.12. Gonion orientation distribution for (HS) *H. sapiens* and (IB) Iberomaurusian by sex.

Likewise, *H. sapiens* male gonions are also mostly straight, but for only 60.87% of them (14 out of 23). The indeterminate sex specimens also follow a similar pattern, with 66.17% of straight gonions (45 out of 68). The eversion is present in 39.13% of *H. sapiens* male (9 out of 23) and 33.83% of indeterminate sex (23 out of 68), a significant portion compared to the females in the same group. Iberomaurusian males also have a greater degree of everted gonions, even if the increase is less significant, 72.22 % of their gonions are everted (13 out of 18) and 27.78% are straight. For the indeterminate sex, the distribution is 50%-50%.

Thus, Iberomaurusians tend to have more everted mandibular gonions than other H. sapiens groups, considering males, females and indeterminate sex individuals. For females, nonetheless, this percentage is remarkably higher, with eversion in 60.87% of Iberomaurusian females against 12.50% of *H. sapiens*.

Chapter IV: Geometric Morphometrics

This chapter introduces the results from the multivariate analysis performed on the hemi-mandibular outline. First, within the geometric morphometrics framework, a Principal Component Analysis (PCA) was conducted on landmarks and semi-landmarks data. Second, an Elliptical Fourier Analysis (EFA) was applied on the curves describing these outlines. The two approaches are described below and their results may be compared.

4.1 Principal Component Analysis on landmarks

The three Principal Components (PCs) were selected for the analysis because together they account for 67.04% of the variability. For each PC, the maximum and minimum outlines were superimposed to comprehend the axis of variability they represent. Then, the PCs were plotted, two at a time, in order to understand the distribution of the groups in them. Last, the PCs boxplots indicate the distribution range per sex in each group, highlighting if there are any remarkable differences inside the groups.

a. Comparing each Principal Component's maximum and minimum outlines.

The morphological nuances of each axis variation are noticeable in the superimposed outlines, for the maximum and minimal variability in the defined PC. This analysis improves the understanding of groups variability when PCs are plotted.

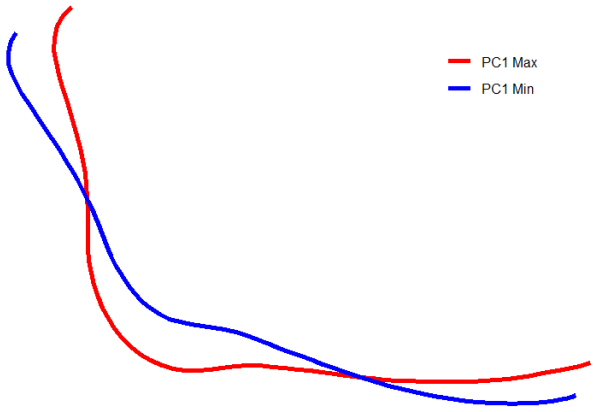

Fig 4.1. PC1 minimal and maximum outlines plotted for comparison.

When comparing PC1 maximal and minimal superimposed outlines (Fig. 4.1), the greatest variation observed is in the opening of the mandibular angle and the ascending ramus position. The minimal PC1 (Fig. 4.1, in blue) is characterized by an obtuse mandibular angle and the posteriorly inclined border of the ascending ramus. In this configuration, the gonion

is reduced in size and the gonial arch is less pronounced, resulting in a less rounded curve. In the opposite direction, the maximal PC1 (Fig. 4.1, in red) is characterized by a mandibular angle closer to 90º, a larger gonion and vertically positioned ascending ramus. A slight incurvation is visible along the posterior border.

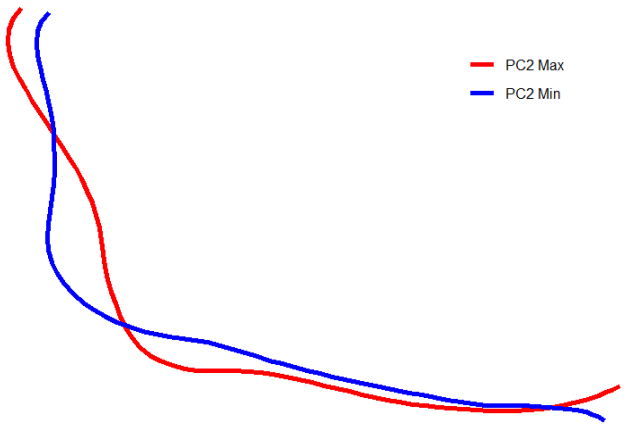

Fig 4.2. PC2 minimal and maximal outlines plotted for comparison.

For PC2, the superimposed minimal and maximal outlines (Fig. 4.2) indicate that the main variation axis concerns the length of the ascending ramus and the gonion shape. The minimal PC2 (Fig. 4.2, in blue) is characterized by a short ascending ramus with a straight posterior border. In this configuration, the gonion is aligned to the posterior border and appears truncated, by a short curvature, relative to the basal border. In contrast, the maximal PC2 (Fig. 4.2, in red) is characterized by regularly curved gonion, anteriorly positioned in relation to the condyle, likely associated with an incurvation along the mid posterior border.

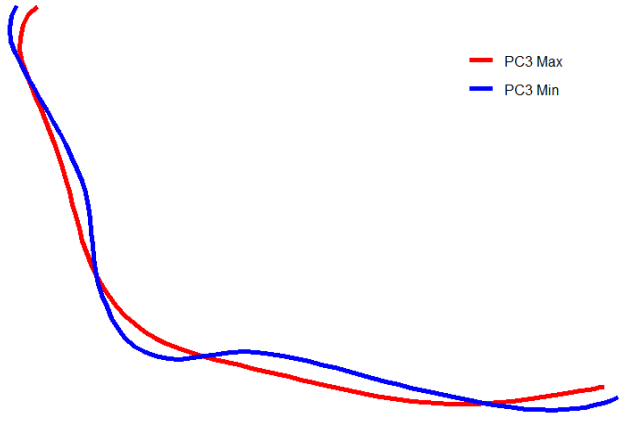

Fig 4.3. PC3 minimal and maximal outlines plotted for comparison.

PC3 maximal and minimal outlines show that the main variation concerns the gonion area and the curvature of the mid posterior border. The minimal PC3 (Fig. 4.3, in blue) is characterized by an expanded, possibly everted gonion, forming an anterior notch at the basal border. In this configuration, the posterior border of the ascending ramus posterior border is also more curved. In contrast, the maximal PC3 (Fig. 4.3, in red) is characterized by a straight ascending ramus and a more regularly curved gonion, without expansion or an anterior gonion notch. In this case, the mandibular arch appears rounder.

	Minimal morphology	***Maximal morphology***
PC1	obtuse gonial angle, posterior border is posteriorly inclined, less pronounced gonial arch	gonial angle closer to 90º, vertical posterior border, larger gonion
PC2	truncated gonion, short and straight ramus, gonion aligned to posterior border	regular gonion, tall and curved ramus, gonion anteriorly positioned
PC3	expanded gonion, curved ramus, anterior gonion arch	regular gonion, straight ramus, rounder mandibular arch

Table 4.1. Summary of minimal and maximal morphologies for each PC.

In summary, the PC1 variation axis is primarily associated with changes in the gonial angle, PC2 with gonion truncation and PC3 with gonion expansion. These variations at the gonion are also associated with the ascending ramus morphological variation: in PC1, the ramus varies in inclination; in PC2, in length; and, in PC3, in incurvation. Further studies are still necessary for a better understanding of these covariations. Table 4.1 provides an overview of minimal and maximal morphological variations for each PC.

b. Analysing plotted Principal Components

Taking into account how the hemi-mandibular outline varies along each variation axis, the species and groups distribution may be analyzed. The distribution of specimens for the three first Principal Components evidences differentiations and overlaps between species and intra-specific groups. Drawn polygons connect extremes for each group, indicated by colors, and symbols refer to sex.

For PC1 (Fig. 4.4 and Fig. 4.7), *H. sapiens* comprises the greatest variability in this axis, with a few specimens in both extremes. Most of its individuals have negative values tending to the minimal PC1, in particular, females for this group are either below zero or approximate to it. The Iberomaurusian population has mostly positive values, towards the PC1 maximal. Out of the thirty-six specimens integrating the group, only four females and two indeterminate sex individuals have PC1 scores smaller than zero, indicating a tendency to positive scores for Iberomaurusians. Upper Pleistocene *H. sapiens,* although very few, are distributed in positive and negative values.

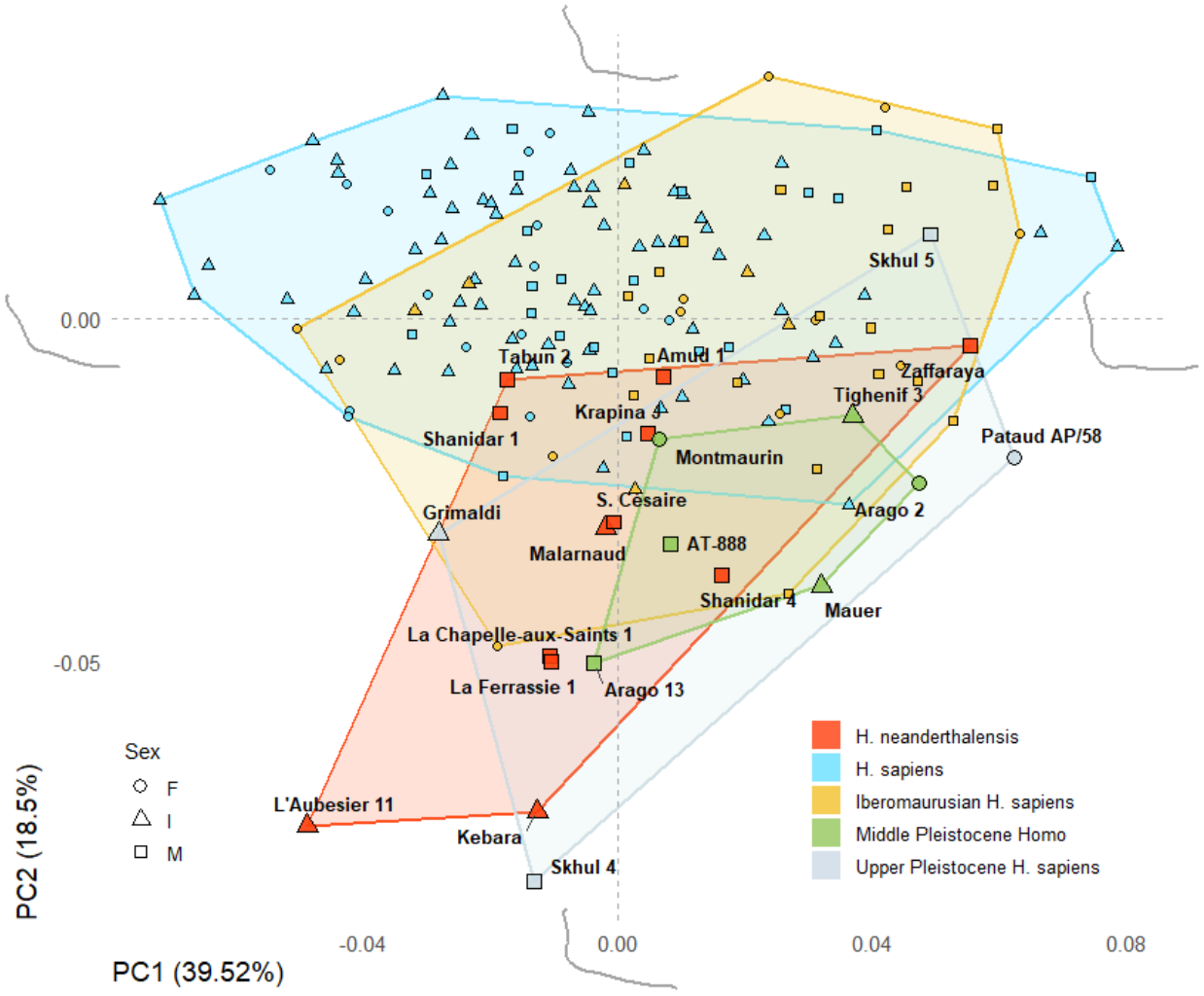

Fig 4.4. PC1 and PC2 plot. Species and population groups are given by colors and sex by symbols. Minimal and maximal outlines are drawn at the axis.

Two-thirds of the *H. neanderthalensis* sample have negative scores for PC1, although most are close to zero and only the L'Aubesier 11 mandible is relatively close to the PC1 minimum. Among the remaining third, Zaffaraya is the most positively positioned

Neanderthal specimen. By contrast, nearly all Middle Pleistocene hominins show positive scores in PC1, only Arago 13 is positioned just below zero. Half of the MP *Homo* sample is close to the *H. neanderthalensis* variability, in particular Arago 13, AT-888 and Montmaurin.

The species show different distributions along the PC2 variation axis (Fig. 4.4 and 4.5). Notably, the negative scores of *H. neanderthalensis* and Middle Pleistocene *Homo* separate them from *H. sapiens*. Lower scoring *H. sapiens* overlap with some Neanderthals (Shanidar 1, Tabun 2, Amud 1, Krapina J and Zaffaraya) and MP hominins (Montmaurin and Tighennif). Nevertheless, the groups show different tendencies: *H. sapiens* range from near zero to the highest positive scores (PC2 maximum), while Neanderthals and Middle Pleistocene *Homo* are consistently negative and clustered toward the PC2 minimum.

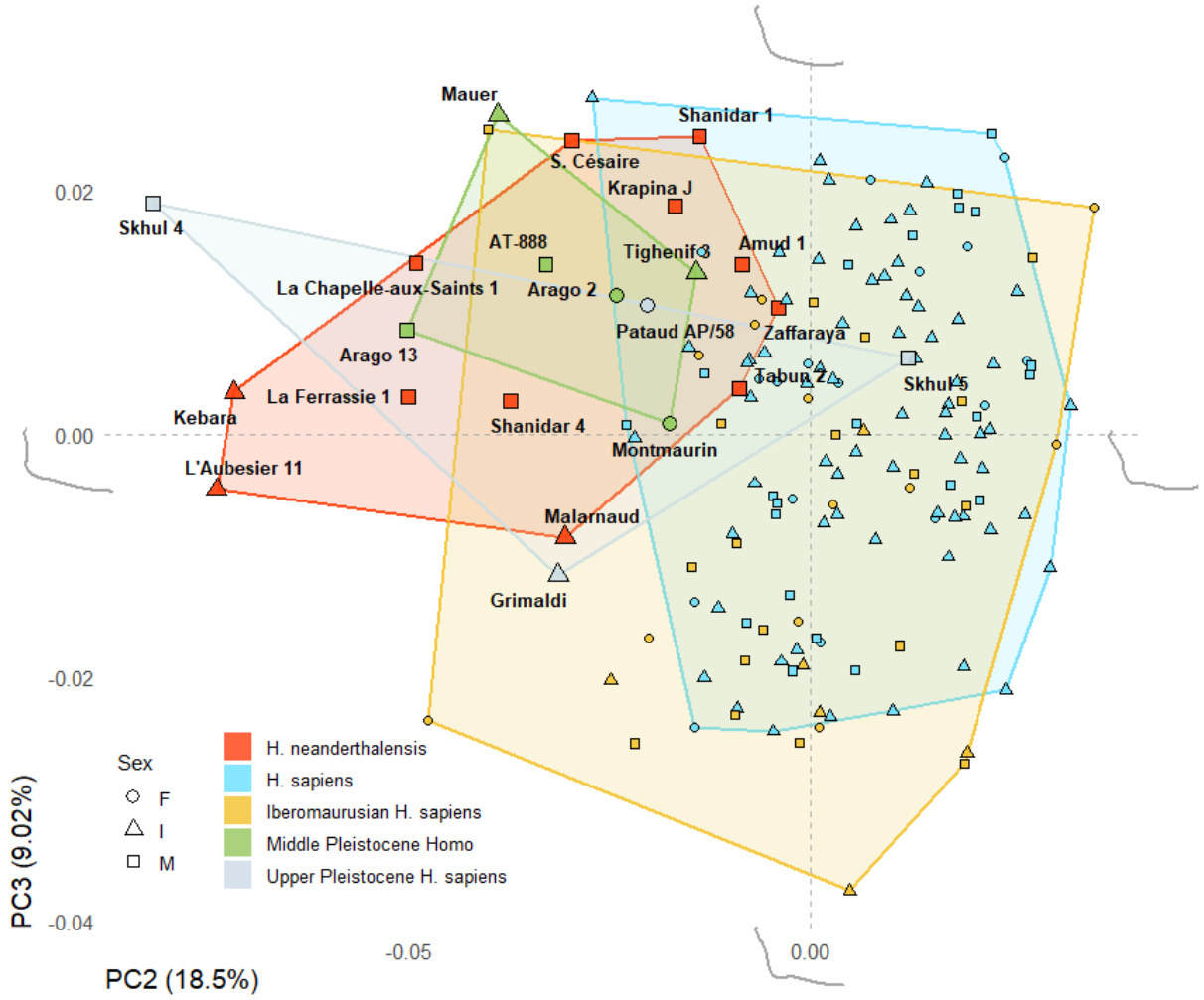

Fig 4.5. PC2 and PC3 plot. Species and population groups are given by colors and sex by symbols. Minimal and maximal outlines are drawn at the axis.

When considering the *H. sapiens* intra-specific variability, the Iberomaurusian population is very similar to the recent *H. sapiens* group, differing only by a slightly greater range for PC2, with a few lower scores. On the other hand, the Upper Pleistocene specimens stand out for their distinct distribution compared to the other modern humans. With the exception of Skhul 5, they all have negative values for PC2, and Skhul 4 (Fig. 4.6) pulls the group towards PC2 minimal, as it represents the lowest score in the axis. Grimaldi and Pataud are in intermediate positions, overlapping with *H. neanderthalensis* and MP *Homo*.

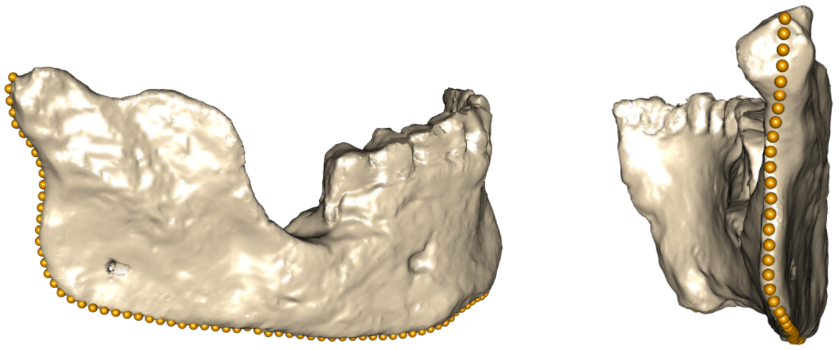

Fig. 4.6. Skhul 4, male. Upper Pleistocene *H. sapiens,* mirrored hemi-mandible with landmark curve.

There is significant overlap on PC3 (Fig. 4.5 and 4.7) between all groups. However, there are important differences to be considered in their distributions. *H. neanderthalensis*, Middle Pleistocene *Homo* and Upper Pleistocene *H. sapien*s are clustered from around zero to the maximal PC3 extreme, with also *H. sapiens* and Iberomaurusian individuals plotted in this direction of variability. The main difference is that both *H. sapiens* and Iberomaurusians extend farther into PC3 negative scores.

When comparing both groups, a substantial part of the Iberomaurusian sample has negative PC3 scores and extends remarkedly towards the minimal PC3. Holocene *H. sapiens* group, however, is more evenly distributed between positive and negative scores and exhibits a narrower range of variability. Therefore, PC3 distinguishes Iberomaurusian from other modern human populations for its consistently lower scores in this axis, likely reflecting gonion expansion and eversion (Fig. 4.8).

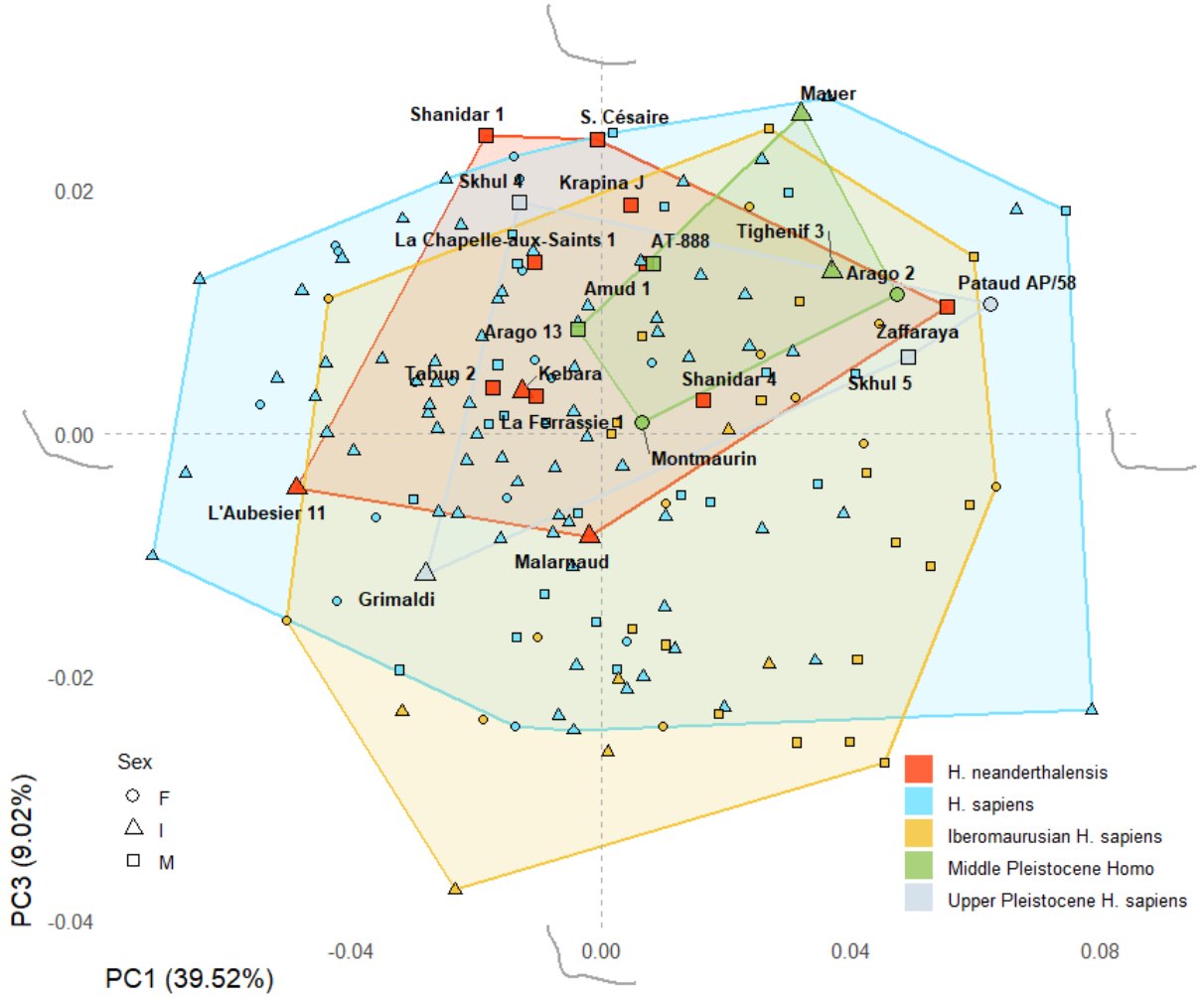

Fig 4.7. PC1 and PC3 plot. Species and population groups are given by colors and sex by symbols. Minimal and maximal outlines are drawn at the axis.

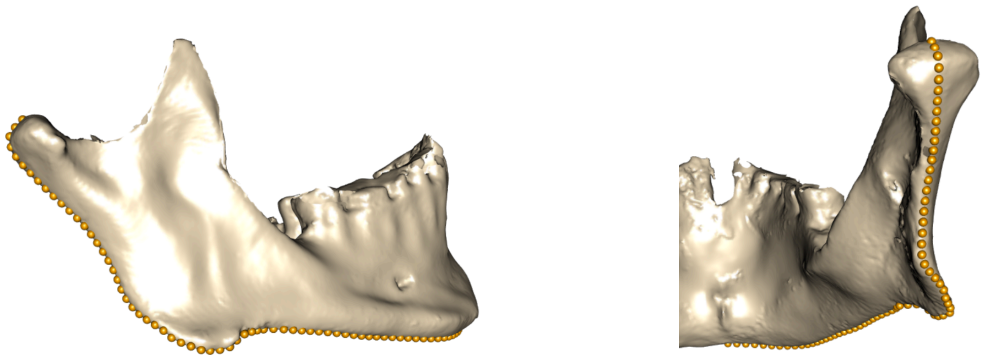

Fig 4.8. Afalou B4, Iberomaurusian, indeterminate sex. Lowest score on PC3. Mandible and landmark curve. Expanded shape and everted orientation are observed at the gonion.

c. PCs score ranges by sex

For a better understanding of each group variability, the range of PC scores was compared by sex (females, males, indeterminate). The boxplots allow to identify if sex explains any variation aspects that stand out. The Upper Pleistocene *H. sapiens* group was excluded because it is composed of only 4 individuals distributed in the three sex categories, which is insufficient for meaningful comparison. Likewise, the *H. neanderthalensis* sample does not include any females, preventing sex-based comparisons.

PC1 scores are indicated in figure 4.9. For *H. sapiens*, the group with the greatest amplitude in this axis, there are important differences between males and females, even though they overlap from zero to negative values. Females extend much further toward PC1 minimal variation axis, the median indicating half of them are clustered around zero. Males, by contrast, tend to distribute toward PC1 maximal, half overlapping with females, since their median is around zero, and the other half extending to positive scores. Indeterminate sex is distributed in the full range of variability for the group.

For Iberomaurusians, the distribution per sex is quite different. The female variability spans the full range for PC1, extending to both minimal and maximal extremes. On the other hand, all the males have positive scores, their median is significantly higher, even when compared to males from the recent *H. sapiens* group. It should be noted that Iberomaursians do not have the highest scores for PC1, although it may seem so from the general group distribution, because *H. sapiens* has a few outliers.

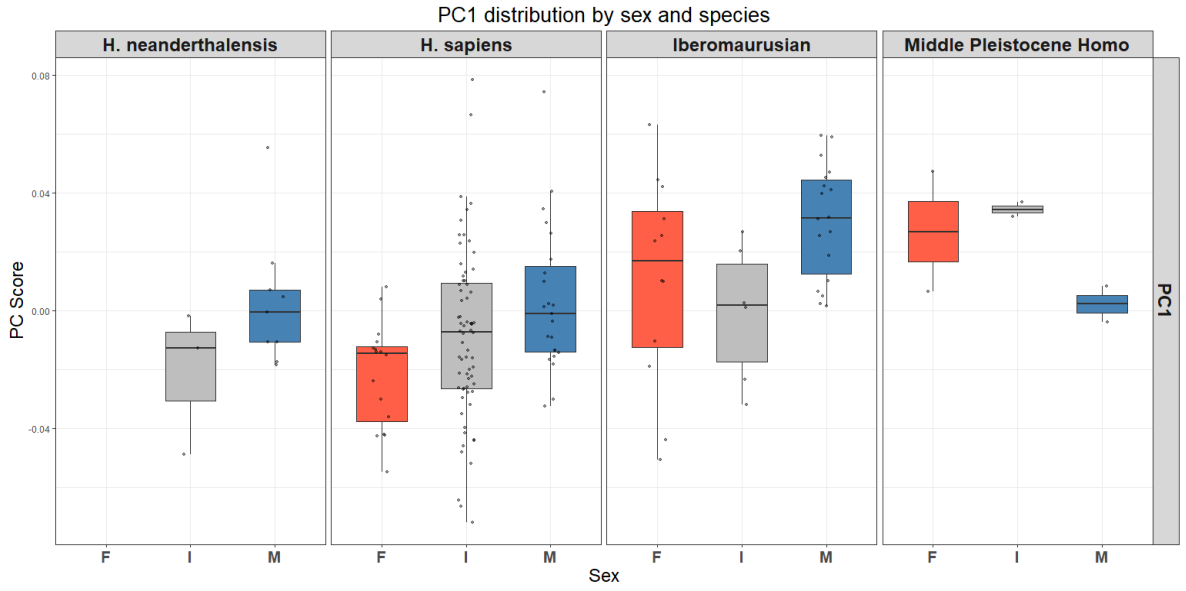

Fig. 4.9. Boxplot of PC1 distribution by group and sex. Red color indicates females, grey indeterminate and blue males.

The Middle Pleistocene *Homo* distribution should be interpreted with caution because only two specimens represent each sex category. In spite of that, males and females score very differently. In PC1, the two males are clustered together just after zero, while the two females have higher scores, towards the PC1 maximal. A similar pattern is observed in PC2 (Fig. 4.10), in which the two sexes are again quite separate and indeterminate individuals are intermediate. In the case of PC2, males have negative scores, tending to PC2 minimum, and females are placed around zero.

When compared to *H. neanderthalensis*, MP *Homo* scores are still inside their variability range. For Neanderthals, two indeterminate sex specimens pull the group's variability in this axis towards PC2 minimum. For males, the pattern differs slightly. The median is placed higher, but still negative. The other half extends greatly in the negative scores, marking the species tendency toward PC2 minimum. In spite of these sex-related differences, the overall distribution of MP *Homo* and *H. neanderthalensis* along this axis converges toward the minimum, setting them apart from the pattern observed in *H. sapiens.*

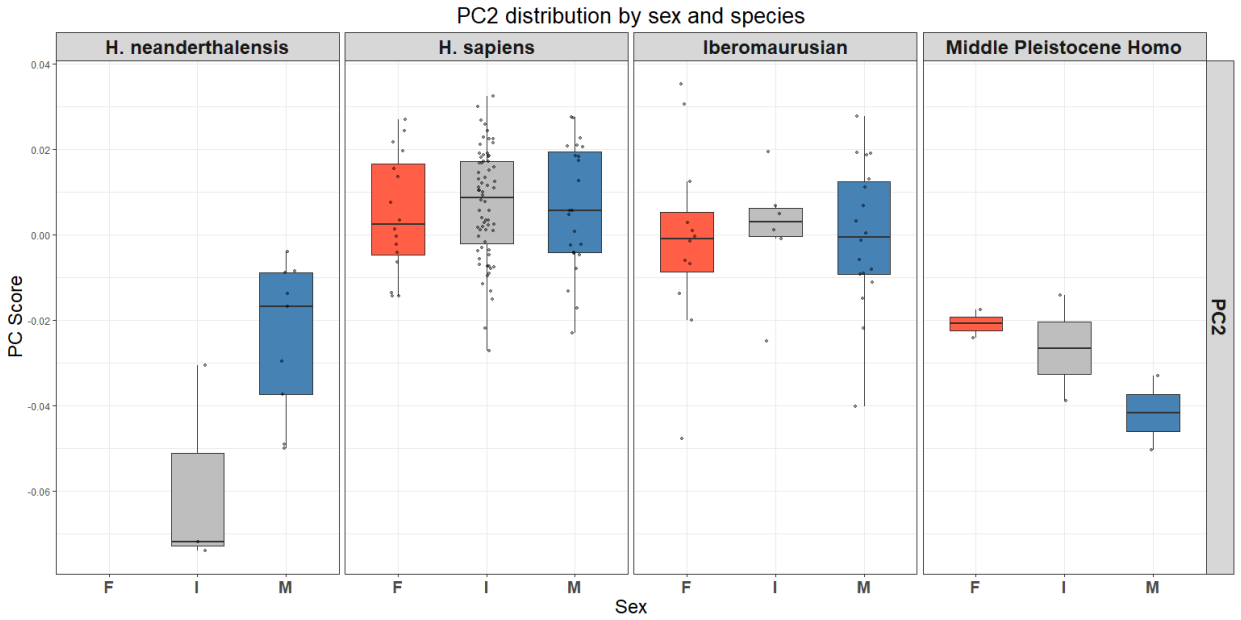

Fig. 4.10. Boxplot of PC2 distribution by group and sex. Red color indicates females, grey indeterminate and blue males.

All the medians are above zero for both *H. sapiens* groups, indicating an overall tendency towards PC2 maximal for the species. All the sex categories in the rencent *H. sapiens* group have a similar distribution pattern in terms of medians and the inter-quartile ranges. Only the lower quartiles overlap with the highest *H. neanderthalensis* scores.

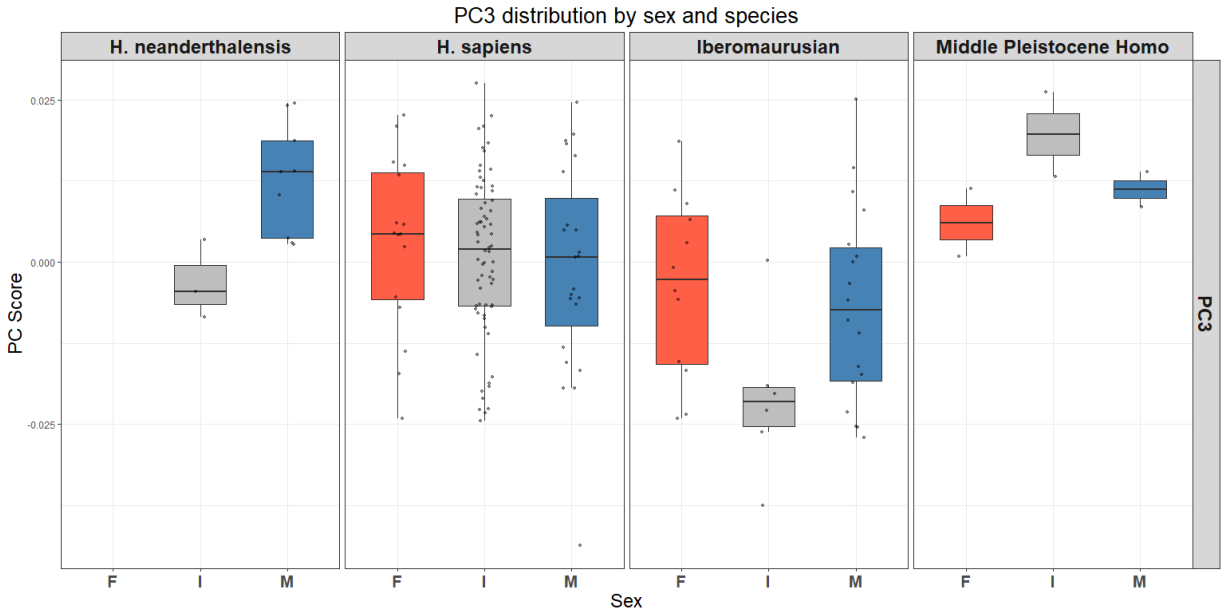

Fig. 4.11. Boxplot of PC3 distribution by group and sex. Red color indicates females, grey indeterminate and blue males.

Among Iberomaurusians, medians are similar across all sex categories, though slightly lower than the ones of the recent *H. sapiens* group. Inter-quartile ranges vary in amplitude, with Iberomaurusian males tending to have higher scores. The main difference lies in the lower quartile and a few outliers, which cause the overlap with *H. neanderthalensis* and Middle Pleistocene *Homo*.

All the groups overlap in positive values for PC3. However, the different distribution patterns indicate some differences between the groups, as shown in figure 4.11. Both Middle Pleistocene *Homo* and *H. neanderthalensis* have scores distributed from around zero towards PC3 maximal. MP hominins of indeterminate sex (Mauer and Tigheniff 3) score higher than their male and female counterparts, but all are always positive. Male Neanderthals also have all positive scores and the high-placed median indicates the tendency towards the maximal axis variation. The indeterminate sex individuals, however, score around zero, spanning into negative values.

In *H. sapiens,* medians lie just above zero, meaning over half of the individuals have positive scores, though inter-quartile ranges extend well into negative values. Compared to females, males' inter-quartile range is slightly lower. Although the whole Iberomaurusian distribution is very similar, their medians are considerably lower, in particular for indeterminate sex individuals, who fall at the PC3 minimum. The inter-quartile ranges also

extend much lower, into negative scores. Therefore, Iberomaurusians differentiate slightly from other *H. sapiens* for their lower PC3 scores.

4.2 Elliptical Fourier Analysis on curves

The Elliptical Fourier method is based on the analysis of outline curves, and as such allows comparison of mean shapes between species and sexes. These outlines are described by harmonics, which can be analysed for the cumulative reconstructive power and ability to explain a curve. Furthermore, Principal Components Analysis can be applied on their coefficients.

a. Comparing outlines: curve and mean shape analysis

Here the outlines are analyzed considering both the species and sex factor. The panel, mean shape and stack functions from Momocs package (Bonhomme et al, 2014) were used to superimpose and compare the outlines.

The panel in figure 4.12 displays the mean outline per group. Middle Pleistocene *Homo*, *H. neanderthalensis* and Upper Pleistocene *H. sapiens* have an overall similar shape. The ascending ramus is fairly vertical and straight, the gonion arch is shorter, indicating possible truncation. *H. sapiens* and its Iberomaurusian population are similar, with a more inclined ramus and regular gonion.

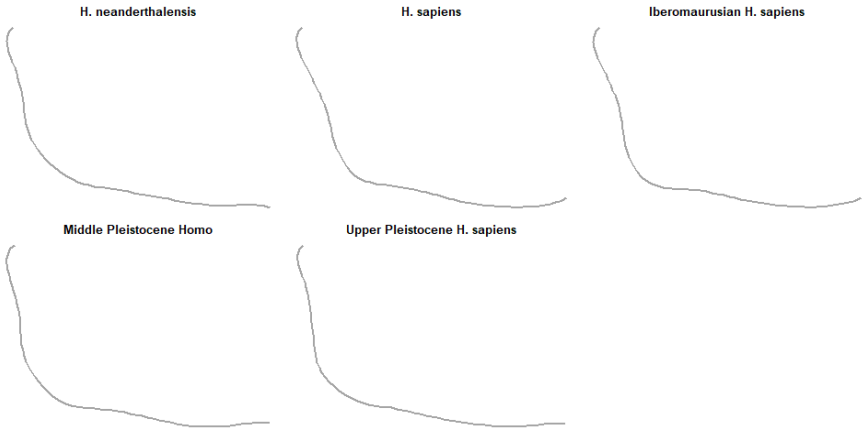

Fig. 4.12 Mean shape panel per group. Gonion shape in *H. neanderthalensis* is similar to MP Homo and UP *H. sapiens*, whereas *H. sapiens* is similar to the Iberomaurusian population.

The mean shape superimposition in figure 4.13 reinforces these comparisons and allows a more detailed analysis. In fact, the *H. neanderthalensis* gonion is more truncated, with a shorter posterior border. On the contrary, *H. sapiens* and its Iberomaurusian population

have a more anteriorly placed ascending ramus, curving posteriorly at the condyle neck. The gonion is also larger, more expanded and regularly curved, especially for Iberomaurusians.

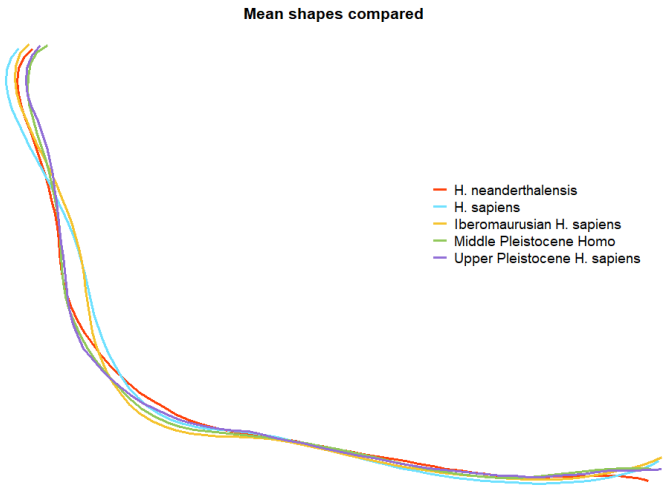

Fig. 4.13. Superposition of group mean shapes.

When comparing the superimposed mean shapes of *H. neanderthalensis*, Middle Pleistocene *Homo* and Upper Pleistocene *H. sapiens* (Fig. 4.14), the ascending ramus is very similar and the gonion is the biggest difference. For *H. neanderthalensis*, the gonion truncation is formed by a third arista between the posterior border of ramus and the basal border, cutting the gonion curve shorter. For MP *Homo*, the truncation is still visible, but less pronounced than *H. neanderthal*. In comparison, the UP *H. sapiens* gonion arch is very similar to MP *Homo* in its extent. However, there are small differences in its smoothness, conferring it a more regularly curved outline instead of the truncation.

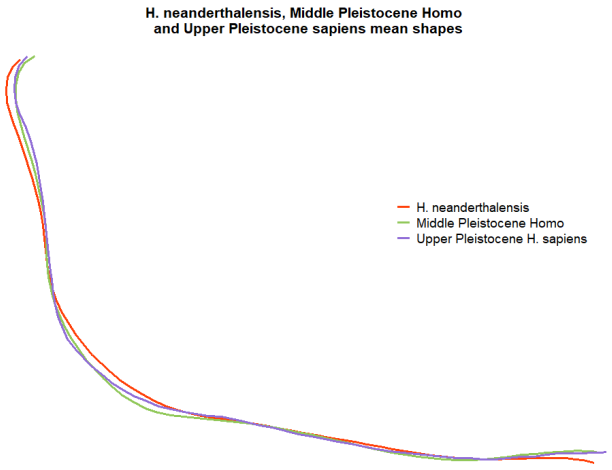

Fig. 4.14. Superimposed mean shapes of *H. neanderthalensis*, Middle Pleistocene Homo and Upper Pleistocene *H. sapiens*.

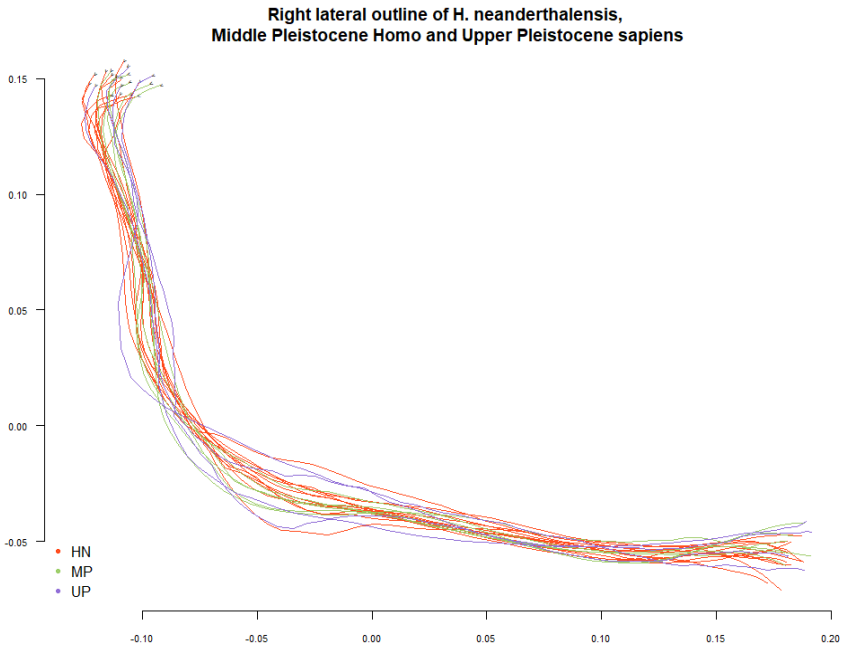

Fig. 4.15. All outlines of *H. neanderthalensis*, MP *Homo* and UP *H. sapiens* superimposed. Stack function, from Momocs R package (Bonhomme et al, 2014).

Analysing the superimposition of all outlines from these groups (Fig. 4.15) it is possible to better understand the composition of the mean shape. Neanderthals do tend to have a more truncated gonion shape; however, there are two outlines in particular that deviate from this morphology, one with a shorter gonion arch and the other with an expanded one. For MP *Homo*, while some outlines are similar to neanderthals, others are rounder, with a more curved gonion arch. Lastly, UP *H. sapien*s outlines have a great variety and the group does not significantly overlap among themselves.

Homo sapiens and the Iberomaurusian, north-african population, have very similar shapes as expected. Both gonion arches are regularly curved, but there are some distinctions. Iberomaurusians have a considerably more extended gonion area and the upper part of the ascending ramus is also more anteriorly positioned, probably indicating a less obtuse mean mandibular angle.

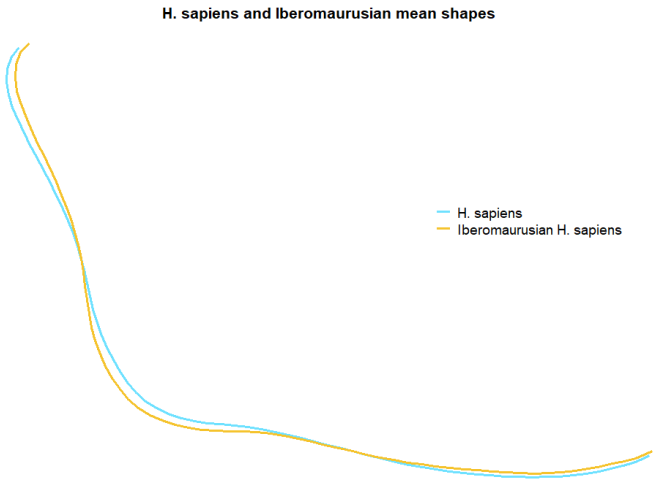

Fig. 4.16. Superimposed mean shapes of *Homo sapiens* and the Iberomaurusian population.

Considering all *H. sapiens* and Iberomaurusian outlines superimposed (Fig. 4.17), it is possible to see that the Iberomarusian tend to have an expanded gonion shape, whereas most *H. sapiens* have a more regularly curved one. Nonetheless, some Iberomaurusian outlines have a smaller gonion arch, drawing its shape among most *H. sapiens*. On the other hand, there are a few *H. sapiens* who have a gonion expanded, similarly to the Iberomaurusian. In regards to the ascending ramus, the difference in the condyle neck is confirmed by the observation of all outlines stacked. For the majority of the Iberomaurusians, it is in fact slightly more anteriorly positioned than other *H. sapiens*.

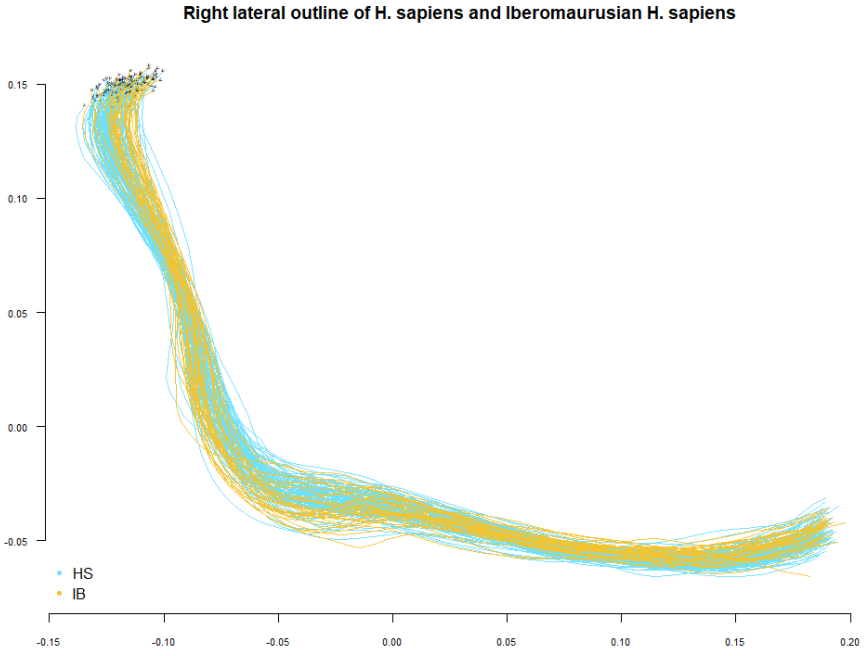

Fig. 4.17. All outlines of *H.sapiens* and Iberomaurusian superimposed. Stack function, from Momocs R package (Bonhomme et al, 2014).

Differences between the sexes may also be considered. While there is an overall similarity between the sexes of the same species, small aspects may highlight the variance and reflect the different distributions observed in the PCs boxplot per species and sex. Some distinctions are hereby highlighted.

In Middle Pleistocene *Homo*, the gonion mean shape is very different between the sexes (Fig. 4.18 and 4.19). For males, the gonion is truncated, similar to the one seen in neanderthals, which makes the ascending ramus shorter. For females, the gonion is regularly curved and the ascending ramus taller.

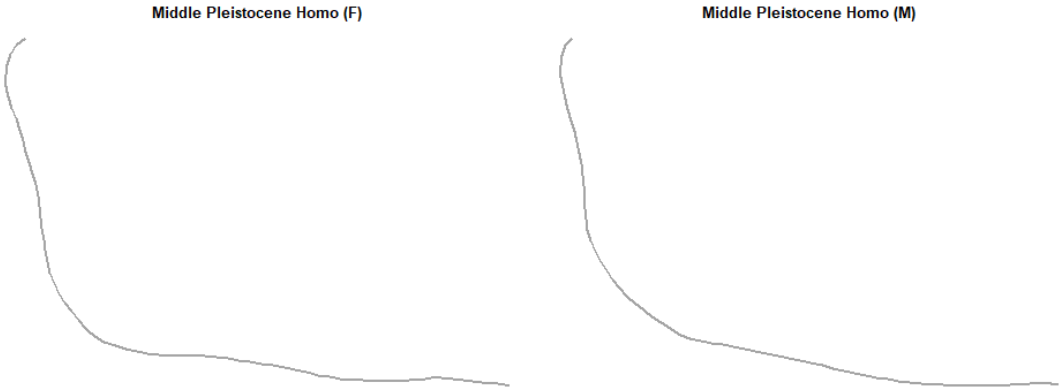

Fig. 4.18. Middle Pleistocene *Homo* mean shape by sex.

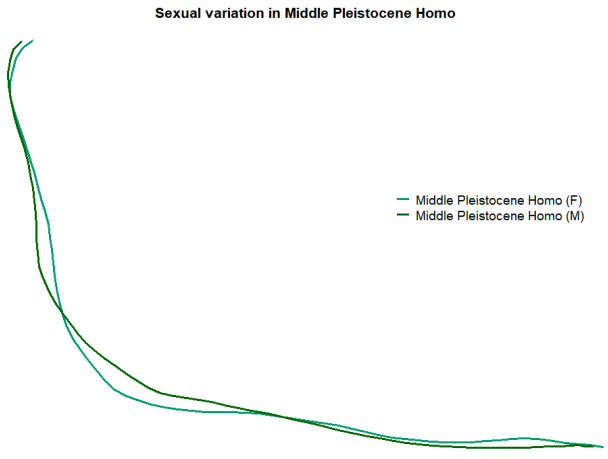

Fig. 4.19. Superimposed mean shapes of female (F) and male (M) Middle Pleistocene *Homo*.

When compared, mean outlines for Middle Pleistocene *Homo* and *H. neanderthalensis* males (Fig. 4.20) are very similar, almost completely superimposing, and exhibiting the same level of gonion truncation.

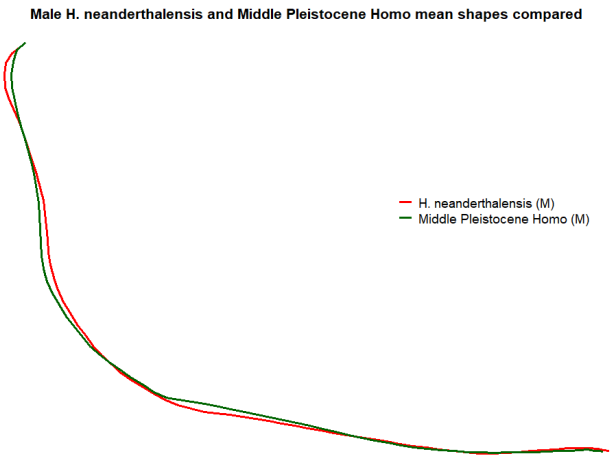

Fig. 4.20. Superimposition of male *H. neanderthalensis* and Middle Pleistocene *Homo* mean shapes.

For *H. sapiens*, when analysing sexual dimorphism for the hemi-mandible outline, males tend to have larger, more expanded gonions and anteriorly placed condyles (Fig. 4.21 and 4.22). This distinction is observed for both the recent *H. sapiens* sample and the Iberomaurusian population. However, when both samples are compared (Fig. 4.23), *H. sapiens* females have a significantly smaller gonion area and the condyle neck is more posteriorly placed. By contrast, the Iberomaurusian male gonion is more expanded and the condyle neck more anteriorly placed. For male *H. sapiens* and female Iberomaurusian there is considerable overlap in an intermediate position.

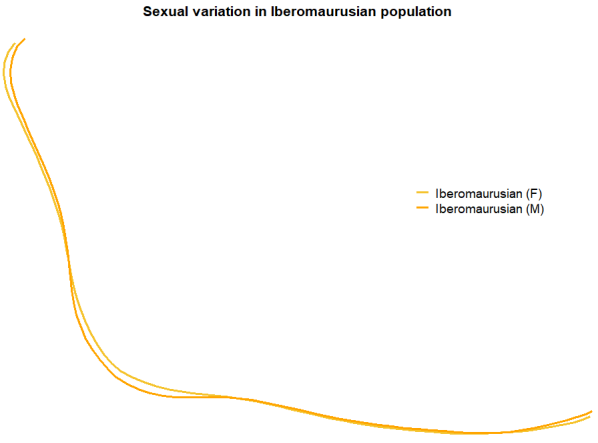

Fig. 4.21. Superimposed mean shapes of female (F) and male (M) Iberomaurusian.

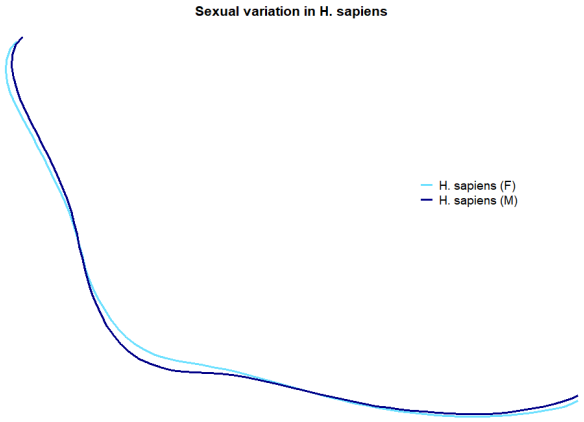

Fig. 4.22. Superimposed mean shapes of female (F) and male (M) *Homo sapiens*.

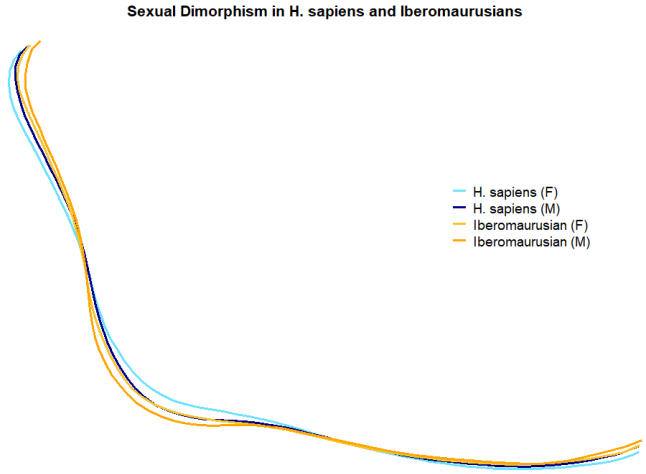

Fig. 4.23. Superimposed mean shapes of female (F) and male (M) *Homo sapiens* and Iberomaurusian.

b. Harmonic Power in Elliptical Fourier Analysis

In the Elliptical Fourier Analysis (EFA), the cumulative effect of harmonics describes the studied outline. As a general rule, the 1st harmonic determines the overall ellipses, 2nd major curves, from the 3rd to the 5th moderate waves and protuberances, from the 6th to the 9th fine details and local shape features. More harmonics may be considered, since their descriptive power varies, depending on the complexity of the outline.

In this study, nine harmonics were included, because their cumulative effect explains 99.9% of the outline (Fig. 4.24). The more harmonics included, the more the outline approaches the original curve. The hemi-mandible outline studied is not a complex curve, by the fourth harmonic 95% of its form is already explained and by the seventh 99%.

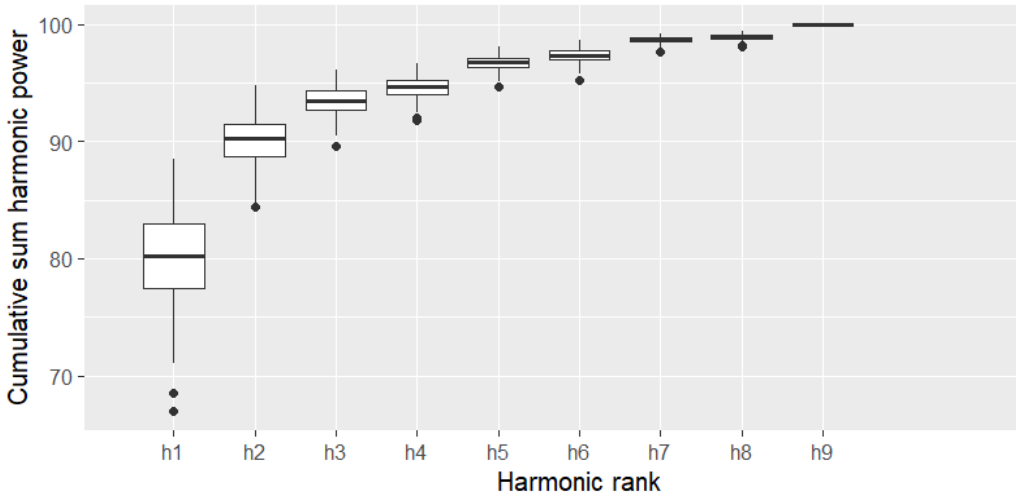

Fig. 4.24. Cumulative effect of the first nine harmonics in explaining the analysed outline.

Considering the varied outlines included in the sample, less harmonics may be necessary to describe the less complex curves. On the other hand, when there are more complex shapes, including as incurvation, notches or accentuated curves, the higher frequency harmonics (from the 6th onwards) may be necessary to better describe it.

In figures 4.25 and 4.26, both a regular (Pataud AP58) and a truncated (La Chapelle-aux-Saints) gonion are already well captured by the 4th harmonic, with little further change beyond this point. Only minor adjustments, particularly in the incurvations of the ascending ramus, appear in the 5th harmonic, and few perceptible changes occur thereafter.

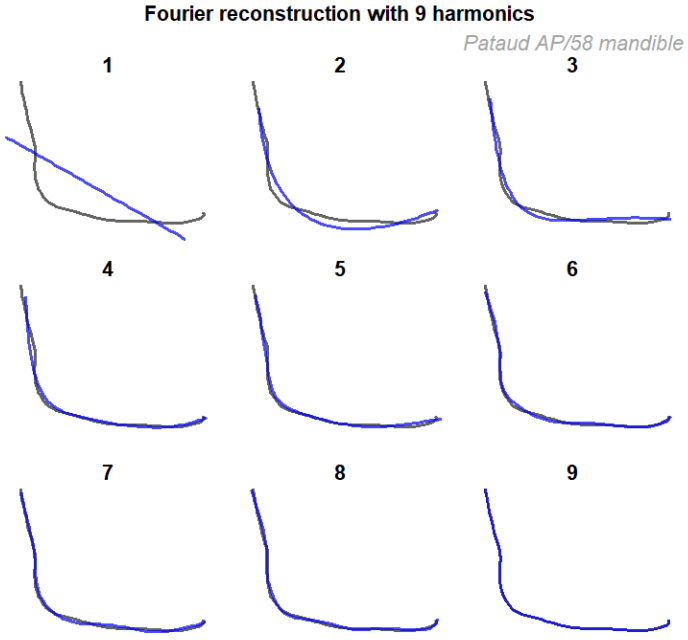

Fig. 4.25. Reconstruction of Pataud AP/58 mandible, H. sapiens, female. Regular and straight gonion.

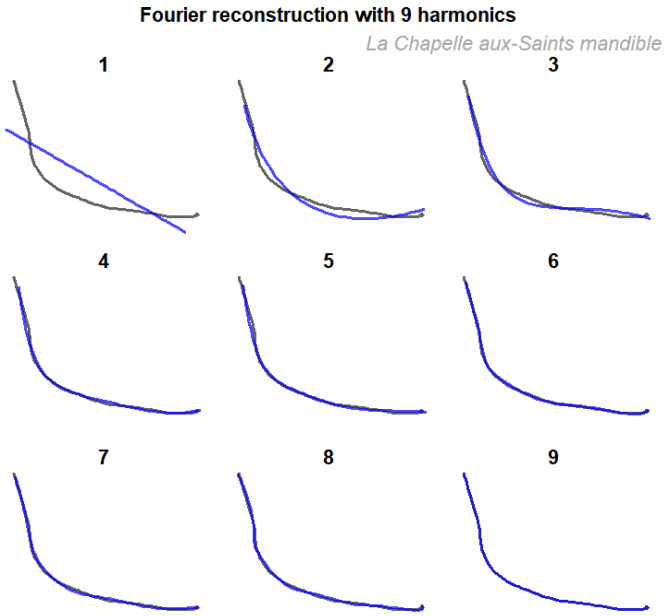

Fig. 4.26. Reconstruction of La Chapelle-aux-Saints mandible, *H. neanderthalensis*, male. Truncated and inverted gonion.

Differently, the Afalou 10 mandible (Fig. 4.27) illustrates a more complex hemi-mandibular outline. The large gonion arch, the incurvations in the ascending ramus and an anterior gonion notch require additional harmonics for an accurate reconstruction. Consequently, higher harmonics play a greater role in capturing this morphology. In fact, the progressive fit of the curve to the gonion shape becomes evident, with a visibly accurate description from the 8th harmonic onwards, instead of the 4th.

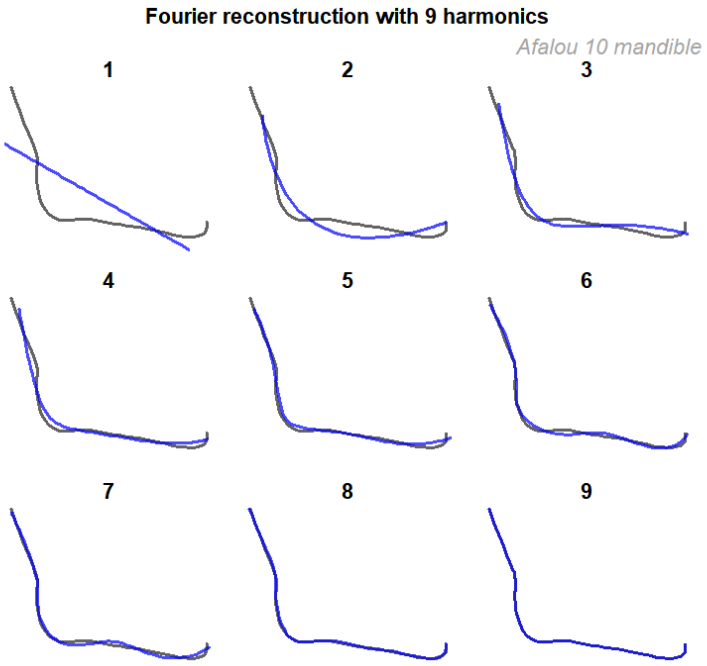

Fig. 4.27. Reconstruction of Iberomaurusian, male mandible, Afalou 10. Expanded and everted gonion.

c. PCA on EFA coefficients - minimal and maximal PC outlines

As with the Principal Component Analysis on landmarks, comparisons between maximal and minimal outlines in each variation axis can also be made for the PCA on Elliptical Fourier coefficients. The superimposed shapes highlight the morphological variation in each PC and provide a basis for direct comparison between the two methods.

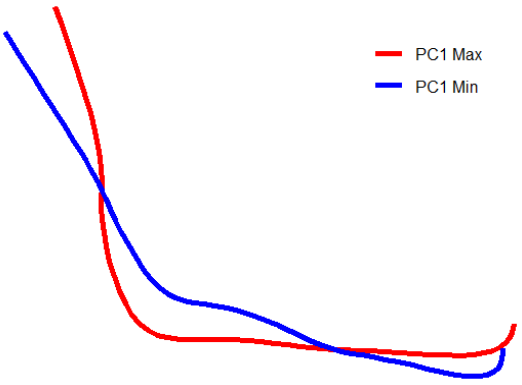

Fig 4.28. PC1 minimal and maximum outlines plotted for comparison. PCA was done on Fourier coefficients.

Comparing the superimposed maximal and minimum outlines for PC1 (Fig. 4.28), the main variation along this axis involves the opening of the gonial angle and the position of the ascending ramus. The PC1 minimum outline (in blue) displays an obtuse mandibular angle, more open, with an inclined and straight ascending ramus. By contrast, the PC1 maximum outline (in red) shows an angle closer to 90º and a vertical, curved ascending ramus.

In comparison with the PCA on landmarks, the Fourier-based PC1 captures overall the same patterns of variance. The main discrepancy lies in the gonial arch, particularly in the PC1 maximum: while PCA on landmarks depicts a more curved and expanded gonion, Fourier PCA shows it with straighter lines and smaller curvatures.

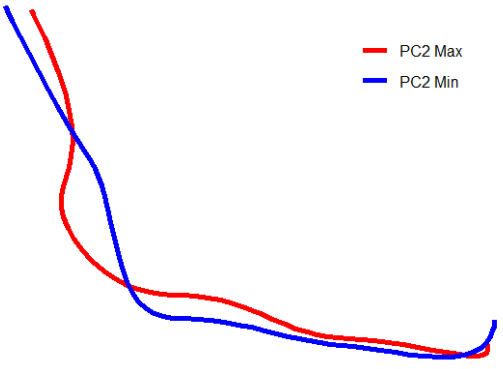

Fig 4.29. PC2 minimal and maximum outlines plotted for comparison. PCA was done on Fourier coefficients.

The PC2 maximal and minimal outlines (Fig. 4.29) characterize the variation along this axis, mainly involving the ascending ramus length and gonion truncation. The PC2 minimum outline (in blue) shows a regularly curved gonion and taller ascending ramus, curving a little in posteriorly at the middle. In the opposite direction, the PC2 maximum outline (in red) displays a short gonion, probably due to the truncation, and a short ascending ramus.

When comparing to PCA on landmarks, Fourier-based PC2 indicates the same variabilities, but inverted: Fourier PC2 maximal corresponds to PC2 minimum on landmarks.

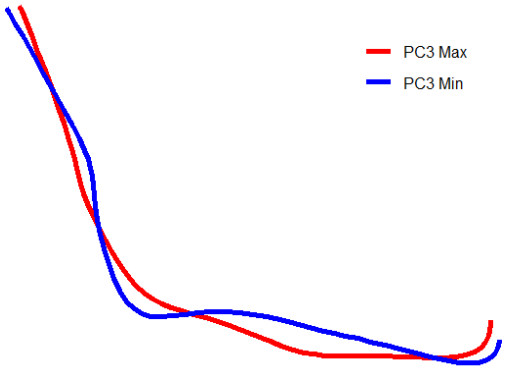

Fig 4.30. PC3 minimal and maximum outlines plotted for comparison. PCA was done on Fourier coefficients.

The superimposition of PC3 maximal and minimal (Fig. 4.30) highlights the main variation along this axis, characterized by gonion expansion and curvature of the borders. The PC3 minimum (in blue) shows an expanded gonion, a curved ascending ramus and an anterior gonion notch. By contrast, the PC3 maximum outline (in red) shows a straight ascending ramus, a regularly curved gonion and the absence of the anterior gonion notch. In fact, the inferior border projects outward where PC3 minimal shows a notch.

In comparison to PCA on landmarks, the Fourier-based PC3 captures a similar variation pattern, with a few distinctions. The minimum PC3 outline shows a less pronounced gonion expansion, while the PC3 maximum has a more pronounced curvature on the mandibular body.

d. Plotted PCA on EFA coefficients

In the PCA based on Fourier coefficients, PC1 explains 53.3% of variability, PC2 23.1% and PC3 11.3%. In total, they account for 87.7% of variation. These values differ

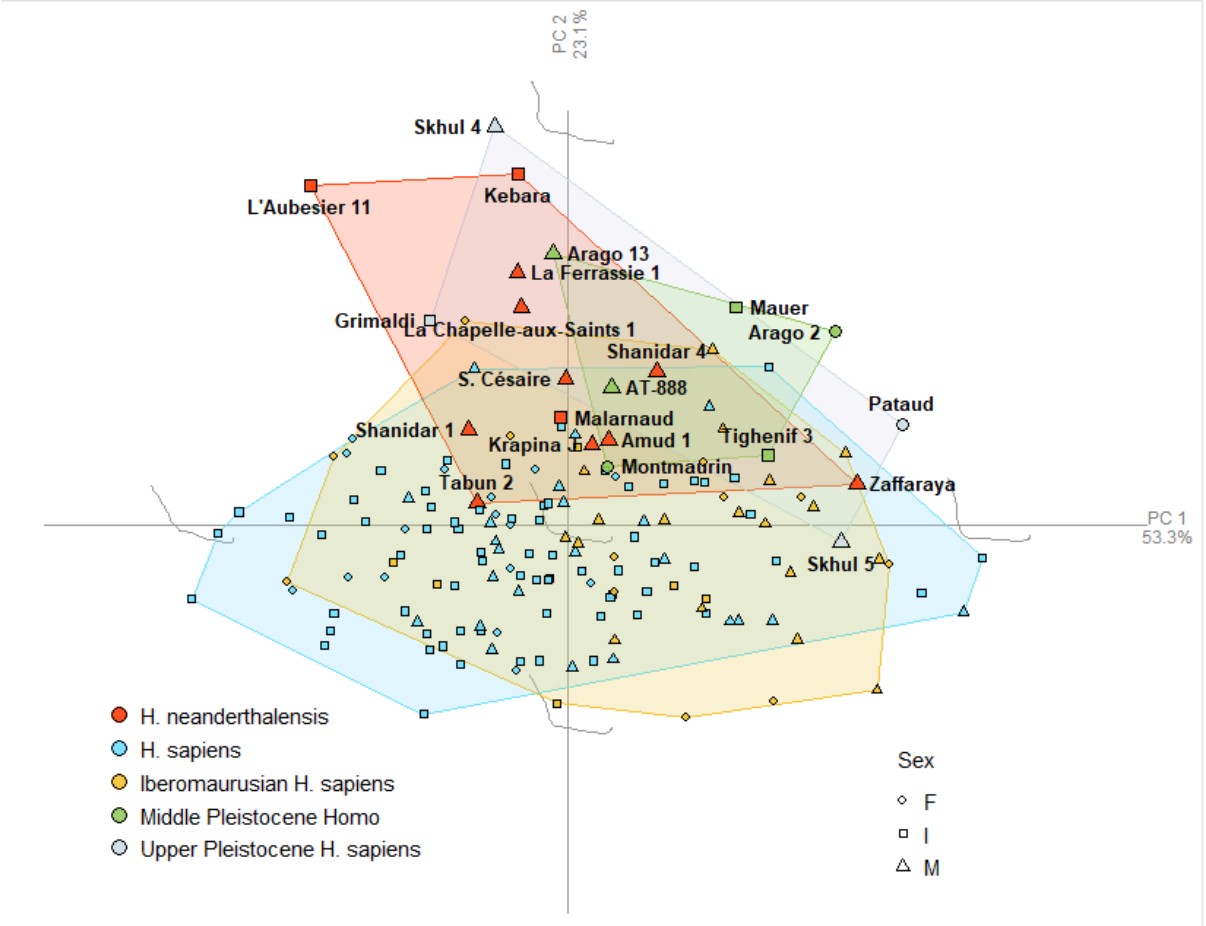

Fig 4.31. PC1 and PC2 plot from Fourier coefficients. Species and population groups are given by colors and sex by symbols. Minimal and maximal outlines are drawn at the axis.

markedly from the PCA on landmarks percentages, respectively 39.52%, 18.5% and 9.02%, explaining in total 67.04% of the variability.

The PC1 - PC2 plot (Fig. 4.31) is overall very similar to the one from PCA on landmarks (Fig. 4.4), with the exception of the inversion on the PC2 axis, since the minimum on landmarks corresponds to the maximal on Fourier. Although mirrored along the x axis, the overall group polygon shapes and distributions remain very similar.

The small differences refer to specimen positions, for example La Ferrassie 1 and La Chapelle-aux-Saints overlap in the PCA on landmarks plot. On Fourier-based PCA, the two Neanderthals are more distant on the PC2 axis, La Ferrassie 1 moving toward PC2 maximal. Comparable shifts are also observed in other fossils: Saint Césaire and Malarnaud do not overlap; Arago 2 plots outside the Upper Pleistocene *H. sapiens* polygon, when in the other plot they overlapped. In general, the groups distribution exhibit the same distribution pattern for PC1 and PC2.

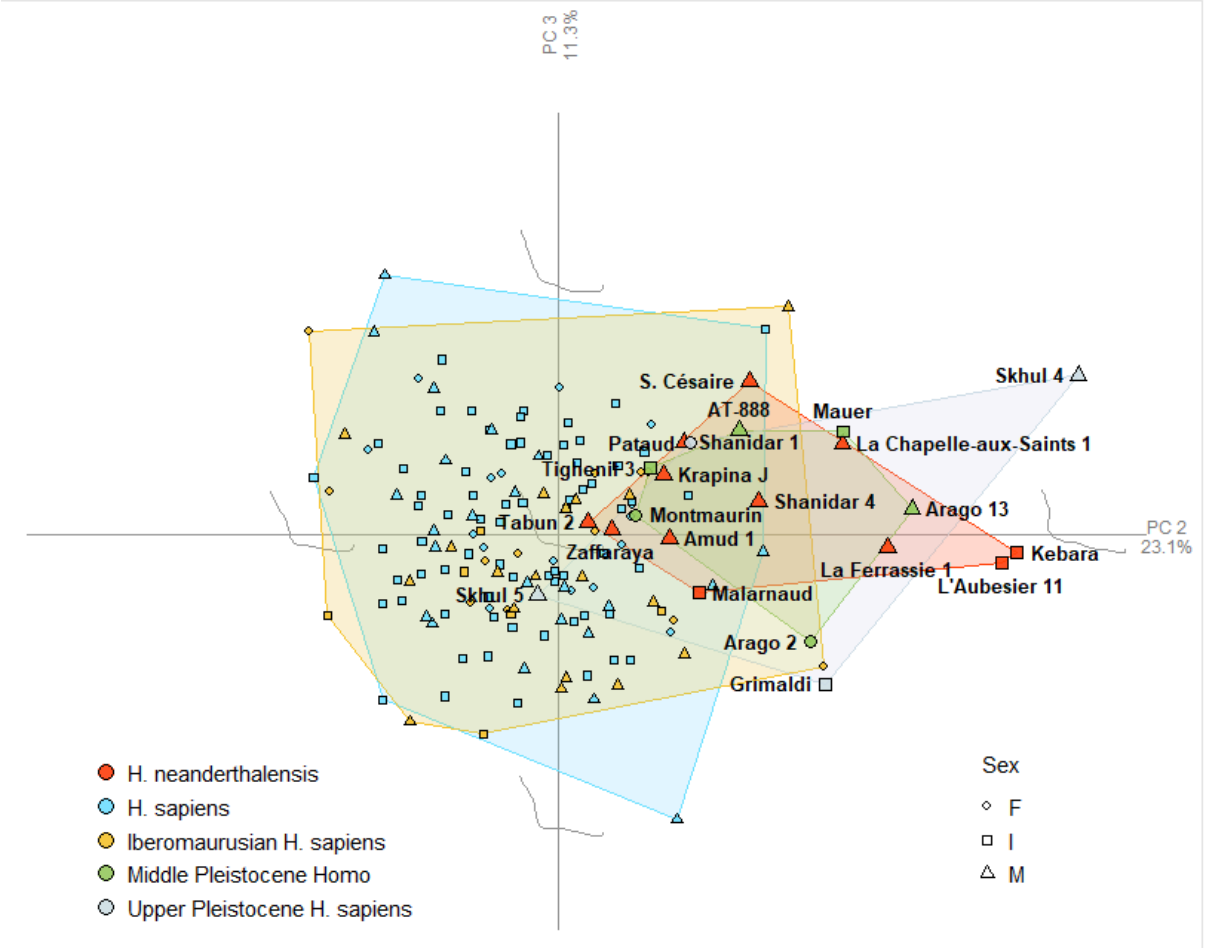

Fig 4.32. PC2 and PC3 plot from Fourier coefficients. Species and population groups are given by colors and sex by symbols. Minimal and maximal outlines are drawn at the axis.

The distribution along the PC3 (Fig. 4.32 and 4.33) is, however, considerably different between landmark-based and Fourier-based PCA. In this second method, the groups separate poorly, since there is great overlap between *H. neanderthalensis*, Middle Pleistocene *Homo* and Upper Pleistocene *H. sapiens*. Moreover, Iberomaurusian variability is inserted into *H. sapiens* distribution, whereas in the PCA on landmarks they were slightly distinguishable.

In the PC2 - PC3 plot (Fig. 4.32), even if there is no clear distinction between the recent *H. sapiens* group and the Iberomaurusian population, it is still noteworthy that most Iberomaurusian specimens plot with negative scores, towards PC3 minimum. H. neanderthalensis and Middle Pleistocene *Homo* are also differently positioned at Fourier-based PC3, where they greatly overlap around the zero line. On landmark-based PC3 (Fig. 4.5 and 4.7), specimens such as Mauer, Shanidar 1 and Saint Césaire had the highest scores, positioned at the maximal extreme of the variation axis.

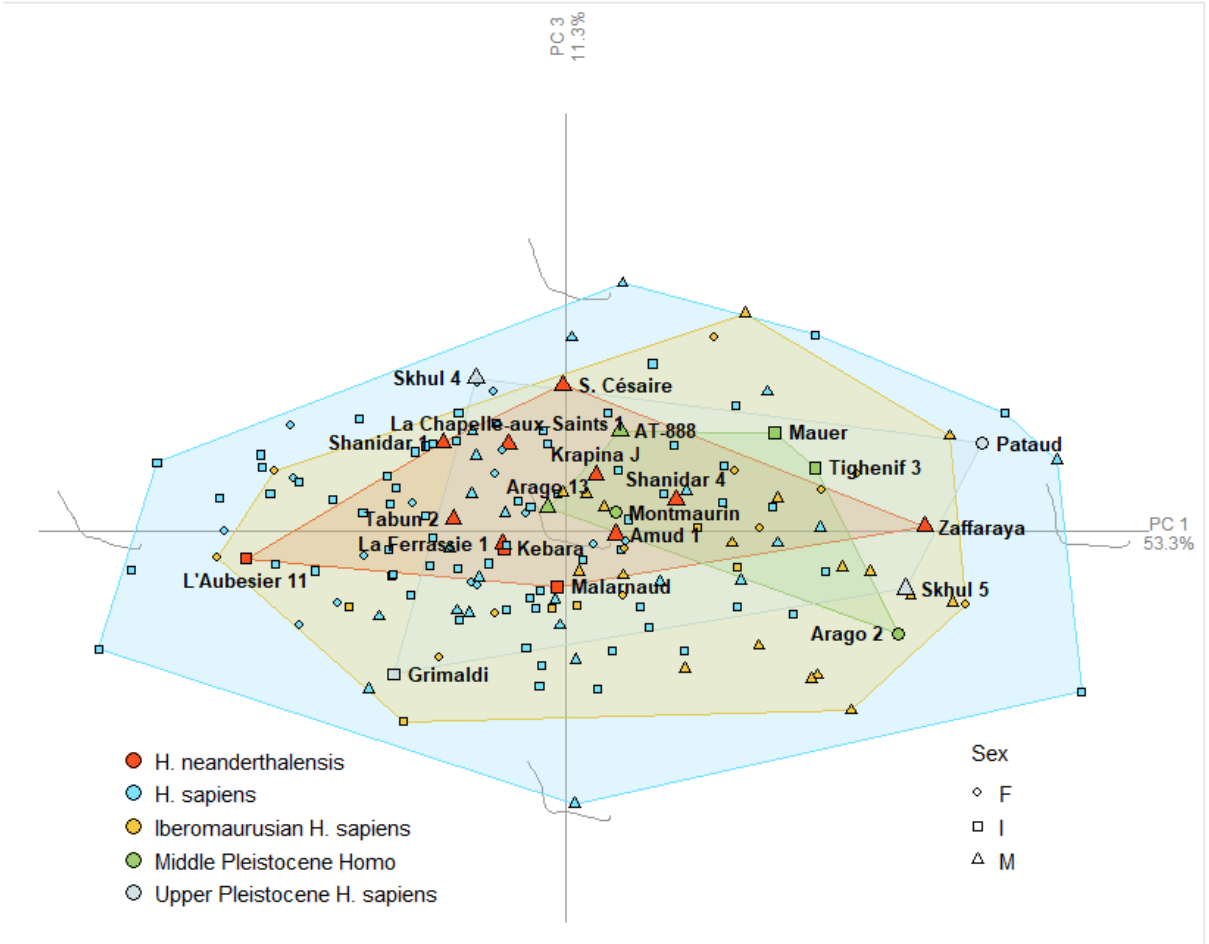

Fig 4.33. PC1 and PC3 plot from Fourier coefficients. Species and population groups are given by colors and sex by symbols. Minimal and maximal outlines are drawn at the axis.

These tendencies are yet confirmed on the PC1 - PC3 plot (Fig. 4.33). Although the group polygons are not separated, more *H. sapiens* tend to plot on the left quadrant, towards PC1 minimum, and Iberomaurusians on the right one, PC1 maximal. Likewise, *H. neanderthalensis* and Middle Pleistocene *Homo* overlap, but have different tendencies. Neanderthals are mostly positioned from the center to the left upper quadrant (the exception is Zaffaraya), with low scores for PC1 and high ones for PC3. On the other hand, Middle Pleistocene hominins are mostly at the right upper quadrant (exception of Arago 2), with similar scores for PC3, but positive for PC1.

Chapter V: Discussion

The study of the mandibular outline contributes to the understanding of the morphological variability in a bone that is frequently present in the fossil record and highly informative for phylogenetic attribution (Lieberman, 1997; Rosas et al, 2019). In particular, the gonion region is relevant to ongoing debates in paleoanthropology, such as its implications for species differentiation, since *H. neanderthalensis* and Middle Pleistocene *Homo* have a distinct gonion morphology compared to *H. sapiens* (Rosas, 2001; Mounier, 2009; Bergmann et al, 2021). Yet, considerable intra-specific variability also exists, especially considering the interplay between the gonion and the posterior border of the ramus, which is observed in the wide variation range within *H. sapiens* (Bergmann et al, 2021).

There are questions about what factors explain these distinct configurations. Growth trajectories may account for part of the variation (Enlow et al, 1996), as well as the correlation with other morphological changes in the cranial-facial complex (Rosas and Bastir, 2004; Rosas et al, 2006; Harvati et al, 2011; Rosas et al; 2019). At the same time, the mandible is constantly involved in biomechanical strains, from the chewing forces and paramasticatory activity, which can influence bone formation processes (Aiello and Dean, 1990; Lieberman, 1997; Van Eijden, 2000; Ruff, 2018; Sella-Tunis et al, 2018).

To explore these aspects, this study applied morphological classification and Principal Components Analysis (PCA) based on landmarks and Fourier harmonics (Lestrel, 1989; Claude, 2008; Arnaud, 2021). These methods aimed to improve the comprehension of nuances in mandibular variability, accounting for the relationship between the different specimens and their group distribution. While Fourier is usually more accurate, given its use of harmonics that contribute to the shape, the 70 semi-landmarks used account for much of the outline, increasing the pattern identification power for the landmark PCA. Thus, the PCs represent the same variation axis in both methods, with only minor shifts in specimen positions. Overall, the three approaches yielded congruent results.

5.1 Gonion morphology in *H. sapiens* and *H. neanderthalensis*

The data analysed in this study indicates distinctive patterns in mandibular outlines, comprising the posterior and inferior borders. In line with previous studies (Enlow et al, 1996; Nicholson and Harvati, 2006; Harvati, 2011) the junction at the gonion region shows intra and inter-specific morphological variability (Rosas, 2001; Mournier, 2009; Bergmann et al, 2021), which may be linked to biomechanical responses and evolutive adaptations according to cranial-mandibular integration processes (Rosas and Bastir, 2004; Rosas et al,

2006). Taking into account these processes, the mandible features may be considered from an evolutionary perspective, in the frequency and consistency in the patterns exhibited by the species.

When comparing *H. sapiens* and *H. neanderthalensis* some individuals exhibit similar morphologies. A regular and straight gonion is displayed by 2 of the 12 Neanderthals and 67 of the 107 *H. sapiens* (table 3.6), the typical morphology for modern humans. Likewise, both the PCA on landmarks and on Fourier coefficients indicate this partial overlap on PC2 (Fig. 4.4 and 4.31), characterized by a truncated gonion and shorter ramus for negative values and a regular gonion and incurved ramus for the positive values. Nevertheless, this superimposition only includes the highest scores of *H. neanderthalensis* and the lowest scores of *H. sapiens*, demonstrating there are clear distinctions in the direction of variability for each group.

In total, 5 Neanderthal specimens are inserted into the lower portion of *H. sapiens* distribution. Among them, Tabun II, Amud I and Zafarraya have the highest scores. Interestingly, the last two individuals have a truncated gonion (Fig. 5.1). For Zafarraya, the truncation is moderate, but the third arista, although inclined, is mostly vertically oriented, the ramus is then very tall in relation to the basal border. For Amud 1, the truncation of the third arista is very subtle and almost horizontal, in spite of that, the ascending ramus is also very tall. Krapina J and Shanidar 1, at the lower extreme of the *H.sapiens* distribution, have a regularly curved gonion, as does Tabun II (Fig. 5.2), with an outline more similar to the *H. sapiens* morphology

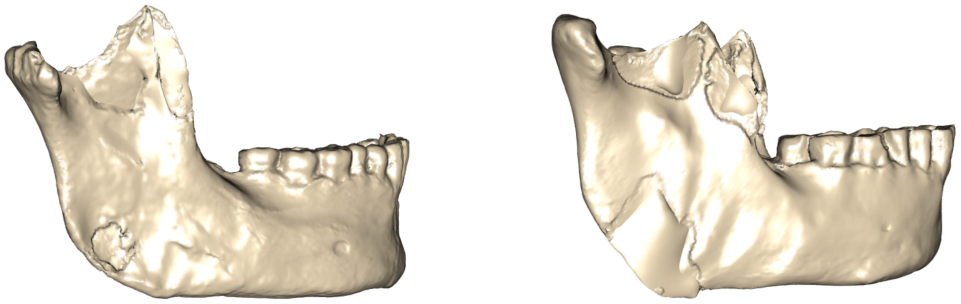

Fig. 5.1. Highest scoring Neanderthals on PC2 with truncate gonion. Amud 1, male, mildly truncated mandible on the left and Zafarraya, male, moderately truncated mandible on the right.

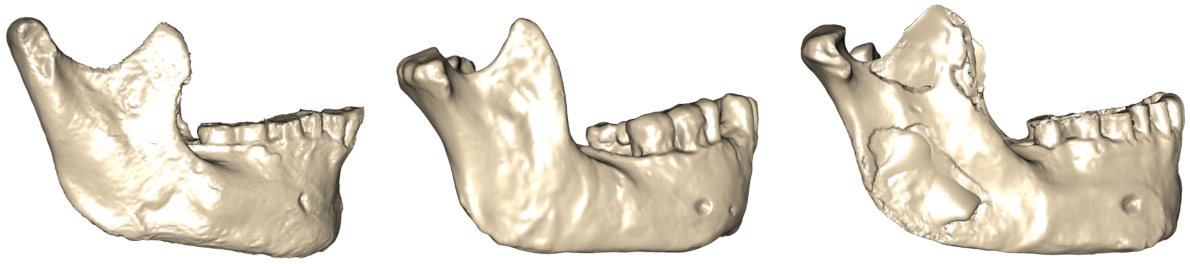

Fig. 5.2 Highest scoring Neanderthals on PC2 with a regular gonion. Tabun II, male, on the left; Krapina J , male, at the center and Shanidar 1, male, on the right.

For *H. sapiens*, when the gonion is not regular and straight, it tends to be everted and expanded. By contrast, *H. neanderthalensis,* do not have any everted or expanded gonions. When their gonions are not regularly shaped, they are truncated and/or inverted. In fact, 10 out of the 12 Neanderthals have at least one of these features, typical for the species. This clearly sets *H. neanderthalensis* and *H. sapiens* apart, since to the later group inversion is never present and truncation only a subtle degree in 3.74% of the sample. These results are aligned with previous studies that list gonion morphology as one of the distinct traits between the two groups (Nicholson and Harvati, 2006; Harvati et al, 2011), in particular due to Neanderthal truncation (Rosas, 2001), but also modern humans eversion (Bergmann et al, 2021).

The classification employed is centered on the gonion region, but the PCA also captures the morphology of the posterior ramus border and the basal border. PC2 maximal and minimal outlines indicate the gonion and the posterior border are significantly varying in this axis (fig 4.2), which is the one that best separates Neanderthals and modern humans. From their superimposition just the PC2 (Fig. 4.4 and 4.31) below the zero line, *H. sapiens* specimens distribute towards positive values, characterized by a regularly curved gonion, a longer and curved posterior border; *H. neanderthalensis* plots towards more negative values, characterized by a truncated gonion, short and straight posterior border.

Other studies also suggest the variation in the ascending ramus morphology is meaningful for *H. neanderthalensis* differentiation. Bergmann et al (2021) enlist the upper ramus configuration as one of the features differentiating *H. neanderthalensis* and Holocene *H. sapiens*, the latter group having a decrease in ramus breadth in respect to the former. According to Terhune et al (2018), Neanderthals differ by a low condylar process in relation to the higher coronoid process, an anterior-superior ramus distinction consistent in adults and during ontogeny.

Although the outlines in this study do not have information about ramus' width or the relation to the anterior border, the PC2 axis indicates variation in their length, inclination and incurvation. These results shed light on other aspects of ascending ramus variability, although it is not yet clear whether gonion and ascending ramus are co-varying or responding to different factors. They could possibly relate to the opening degree of the mandibular angle and the shape of the gonion. When the gonion is truncated, the posterior border may be shortened by the formation of the diagonal third arista.

Notably, the *H. neanderthalensis* positioned at the extreme of this variation axis (Kebara ana L'Aubesier) have a regular gonion, instead of the truncated shape illustrated in PC2 minimum (Fig. 4.2) and most characteristic for the species (Rosas, 2001). On the other hand, their ramus is significantly shorter, while for the higher scoring Neanderthals it is taller (Fig. 51 and 5.2). This implies that the ascending ramus length and morphology have a great influence in this variation axis, although the gonion morphology is associated. Further inquiries are needed to better understand the relationship between the gonion region and the ascending ramus posterior border.

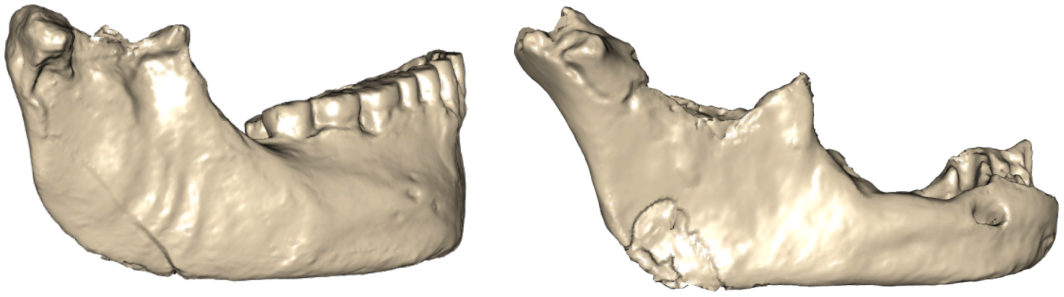

Fig. 5.3. Lowest scoring Neanderthals on PC2. Kebara, indeterminate sex, on the left and L'Aubesier, indeterminate sex, on the right. Both display regular gonion morphology and short ascending ramus.

Integration and allometric studies have inquired into the associations between different mandibular parts. Testing for different allometric trajectories between anterior and posterior mandibular portions, Harvati et al (2011) obtained a Partial Least Square (PLS) result that associated wider rami and medial drawn gonion to retracted symphysis and posteriorly positioned mental foramen. On the other extreme, the narrow rami and laterally expanded gonion were connected to forward symphysis and anteriorly positioned mental foramen. Rosas and Bastir (2004) also investigate the allometric effect, but on mandibular supra and inferior-alveolar units, finding an allometric signal only on the first, which associates the retromolar space to size. The gonion and the posterior border are part of the inferior-alveolar unit, and as such are not included. The authors highlight the tendency for

ramus verticalization, seen increasingly in *H. sapiens* in comparison to the Middle Pleistocene.

The mechanism for gonion and ascending ramus variation are not yet fully understood. This region is particular because of its role in muscular attachment and bone remodeling. It is an active site for bone resorption and deposition responding to different stimuli, at the same time, subject to biomechanical effects, from chewing and bite force, and cranio-mandibular integration, to maintain occlusal relation. According to Enlow et al (1996), the ascending ramus maintains the mandibular body in a functional position, ensuring occlusal fitting. In this process, the ramus configuration responds to changes in the facial structure, the remodelling altering according to changes in other cranial-facial features.

The ontogenesis evidences some of the ramus regions for bone resorption and deposition. For *H. sapiens*, during growth, the ramus must increase vertically more than it does horizontally, a growth trajectory guaranteed by greater bone deposition in the inferior part of the posterior border than in the superior. Thus, the gonion region undergoes changes to maintain the relationship between maxillary and mandibular arches, with the posterior border acting as a deposition area. Notwithstanding, the whole ramus shows adaptive capabilities (Enlow et al, 1996), for instance the gonial basal margin may act as a resorptive field. Then, one must consider factors such as the muscular alterations associated with mandibular shift, as well as facial and basal cranial variations that may affect the mandible.

Further clarification of these responses is needed, especially regarding other *Homo* species. Do the observed morphological variations reflect muscular adaptations linked to increased bite force or specific activities? Or do they instead represent musculoskeletal changes associated with broader craniofacial reorganization? Understanding this variability is key to evaluating the phylogenetic significance of the gonion, whether its changes primarily reflect functional factors or structural modifications connected to the emergence of the *H. neanderthalensis* lineage

5.2 Gonion morphology in *H. neanderthalensis* and Middle Pleistocene *Homo*

Better distinguishing the implications of functional and structural factors in gonion morphology is key to understanding what it represents in terms of an evolutive adaptation, ontogenetic patterns and mandibular activity. The gonion and ramus modelling pattern is not fully comprehended for other *Homo* species, which creates a degree of uncertainty about the phylogenetic significance of the morphological variation. The typical *H. neanderthalensis* truncated gonion is largely considered one of features in the “neanderthalization process”

(Rosas, 2001; Hublin, 2009). However, the appearance of the trait without a major association to other clear Neanderthal features is still a source of debate (Mounier, 2009b; Quam et al, 2024).

The Mauer mandible, holotype for *H. heidelbergensis*, is considered ancestral to *H. neanderthalensis,* because it displays a combination of plesiomorphic characteristics and Neanderthal apomorphies (Mounier 2009b). Mauer's pronounced truncated gonion is listed among these last ones. Quam et al (2024) also recognizes that the gonion in Mauer is its most-Neanderthal feature, but says that Neanderthal apomorphies are difficult to identify in the mandible, unlike the Sima de los Huesos (SH) Middle Pleistocene population. The similarities are then attributed to a common structural base, where Neanderthal apomorphies will develop, a differentiation that for the authors excludes Mauer from their lineage.

On the other hand, Rosas et al. (2006; 2019) adopt a structural perspective, emphasizing cranial–mandibular integration within ontogenetic and remodeling processes that shape morphology. In *H. neanderthalensis*, midfacial prognathism affects the gonion and ramus in order to maintain proper occlusal relations with the maxilla, although additional traits may co-vary. Furthermore, while facial growth in *H. sapiens* is predominantly vertical, in *H. neanderthalensis* and Middle Pleistocene *Homo* it follows a more horizontal trajectory, producing corresponding mandibular modifications. The authors also argue that shifts in the lateral basicranium - particularly in the temporal petrosa and glenoid fossa - are associated with ascending ramus breadth, linking mandibular position to cranial architecture. In this model, variation in cranial morphology would explain the differences in the mandibles observed between Mauer and Sima de los Huesos.

In the results hereby presented, *H. neanderthalensis* and Middle Pleistocene *Homo* plot very similarly in all three PCA variation axis. They also differentiate best from *H. sapiens* in PC2, with negative scores, inserted in the *H. neanderthalensis* distribution, although with a smaller, less-extreme variation range. The outlines' mean shape per group supports these similarities, approximating the two groups by a more straight posterior border and truncated gonion, in opposition to the *H. sapiens* curved ramus and regular anteriorly-placed gonion. Our results are consistent with a similar mandibular outline pattern for *H. neanderthalensis* and Middle Pleistocene *Homo*, distinct from the *H. sapiens* variation for its morphological configuration.

If observed in greater detail, the *H. neanderthalensis* and Middle Pleistocene *Homo* distribution shows different variation trends in PC1 (Fig. 4.4 and 4.31). Although the groups are mostly completely superimposed in this variation axis, most Middle Pleistocene

specimens have positive scores, only Arago 13 is positioned below the zero line. On the contrary, most Neanderthals are on the negative half of the axis, with only Zafarraya, Shanidar 4 and Krapina J plotting with MP *Homo*. This variation is very subtle, most individuals plotting around the zero line and significant overlap. It does indicate, however, a repositioning of the ramus, in relation to the basal border.

Although the overall group is inserted into the *H. neanderthalensis* variability, the six Middle Pleistocene fossils display different morphological combinations, slightly approaching or distancing different Neanderthal individuals. In the PC1-PC2 (Fig. 4.4) plot the position of each specimen in relation to these variation axis is illustrated. Mauer and Arago 2 (Fig. 5.4) are plotted a little outside of the Neanderthal distribution, due to their higher scores in the PC1 axis, indicating a more vertical and ascending ramus. While the two individuals have different gonion configurations, Mauer truncated and Arago 2 regular, they both exhibit a similar ramus, wide, straight and not significantly long.

The other MP *Homo* are inserted into the *H. neanderthalensis* variability. Tigheniff 3 and Montmaurian (Fig. 5.5) are at the extreme of the *H. sapiens* distribution, closer to the overlapping Neanderthals, Zafarraya and Krapina J respectively. They also have different gonion morphologies, one truncated and the other regular, but the ascending ramus is similarly taller. By contrast, Arago 13 and AT-888 (Fig. 5.6) plotted in the center of Neanderthal distribution (close toShanidar 4, La Ferrassie 1, Saint-Césaire, La Chapelle-aux-saints) and have a medium-length ramus and a mildly truncated gonion.

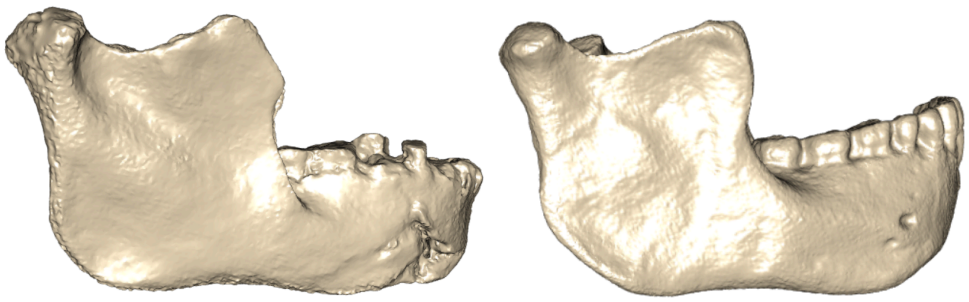

Fig. 5.4 Middle Pleistocene *Homo* plotted outside of *H. neanderthalensis* distribution in PC1-PC2. Arago 2, on the left, regular gonion, and Mauer on the right, truncated gonion.

For both *H. neanderthalensis* and Middle Pleistocene *Homo*, specimens with a truncated gonion are to a certain degree dispersed in the group's distribution. They are mostly clustered towards PC2 minimal, not at the axis' extreme, but rather at mid-negative scores, where the following fossils plot together: Arago 13, Shanidar 4, La Ferrasie 1, La Chapelle-aux-saints, AT-888, Saint Césaire, Malarnaud and, to some degree, Mauer. In

comparison, Amud 1, Zafarraya (Fig. 5.1) and Tigheniff (Fig. 5.5), the other fossils with a truncated gonion, appear overlapping within the *H. sapiens* distribution. However, their gonion truncation and ramus configuration is quite different, since the third arista is more verticalized, while for the lower-score fossils it is more horizontal. This observed variability in truncation needs further understanding, in particular regarding the relation to other aspects of the ramus and mandible. It is worth noting that this more vertical truncation was observed in both Neanderthals and MP *Homo*, not being a factor in the differentiation of the two species.

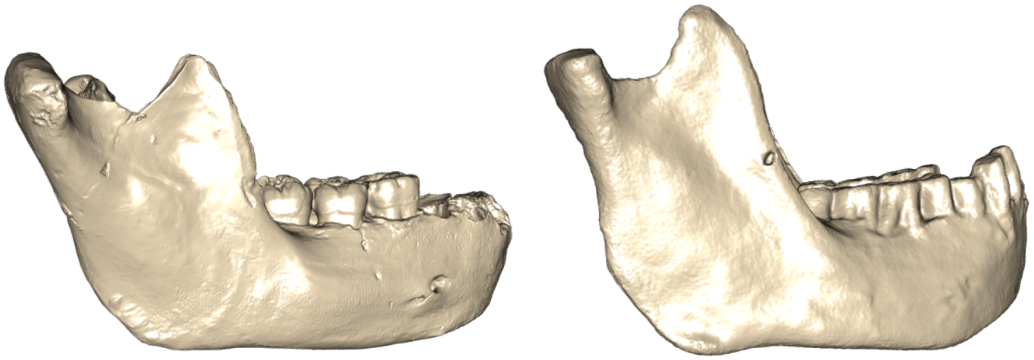

Fig. 5.5 Middle Pleistocene *Homo* plotted closer to high-scoring *H. neanderthalensis* in PC2. Montmaurin, on the left, regular gonion, and Tighenif 3 on the right, truncated gonion.

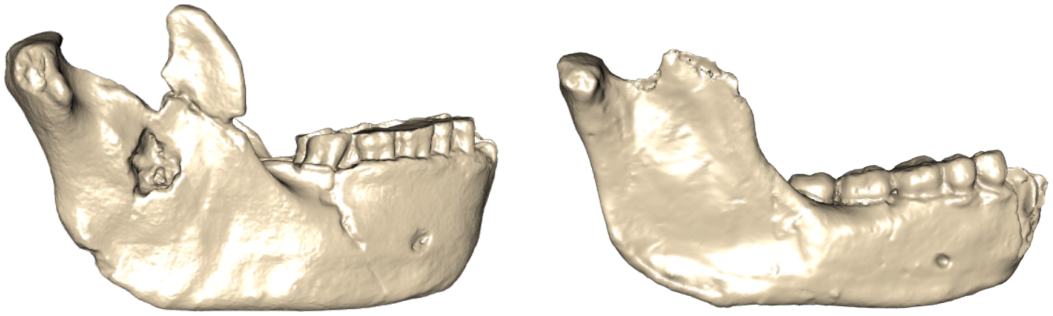

Fig. 5.6 Middle Pleistocene *Homo* plotted at the center of *H. neanderthalensis* distribution in PC1-PC2. AT-888, on the left, truncated gonion, and Arago 13 on the right, truncated gonion

Therefore, Middle Pleistocene *Homo* have different morphological configurations for ramus and gonion regions, but are closely associated with *H. neanderthalensis*. This conclusion is aligned with the current paleoanthropological framework, in which the Neanderthal lineage originated in Eurasia from one or more Middle Pleistocene population (Mounier et al, 2009; Hublin, 2009; Dennel et al, 2011; Rightmire, 2015; Roksandic et al, 2018; Rosas et al, 2019; Di Vincenzo and Manzi, 2023; Quam et al, 2024; Hautaviane et al, 2024). Nevertheless, further inquiries are needed into the process that drive the gonion morphological variation and its relation to other ascending ramus features.

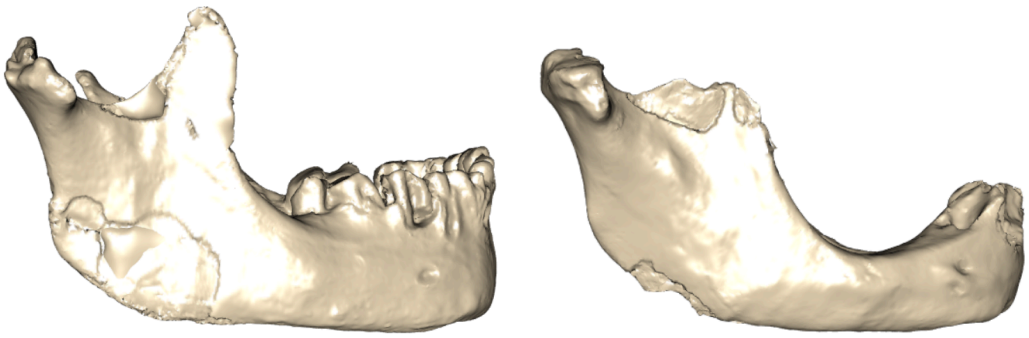

Fig. 5.7 *H. neanderthalensis* plotted close to Middle Pleistocene *Homo* Arago 13. La Ferrasie 1, truncated gonion, on the left, and La Chapelle-aux-saints, truncated gonion on the right.

5.3 *Homo sapiens* intra-specific variability

The *Homo sapiens* species in this study is divided into three groups: 1) 4 specimens are clustered for their chronology, since they date from the Upper Pleistocene; 2) 36 also from the Upper Pleistocene, are assembled into the Iberomaurusian group, for their cultural-population affinity; 3) 107 represent a recent Holocene sample, from the Neolithic and XIXth century reference collections. This group division provides a better comprehension of the species variability, in line with distinctions done in previous studies (Sella-Tunia et al, 2018; Bergmann et al, 2021).

The Upper Pleistocene *H. sapiens* show a large variability, although the sample is only composed of four specimens. Only Skhull 5 (Fig. 3.1) plots inside the Holocene *H. sapiens* distribution in all PCs studied. The others are more associated with the *H. neanderthalensis* variation pattern, distinguished in PC2 (Fig. 4.4 and 4.5) by a short, straight ramus and truncated gonion. Pataud AP/58 and Grimaldi (Fig. 5.8) plot at mid-negative axis, considerably below the highest scoring Neanderthals, but not at the extremes. Skull 4 (Fig. 4.6), on the other hand, is the lowest score for the axis.

This is in accordance with Bergmann et al (2021), who classify the *Early H. sapiens* group as diverse, in terms of mandible morphology, large specimens approximating the *H. neanderthalensis* configuration of inverted gonion and wide rami. This is also reflected in this study by the mean shape analysis for the group and the superimposition of the outlines (Fig. 4.14 - 4.16), which show a great variation in shape, approximating the group to *H. neanderthalensis* and Middle Pleistocene *Homo* more than other *H. sapiens*.

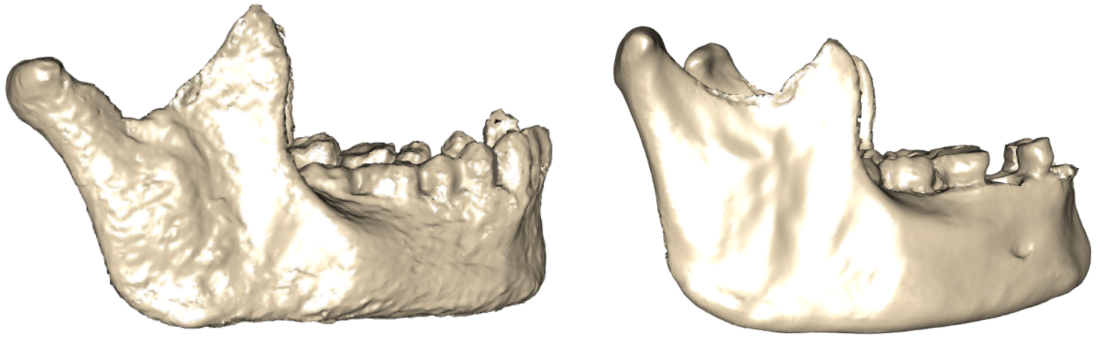

Fig. 5.8. Upper Pleistocene *H. sapiens* plotted towards PC2 minimal. Grimaldi mandible, on the left. Pataud AP/58 on the right.

In turn, the lower scoring Upper Pleistocene *H. sapiens* have a regular and straight gonion morphology. Instead, they approximate the Neanderthal-like shape by their short and wide ascending ramus. In fact, it is Skhull 5 (Fig. 3.1) who has a truncated and slightly inverted gonion, despite plotting among Holocene specimens. By contrast to the group counterparts, Skull 5 ramus is tall and narrow, indicating that its length is greatly influencing this axis of variation. The gonion morphology is also peculiar because, although truncated, it is very large and posteriorly projecting, more similar to an expanded gonion in some instances.

Bergmann et al (2021) argue that, while large *Early H. sapiens* individuals reminisce Neanderthal features, the large later *H. sapiens* exhibit an everted gonion, outward projection never seen in *H. neanderthalensis.* The Iberomaurusian population's particular morphology could be indicative of this trend, since it differs slightly from the other *H. sapiens*, but overlapping significantly. This would also be chronologically consistent, since they date from the end of the Upper Paleolithic, approaching a transitional period to the Holocene (Mariotti et al, 2009; De Groote and Humphrey, 2016).

The morphological investigation shows this pattern, with 66.67% of everted gonions in the Iberomaurusian sample and only 31.78% in the Holocene *H. sapiens* (table 3.10). The landmark-based PCA shows a similar division, most Iberomaurusian's plotting towards the PC3 minimal (Fig. 4.5 and 4.7), characterized by gonion expansion and eversion, forming an anterior gonion-notch (Fig. 4.3). On the other hand, the Fourier-based PC3 (Fig. 4.32 and 4.33) does not illustrate the same distribution pattern. Even if most Iberomaurusians continue to plot towards the gonion eversion, a few Holocene *H. sapiens* have similar scores, overlapping the two groups distribution. Since it is based on harmonics, EFA method tends to

be more sensitive, demonstrating that, while there are different tendencies in the Iberomaurusian morphology, they are not outside of the range for other *H. sapiens*.

Furthermore, there are important co-variations in gonion and ramus morphology, consistently present in the Iberomaurusian sample. The mean shape and superimposed outlines (Fig. 4.16 and 4.17) capture the gonion eversion and associate it to differences in upper ramus configuration. For the Iberomaurusians, who have an expanded gonion, the ramus border is straighter and the condyle more anteriorly placed. On the other hand, Holocene *H. sapiens*, with a regular gonion, tend to have an inclined ramus border and posterior condyle. This reinforces that gonion and ramus morphological configurations are related.

A relation in gonion and ascending ramus morphology is also observed in the axis that accounts most for this variation. On landmark-based PC1 (Fig. 4.4 and 4.7), 39.52% of the variability is explained, but no species or groups are differentiated in this axis. It is in fact, the recent *H. sapiens* sample that represents the full axis'range. Most of the specimens are plotted towards the minimal shape (Fig. 4.1), characterized by an obtuse gonial angle and a posteriorly inclined ramus. Nevertheless, some individuals from the same group plot at the maximal extreme (Fig. 4.1), characterized by a gonion angle closer to 90º and a straight ramus. The same variation is captured by Fourier-based PC1 (Fig. 4.28), as well as the overall range of *H. sapiens* distribution (Fig. 4.31 and 4.33). The main difference is that in Fourier, PC1 accounts for a large portion of the variability, explaining 53.3% of it.

Notably, this variation does not indicate significant changes in the gonial morphology, considering that both PC1(Fig. 4.1 and 4.28) minimal and maximal outlines describe regularly shaped gonions. It also does not play a significant role in species differentiation, since all groups overlap inside of the *H. sapiens* range. An identical variation can be observed in Sella-Tunis et al (2018), a study correlating mandibular morphology with masseter muscle cross-sectional area. The gonion, as the attachment site for the muscle, may be responding to changes in its configuration or in the force exerted by it. Likewise, the ramus also is subject to muscular insertions and activities.

For both males and females, mandibles with smaller cross-sectional area muscles are characterized by tall and narrow ascending ramus. According to the warping provided by Sella-Tunis et al (2018) (Fig. 5.9), these could also be described by an obtuse gonial angle and posteriorly inclined ramus. By contrast, for mandibles with large masseter cross-sectional areas (Fig. 5.9), the ramus are wide, trapezoid-like. The warpings indicate a more straight, vertically positioned posterior border and a larger gonion, in terms of area, even if regularly

shaped. The observed PC1 variability is consistent with this description, and aligned with a general gracilization trend. This process, particularly emphasized for Holocene populations, implies a more obtuse gonion angle, the reduction of its area and ramus breadth (Bergmann et al, 2021).

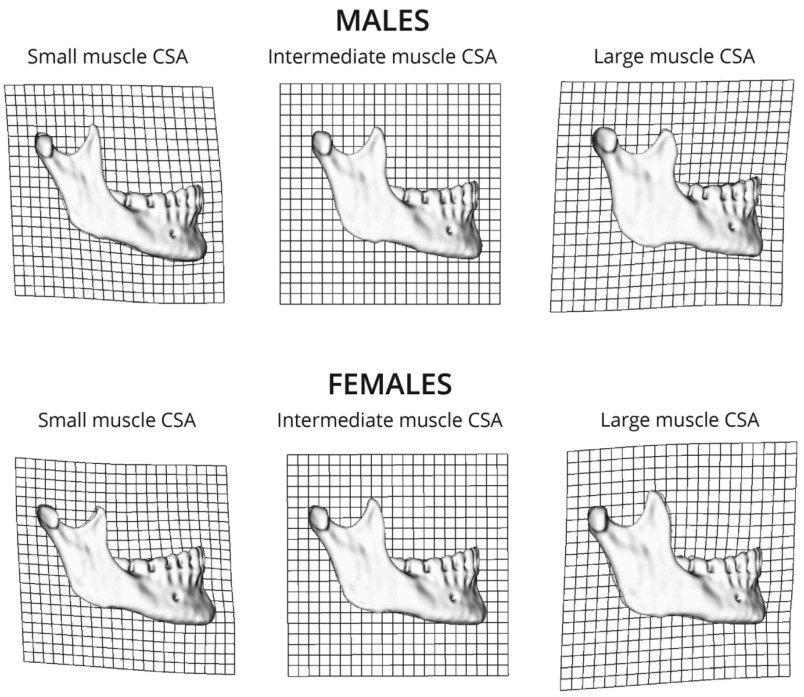

Fig. 5.9 Wrappings showing mandibular morphology associated with muscular cross-sectional area (CSA). From Sella-Tunis et al (2018).

Sella-Tunis et al (2018) highlight differences between the sexes, especially regarding the individuals with large muscle cross-sectional areas. Comparatively to females, males have slightly wider rami, straighter posterior border and larger gonion area, more expanded (Fig.5.9). The variation observed in this study follows accordingly. For PC1 (Fig. 4.9), *H. sapiens* females are distributed towards lower scores, characterized by the obtuse gonial angle. By contrast, males have more positive scores, towards a more vertical ramus and gonial angle closer to 90º. Therefore, there are indications that muscle mass differences are factors in the variability observed in PC1; nonetheless, future studies are still needed for a better understanding of muscle mass implications for gonion and ramus morphologies.

Sex differences may also be compared considering different *H. sapiens* populations. The superimposed mean shapes (Fig. 4.21 - 4.23) indicate consistent sex differences for both Iberomaurusians and the recent *H. sapiens* group. In either group, males' mean shape show a more expanded gonion and anteriorly placed condyle than their female counterparts, with more obtuse gonial angles and posteriorly placed condyles. Moreover, *H. sapiens* females and

Iberomaurusian males are at the two extremes of this variation, with Iberomaurusian females and *H. sapiens* males overlapping intermediary. Therefore, the Iberomaurusian tendency for gonion expansion is true for both sexes, but keeps the same inter-sex pattern inside the group.

The morphological investigation (table 3.11 and 3.12) of the sample studied reinforces this pattern, given that all *H. sapiens* females have regular gonions, and only 12.50% are everted. In contrast, for Iberomaurusians females, there is a prevalence for the morphology, as 60.87% show some degree of eversion. The eversion is even more frequent than for the 39.13% *H. sapiens* males, but still less than the Iberomaurusian males at 72.22%. A similar distribution is observed at the landmark-based PC3 scores per sex (Fig. 4.11). Compared to other *H. sapiens*, Iberomaurusians tend to have lower medians and inter-quartile ranges, towards gonion eversion; however, scores for males extend lower than for females. The same pattern is observed for *H. sapiens*, but with slightly higher scores than Iberomaurusians, indicating less eversion

Moreover, since the bone remodelling process is also influenced by the biomechanical forces at play, the impact of antemortem tooth-loss was investigated, in particular for molars. The purpose was to inquire if gonion morphology may be affected by a considerable lack of teeth, which alters the chewing pattern and may, in turn, alter the morphology.

From the 165 individuals included in the sample, 74 registered some kind of ante-mortem tooth loss, 68 on the right side. Considering the classification applied in the morphological investigation, the results were filtered for shape and orientation to understand if there is any change in the distribution pattern. First we considered all individuals with antemortem right tooth loss, the same side of the outline. Then, progressively, we analyzed the impact of molar tooth loss, filtering first for the antemortem absence of one molar (be it the first, second or third), then two and all three finally.

	Gonion orientation distribution				
	Everted	Inverted	Straight	Total	Sample size
Full sample	35.15%	6.67%	58.18%	100%	165
Right side tooth loss	41.18%	5.88%	52.94%	100%	68
Loss of 1 molar	38.60%	5.26%	56.14%	100%	57
Loss of 2 molars	41.94%	6.45%	51.61%	100%	31
Loss of all molars	40%	6.67%	53.33%	100%	15

Table 5.1. Distribution of gonion orientation in everted, inverted or straight, according to molar loss.

	Gonion shape distribution				
	Expanded	Regular	Truncated	Total	Sample size
Full sample	13.94%	74.55%	11.52%	100%	165
Right side tooth loss	19.12%	70.59%	10.29%	100%	68
Loss of 1 molar	17.54%	73.68%	8.77%	100%	57
Loss of 2 molars	16.13%	70.97%	12.90%	100%	31
Loss of all molars	20%	60%	20%	100%	15

Table 5.2 Distribution of gonion shape in expanded, regular or truncated, according to molar loss.

The results (table 5.1 and 5.2) do not indicate any significant changes in morphology pattern, considering gonion shape and orientation. The percentages are stable, not varying greatly, in spite of the reduction on the total sample and on the number of teeth. Therefore, there is no indication that edentulism affects the gonion morphology or explain any of the intra and inter-specific variability observed.

Studying the intra-specific variability of gonion and ramus morphologies may offer considerable insights into the factors influencing their variability, with more nuanced phylogenetic implications. Evolutionary aspects should be considered, as the gracilization trend (Sella-Tunis et al, 2018; Bergmann et al, 2021), but other factors must be explored, such as the integration to other cranial-facial elements, the growth process and responses to different biomechanical factors. Indeed, the study of living populations grants the possibility of adding new data, new perspectives to consider ramus and gonion responses to muscular adaptations and other factors.

Conclusions

The posterior portion of the mandible has significant information power, with considerable variance at the ascending ramus posterior border and the gonion region, at the junction with the basal border. *Homo neanderthalensis* differentiates from *Homo sapiens*, but not only by the previously observed truncated gonion shape. A shorter and straighter ramus is associated with the truncated gonion, although their distribution does not allow a clear insight into the relation of these features. A better understanding of the factors influencing ramus length and incurvation is necessary as well as their integration to gonion morphology.

The studied outline approximates Middle Pleistocene *Homo* to Neanderthals, both presenting a very similar variation pattern. Arago 13, who has a truncated gonion and short ramus, plots very closely to classical Neanderthals, such as La Ferrassie 1 and La Chapelle-aux-saints. On the other hand, Arago 2 and Mauer, who have wider and straighter ramus, plot slightly outside the *H. neanderthalensis* distribution pattern, a difference of dubious significance. Both have wider and more vertical ramus, but one gonion is truncated and the other regular, hindering the interpretation of the feature as an adaptive response or a population variance.

Intra-specific studies in *Homo sapiens* groups offer some insight into these factors. Our results indicate a wide range for the Holocene *H. sapiens*, an obtuse gonial angle associated with an inclined posterior ramus border, and an angle closer to 90º is connected to a more vertical, straighter border. Moreover, this variation reflects sexual dimorphism, since females frequently have more obtuse gonions than their male counterparts. Ante-mortem tooth loss was not identified as a factor that correlated to specific morphologies.

In terms of populational differences, most Upper Pleistocene *H. sapiens* show a Neanderthal-like ramus morphology, aligned with studies that describe these similarities that will not be present in later *H. sapiens*. The Iberomaurusians, a North-African population dating from the end of the Upper Paleolithic, variate in another direction. Although very close to the recent *H. sapiens* distribution, they show a more frequent and pronounced gonion eversion and expansion, associated with a more anteriorly placed condyle. This is true, for both males and females, when compared to their respective groups.

Other questions regard the factors influencing the everted, regular and truncated gonion morphology. Do they have different growth trajectories? Or are they remodelling responses to different cranial-mandibular integration patterns? As the site for masticatory muscle attachment, how does the gonion configuration reflect distinct bite forces? Addressing these questions may offer new perspectives on bone deposition and resorption patterns, in

function of different stimuli - growth, biomechanics and cranial-mandibular integration. Including the full ramus outline in the study may be informative, since the anterior border is also a place of muscular attachment and known bone resorption center. It may enhance the comprehension of gonion morphology in terms of populational differences and the phylogenetic significance.

Bibliographical References

Aiello, L., & Dean, C. (1990). An introduction to human evolutionary anatomy. Academic Press.

Arambourg, C. (1954). The fossil man of Ternifine (Algeria). Comptes rendus hebdomadaires des séances de l'Académie des sciences, 239(15), 893-895.

Arnaud, J., Peretto, C., & Grimaud-Hervé, D. (2015). The Grotta Guattari mandibular remains in the Italian human evolutionary context: A morphological and morphometrical overlook of the Neanderthal jaw. Quaternary International, 388, 206-217.

Arnaud, J. (2021). Les restes mandibulaires d'Homo neanderthalensis d'Archi, Caverna delle Fate et Guattari. BAR Publishing.

Balout, L., & Briggs, L. C. (1949). Débris humains de l'escargotière de Gambetta. Imprimeries la Typo-Litho et Jules Carbonel réunies.

Barroso Ruiz, C., 2001. Le site moustérien de la grotte du Boquete de Zafarraya, province de Malaga en Andalousie, Espagne. Muséum National d'Histoire Naturelle, Paris.

Barton, R. N., Bouzouggar, A., Collcutt, S. N., Gale, R., Higham, T. F., Humphrey, L. T., ... & Malek, F. (2005). The Late Upper Palaeolithic occupation of the Moroccan northwest Maghreb during the last glacial maximum. African Archaeological Review, 22, 77-100.

Bastir, M. (2018). Back to basics: morphological analysis in paleoanthropology. Biological theory, 205-227.

Bergmann, I., Hublin, J. J., Gunz, P., & Freidline, S. E. (2021). How did modern morphology evolve in the human mandible? The relationship between static adult allometry and mandibular variability in Homo sapiens. Journal of Human Evolution, 157, 103026.

Bergmann, I., Hublin, J. J., Ben-Ncer, A., Sbihi-Alaoui, F. Z., Gunz, P., & Freidline, S. E. (2022). The relevance of late MSA mandibles on the emergence of modern morphology in Northern Africa. Scientific Reports, 12(1), 8841.

Bermúdez de Castro, J. M., Martinón-Torres, M., Gómez-Robles, A., Prado, L., & Sarmiento, S. (2007). Comparative analysis of the Gran Dolina-TD6 (Spain) and Tighennif (Algeria) hominin mandibles. Bulletins et mémoires de la Société d'Anthropologie de Paris. BMSAP, 19(19 (3-4)), 149-167.

Billy, G., Vallois, H.V., 1977. La mandibule pré-rissienne de Montmaurin. Anthropologie 81, 273-312, 411-458.

Black, S. M., Schaefer, M., & Scheuer, L. (2009). Juvenile Osteology: A Laboratory and Field Manual

Bonhomme V, Picq S, Gaucherel C, Claude J (2014). Momocs: Outline Analysis Using R, volume 56 number 13. https://www.jstatsoft.org/v56/i13/.

Broca, P. (1872). Laboratoire d'Anthropologie. Annuaires de l'École pratique des hautes études, 1(1), 40-46.

Broca, P. (1873). Laboratoire d'Anthropologie. Annuaires de l'École pratique des hautes études, 1(1), 50-55.

Claude, J. (2008). Morphometrics with R. Springer Science & Business Media.

Condemi, S., 2001. Les Néanderthaliens de La Chaise. Comité des Travaux Historiques et Scientifiques (CTHS), Paris, p 175.

De Groote, I., & Humphrey, L. T. (2016). Characterizing evulsion in the Later Stone Age Maghreb: Age, sex and effects on mastication. Quaternary International, 413, 50-61.
Demoulin, Françoise. 1996. In memorium Georges Olivier (1912–1996). Bulletins et Mémoires de la Société d'anthropologie de Paris 8 (3–4): 511.

De Lumley, M. A. (2015). L'homme de Tautavel. Un Homo erectus européen évolué. Homo erectus tautavelensis. l'Anthropologie, 119(3), 303-348.

Dean, D., Hublin, J. J., Holloway, R., & Ziegler, R. (1998). On the phylogenetic position of the pre-Neandertal specimen from Reilingen, Germany. Journal of Human Evolution, 34(5), 485-508.

Dennell, R. W., Martinón-Torres, M., & de Castro, J. M. B. (2011). Hominin variability, climatic instability and population demography in Middle Pleistocene Europe. Quaternary Science Reviews, 30(11-12), 1511-1524.

Di Vincenzo, F., & Manzi, G. (2023). Homo heidelbergensis as the Middle Pleistocene common ancestor of Denisovans, Neanderthals and modern humans. Journal of Mediterranean Earth Sciences, 15.

Easton, V. J. (2000). Describing size and shape changes in the human mandible from 9 to 15 years-comparison of elliptical Fourier function and Procrustes methods (Doctoral dissertation, University of Glasgow).

El Hajraoui, M. A., Nespoulet, R., Debénath, A., & Dibble, H. L. (2012). La Préhistoire de la région de Rabat-Témara (Vol. 3, p. 300). Institut National des Sciences de l'Archéologie et du Patrimoine.

Ely, B. (1967). Les crânes tziganes des collections du Musée de l'Homme. Bulletins et Mémoires de la Société d'Anthropologie de Paris, 1(2), 177-192.

Enlow, D. H., Hans, M. G., & McGrew, L. (1996). Essentials of facial growth (Vol. 35). Philadelphia: Saunders.

Fedorov A., Beichel R., Kalpathy-Cramer J., Finet J., Fillion-Robin J-C., Pujol S., Bauer C., Jennings D., Fennessy F.M., Sonka M., Buatti J., Aylward S.R., Miller J.V., Pieper S., Kikinis R. (2012). 3D Slicer as an Image Computing Platform for the Quantitative Imaging Network . Magnetic Resonance Imaging. 30(9):1323-41. PMID: 22770690. PMCID: PMC3466397.

Grün, R., Beaumont, P., Tobias, P. V., & Eggins, S. (2003). On the age of Border Cave 5 human mandible. Journal of human Evolution, 45(2), 155-167.

Harvati, K., Singh, N., & López, E. N. (2011). A three-dimensional look at the Neanderthal mandible. In Continuity and discontinuity in the peopling of Europe: one hundred fifty years of Neanderthal study (pp. 179-192). Dordrecht: Springer Netherlands.

Hautavoine, H., Arnaud, J., Balzeau, A., & Mounier, A. (2024). Quantifying hominin morphological diversity at the end of the middle P leistocene: Implications for the origin of Homo sapiens. American Journal of Biological Anthropology, 184(2), e24915.

Heim, J. L., & Cranat, J. (1995). La mandibule de l'enfant néandertalien de Malarnaud (Ariège): Une nouvelle approche anthropologique par la radiographie et la tomodensitométrie. Anthropologie et préhistoire, 106, 75-96.

Henry-Gambier, D., Villotte, S., Beauval, C., Brůžek, J., & Grimaud-Hervé, D. (2013). Les vestiges humains: un assemblage original. Le Gravettien final de l'abri Pataud (Dordogne, France): fouilles et études 2005-2009, 2458, 135-177.

Hovers, E., Rak, Y., Lavi, R., & Kimbel, W. H. (1995). Hominid remains from Amud Cave in the context of the Levantine Middle Paleolithic. Paléorient, 47-61.

Hublin, J. J. (2009). The origin of Neandertals. Proceedings of the National Academy of Sciences, 106(38), 16022-16027.

Hublin, J. J., Ben-Ncer, A., Bailey, S. E., Freidline, S. E., Neubauer, S., Skinner, M. M., ... & Gunz, P. (2017). New fossils from Jebel Irhoud, Morocco and the pan-African origin of Homo sapiens. Nature, 546(7657), 289-292.

Humphrey, L. T., & Bocaege, E. (2008). Tooth evulsion in the Maghreb: Chronological and geographical patterns. African Archaeological Review, 25, 109-123.

Humphrey, Freyne, Bouzouggar, Gaudzinski-Windheuser, S., & Jöris, O. (2021). Mind the gap: funerary behavior during the Iberomaurusian. The beef behind all possible pasts: the tandem festschrift in honour of Elaine Turner and Martin Street. RGZM, 459-70.

Irish, J. D. (2000). The Iberomaurusian enigma: North African progenitor or dead end?. Journal of human evolution, 39(4), 393-410.

Kuhl, F. P., & Giardina, C. R. (1982). Elliptic Fourier features of a closed contour. Computer graphics and image processing, 18(3), 236-258.

Knüsel, C. and Maureille, B. (2018). Archaeological Approaches to Human Remains: France. Archaeological Human Remains. Legacies of Imperialism, Communism and Colonialism., ff10.1007/978-3-319-89984-8_5ff. ffhal-02123301f

Lebel, S., Trinkaus, E., Faure, M., Fernandez, P., Guérin, C., Richter, D., ... & Wagner, G. A. (2001). Comparative morphology and paleobiology of Middle Pleistocene human remains from the Bau de l'Aubesier, Vaucluse, France. Proceedings of the National Academy of Sciences, 98(20), 11097-11102.

Lebel, S., & Trinkaus, E. (2002). Middle Pleistocene human remains from the Bau de l'Aubesier. Journal of Human evolution, 43(5), 659-685.

Lestrel, P. E. (1989). Method for analyzing complex two‐dimensional forms: Elliptical Fourier functions. American Journal of Human Biology, 1(2), 149-164.

Lieberman, D. E. (1997). Making behavioral and phylogenetic inferences from hominid fossils: considering the developmental influence of mechanical forces. Annual Review of Anthropology, 26(1), 185-210.

Mariotti, V., Bonfiglioli, B., Facchini, F., Condemi, S., & Belcastro, M. G. (2009). Funerary practices of the Iberomaurusian population of Taforalt (Tafoughalt; Morocco, 11–12,000 BP): new hypotheses based on a grave by grave skeletal inventory and evidence of deliberate human modification of the remains. Journal of Human Evolution, 56(4), 340-354.

Maureille, B., & Vandermeersch, B. (2007). Les sépultures néandertaliennes. Doc Prehist, 23, 311-322.

Mercier, G. (1915). L'Homme de Mechta-Châteaudun (Algérie). Bulletin de la Société préhistorique de France, 12(3), 160-166.

McCown, T.D., Keith, A., 1939. The Stone Age of Mount Carmel, Vol. II: The Fossil Human Remains from the Levallois-Mousterian, 2. Oxford University Press, London, p 390.

Mounier, A., Marchal, F., & Condemi, S. (2009). Is Homo heidelbergensis a distinct species? New insight on the Mauer mandible. Journal of Human Evolution, 56(3), 219-246.

Mounier, A. (2009b). Validité du taxon Homo heidelbergensis Schoetensack, 1908 (Doctoral dissertation, Université de la Mediterranee).

Nicholson, E., & Harvati, K. (2006). Quantitative analysis of human mandibular shape using three‐dimensional geometric morphometrics. American Journal of Physical Anthropology: The Official Publication of the American Association of Physical Anthropologists, 131(3), 368-383.

Oujaa, A., & Lacombe, J. P. (2012). L'occupation humaine paléolithique de la région de Témara: les grottes d'El Harhoura 2 et d'El Mnasra (Chapitre XIX). Préhistoire de la région de Rabat-Témara, 3, 136-149.

Prüfer, K., Racimo, F., Patterson, N., Jay, F., Sankararaman, S., Sawyer, S., ... & Pääbo, S. (2014). The complete genome sequence of a Neanderthal from the Altai Mountains. Nature, 505(7481), 43-49.

Putz, R., Pabst, R. (2006). Sobotta: Atlas of Human Anatomy (Volume 1, 14th edition). Germany: Elsevier GmbH.

Quam, R., Martínez, I., Rak, Y., Hylander, B., Pantoja, A., Lorenzo, C., ... & Arsuaga, J. L. (2024). The Neandertal nature of the Atapuerca Sima de los Huesos mandibles. The Anatomical Record, 307(7), 2343-2393.

R Core Team (2024) R: A Language and Environment for Statistical Computing. R Foundation for Statistical Computing. https://www.R-project.org/

Rightmire, G. P. (2008). Homo in the Middle Pleistocene: hypodigms, variation, and species recognition. Evolutionary Anthropology: Issues, News, and Reviews: Issues, News, and Reviews, 17(1), 8-21.

Rightmire, G. P. (2015). Later middle pleistocene homo. In Handbook of paleoanthropology (pp. 2221-2242). Springer, Berlin, Heidelberg.

Roksandic, M., Radović, P., & Lindal, J. (2018). Revising the hypodigm of Homo heidelbergensis: A view from the Eastern Mediterranean. Quaternary International, 466, 66-81.

Roksandic, M., Radović, P., Wu, X. J., & Bae, C. J. (2021). Resolving the "muddle in the middle": The case for Homo bodoensis sp. nov. Evolutionary Anthropology: Issues, News, and Reviews, 31(1), 20-29.

Rosas, A. (1997). A gradient of size and shape for the Atapuerca sample and Middle Pleistocene hominid variability. Journal of Human Evolution, 33(2-3), 319-331.

Rosas, A., & De Castro, J. M. B. (1998). The Mauer mandible and the evolutionary significance of Homo heidelbergensis. Geobios, 31(5), 687-697.

Rosas, A. (2001). Occurrence of Neanderthal features in mandibles from the Atapuerca‐SH site. American Journal of Physical Anthropology: The Official Publication of the American Association of Physical Anthropologists, 114(1), 74-91.

Rosas, A., & Bastir, M. (2004). Geometric morphometric analysis of allometric variation in the mandibular morphology of the hominids of Atapuerca, Sima de los Huesos site. The Anatomical Record Part A: Discoveries in Molecular, Cellular, and Evolutionary Biology: An Official Publication of the American Association of Anatomists, 278(2), 551-560.

Rosas, A., Bastir, M., Martínez-Maza, C., García-Tabernero, A., & Lalueza-Fox, C. (2006). Inquiries into Neanderthal craniofacial development and evolution: "accretion" versus "organismic" models. In Neanderthals revisited: New approaches and perspectives (pp. 37-69). Dordrecht: Springer Netherlands.

Rosas, A., Bastir, M., & Alarcón, J. A. (2019). Tempo and mode in the Neandertal evolutionary lineage: A structuralist approach to mandible variation. Quaternary Science Reviews, 217, 62-75.

Ruff, C. B. (2018). Biomechanical analyses of archaeological human skeletons. Biological anthropology of the human skeleton, 189-224.

Sawyer, S., Renaud, G., Viola, B., Hublin, J. J., Gansauge, M. T., Shunkov, M. V., ... & Pääbo, S. (2015). Nuclear and mitochondrial DNA sequences from two Denisovan individuals. Proceedings of the National Academy of Sciences, 112(51), 15696-15700.

Scheuer, L., & Black, S. (2000). Developmental juvenile osteology. Academic press.

Scheuer, L., & Black, S. (2004). The juvenile skeleton. Elsevier.

Schlager S (2017). "Morpho and Rvcg – Shape Analysis in R." In Zheng G, Li S, Szekely G (eds.), Statistical Shape and Deformation Analysis, 217–256. Academic Press. ISBN 9780128104934.

Schmittbuhl, M., Rieger, J., Le Minor, J. M., Schaaf, A., & Guy, F. (2007). Variations of the mandibular shape in extant hominoids: generic, specific, and subspecific quantification using elliptical Fourier analysis in lateral view. American Journal of Physical Anthropology: The Official Publication of the American Association of Physical Anthropologists, 132(1), 119-131.

Schwartz, J. H., & Tattersall, I. (2005). The human fossil record, craniodental morphology of genus Homo (Africa and Asia) (Vol. 2). John Wiley & Sons.

Sella-Tunis, T., Pokhojaev, A., Sarig, R., O'Higgins, P., & May, H. (2018). Human mandibular shape is associated with masticatory muscle force. Scientific reports, 8(1), 6042.

Sens, X., Oujaa, A., Grimaud-Hervé, D., Zazzo, A., Lebon, M., Tombret, O. & Nespoulet, R. (2016). Premiers résultats de l'étude anthropologique des restes humains de la grotte de M'Tsogatin 1 (Région d'Oulmès, Maroc). Bulletin de l'Institut Scientifique, Rabat., 7(10), 3746-3762.

Smith, F.H., 1976. The Neandertal Remains from Krapina: A Descriptive and Comparative Analysis. Department of Anthropology. University of Tennessee, Knoxville, Tennessee, p 359.

Stringer, C. (2012). The status of Homo heidelbergensis (Schoetensack 1908). Evolutionary Anthropology: Issues, News, and Reviews, 21(3), 101-107.

Solecki, R. S. (1975). Shanidar IV, a Neanderthal flower burial in northern Iraq. Science, 190(4217), 880-881.

Tappen, N. C. (1985). The dentition of the "old man" of La Chapelle‐aux‐Saints and inferences concerning Neandertal behavior. American Journal of Physical Anthropology, 67(1), 43-50.

Tattersall, I. (2011). Before the Neanderthals: Hominid Evolution in Middle Pleistocene Europe. In Continuity and discontinuity in the peopling of Europe: one hundred fifty years of Neanderthal study (pp. 47-53). Dordrecht: Springer Netherlands.

Terhune, C. E., Ritzman, T. B., & Robinson, C. A. (2018). Mandibular ramus shape variation and ontogeny in Homo sapiens and Homo neanderthalensis. Journal of Human Evolution, 121, 55-71.

Tillier, A. M., Duday, H., & Arensburg, B. (1989). La mandibule et les dents du néanderthalien de Kebara (Homo 2) Mont Carmel, Israel. Paléorient, 39-58.

Trinkaus, E., 1983. The Shanidar Neanderthals. Academic Press, New York.

Trinkaus, E. (2011). The postcranial dimensions of the La Chapelle‐aux‐saints 1 Neandertal. American Journal of Physical Anthropology, 145(3), 461-468.

Van Eijden, T. (2000). Biomechanics of the mandible. Critical reviews in oral biology & medicine, 11(1), 123-136.

Vialet, A., Modesto-Mata, M., Martinón-Torres, M., Martínez de Pinillos, M., & Bermúdez de Castro, J. M. (2018). A reassessment of the Montmaurin-La Niche mandible (Haute Garonne, France) in the context of European Pleistocene human evolution. PLoS One, 13(1), e0189714.

White, T. D., Black, M. T., & Folkens, P. A. (2011). Human osteology. Academic press.

Zanolli, C., & Mazurier, A. (2013). Endostructural characterization of the H. heidelbergensis dental remains from the early Middle Pleistocene site of Tighenif, Algeria. Comptes Rendus Palevol, 12(5), 293-304.